

MINISTRY OF EDUCATION AND SCIENCE OF UKRAINE

National Aerospace University

Kharkiv Aviation Institute

Faculty of Aircraft Engineering

Department of Aircraft and Helicopter Design

**Explanatory note
to the diploma project**

Master's Degree

(educational level)

On the topic: «**Medium – range passenger aircraft and in -air**

noise reduction study»

XAI.103.161FD.23S.134.10032801 EN

Executed by: student of 2 year group № 161FD

Field of knowledge : 13 Mechanical Engineering

Specialty 134 «Aerospace Engineering»

(code and name)

Educational program «Aircraft Designing»

(name)

Kalaivani Muthuramalingam Krishnakumar

(surname and initials of the student)

Supervisor: Filipkovskij S. V.

(surname and initials of the student)

Reviewer: S. M. Ivanov

(surname and initials of the student)

Kharkov- 2023

**Ministry of Science and Education of Ukraine
National Aerospace University
«Kharkiv Aviation Institute»**

Faculty _____ *Aircraft Engineering*
Department _____ *103 Airplane and Helicopter Design*
Degree _____ *First (Bachelor)*
Field of knowledge _____ *13 Mechanical Engineering*
Specialty _____ *134 Aerospace Engineering*
(Code and name)
Educational Program _____ *Airplanes and helicopters*
(Name)

**APPROVED by
Head of Chair**

PhD, Ass. Prof. _____ Andrii HUMENNYI
“ _____ ” _____ 2023 _____

**TASK
FOR DIPLOMA PROJECT**

_____ Kalaivani Muthuramalingam Krishnakumar _____
(Name)

Subject of qualification paper _____ Medium-range passenger aircraft and in-air noise reduction study _____

Supervisor of qualification paper _____ Sergey Filipkovskij, Prof., DSc _____
(name, degree, scientific degree)

Approved by University order No 413-уч from “ 20 ” 03 2023

Qualification paper presentation deadline _____ 15/05/2023 _____

Initial data for the qualification _____ L=6000 km; L_{TO}=2000 m; H_{cruis}=12.5 km; V_{cruis}=955 km/h; V_{max}=1000 km/h; n_{crew}=5 pers; n_{pass}=189 pers. _____

Content of explanatory note (list of problems to solve)

Abstract

1 Design section

1.1 Automated formation of an airplane view

1.2 Analysis of optimized aircraft design parameters influence on its aerodynamic and mass characteristics

2 Research Section

2.1 Integrated design and noise reduction inside aircraft

2.2 Noise reduction outside aircraft

3 Economics Section

3.1 Competitive advantages of the designed aircraft and assessment of its possible volumes of its implementation in the sales markets.

3.2 Initial data for the calculation of technical and economic performance indicators for the creation of an aircraft

3.3 Calculation of the main technical and economic indicators of design and production of aircraft

Conclusion

Reference

List of drawings (with the exact indication of obligatory drawings)

- Master geometry of aircraft surface, general view drawing.
- Load carrying structure layout of the aircraft.

Advisors of diploma project sections

Section	Name and duty of advisor	Signature, Date	
		Task is given	Task is submitted
1	Prof., DSc, Sergey Filipkovskij	10/02/2023	23/03/2023
2	Prof., DSc, Sergey Filipkovskij	10/02/2023	11/05/2023
3	Ass. Prof., PhD, Tatiana Pavlenko	10/02/2023	15/05/2023
4			
5			

Normative inspection _____ Sergey Filipkovskij « _____ » _____ 2023
 (Signature) (Name)

Date when task is given _____ 2023 February 10 _____

CALENDAR PLAN

№	Diploma project milestones	Diploma project milestone deadlines	Notes
1	Design Section	23/03/2023	
2	Research Section	11/05/2023	
3	Economic Section	15/05/2023	
4			
5			

Applicant

_____ Kalaivani
Muthuramalingam
Krishnakumar
 (Signature) (Initials and surname)

Supervisor of diploma project

_____ Sergey Filipkovskij
 (Signature) (Initials and surname)

SUMMARY

The master project contains 89 p., 14 Tables, 86 Fig., 13 References.

Object of research: Medium – Range Passenger Aircraft

The purpose of the work: The aim of this diploma project is to design a medium – range passenger aircraft with 120 passengers, including determining the take-off mass and geometric parameters in the three approximations, developing general view drawing and load-carrying structure, modelling aircraft master-geometry and space distribution model, calculating aerodynamic and flight characteristics, noise reduction inside and outside aircraft, cost calculation of manufacturing the designed aircraft.

Research methods: Building structure in Siemens NX, Aero – Acoustic analysis in ANSYS Fluent, Noise absorption analysis in impedance tube.

The results of the master's diploma project and its novelty: As a result of the master's diploma project the following results were obtained:

1) Determined basic geometric and mass parameters of a medium – range passenger aircraft. The influence of geometric parameters on the take-off mass of the aircraft in three approximations. The take-off mass of the aircraft in the third approximation is 11977 kg, and the masses of the main components of the aircraft: wing – 27370 kg; fuselage – 24990 kg; tail – 4970 kg; landing gear – 12670 kg; power plant – 7000 kg; fuel – 19776.8 kg. The main geometric parameters are wingspan – 40 m, mean aerodynamic chord of wing – 3.64 m, fuselage length – 40 m, wing aspect ratio – 10.

2) Developed a master geometry and a space distribution model of an airplane. Models created using Siemens NX, General view and load-carrying structure created using AUTO CAD v20.

3) Calculated aerodynamic and flight characteristics of the designed aircraft. The highest aerodynamic quality is 15.7 units.

4) Modelling winglet using Siemens NX.

5) Winglet is designed to be reduced for noise reduction. In this we have modified the design of the wing and winglet. Among this 5 types of design, we have analysed each wing with velocity of 75 m/s. By comparing the results, Winglet 5 has suitable range of acoustic power with 102.15 dB. Which is less than Existing Winglet, it has 105.02 dB.

6) The estimated cost of the projected aircraft for the design bureau, which is 41.5 million dollars. The estimated cost of manufacturing the aircraft, which amounted to 6.76 billion dollars.

MEDIUM – RANGE AIRCRAFT, WING, TAIL UNIT, FUSELAGE, LANDING GEAR, AERODYNAMIC CHARACTERISTICS, MATERIAL ANALYSIS, WINGLET, PRICE OF THE AIRCRAFT.

CONTENT

1 DESIGN SECTION	6
1.1 Automation formation of an airplane view	6
1.1.1 Development of the concept of creating a projected aircraft and a scientific and technical program to achieve its characteristics	6
1.1.2 Purpose, tactical and technical requirements for the aircraft, the conditions for its production and operation, restrictions imposed by aviation regulations in the design of the aircraft	7
1.1.3 Collection, processing and analysis of statistical data. Selection of the basic relative initial parameters of the aircraft.	9
1.1.4 Selection and justification of the scheme of the aircraft	13
1.1.5 Calculation of aircraft mass in three approximations	15
1.1.6 Selection of engines and checking of run length	29
1.1.7 Determination and optimization of design parameters of the aircraft and its units	30
1.1.8 Calculation of centering and moments of inertia of the aircraft...	34
1.1.9 Conclusion	36
1.2 Analysis of optimized aircraft design parameters influence on its aerodynamic and mass characteristics	36
1.2.1 Determination of the drag of the designed aircraft.....	36
1.2.2 Lift force, inductance, aircraft polar, aerodynamic quality of the aircraft, aircraft polarities in take-off and landing configurations	38
1.2.3 The longitudinal moment and the location of the aerodynamic focus of the aircraft	41
1.2.4 Conclusions	43
2 RESEARCH SECTION	44
2.1 Integrated design and noise reduction inside aircraft	44
2.1.1 Objective of the project	44
2.1.2 Application of sound absorbing material	44
2.1.3 Fiber selection and description	46
2.1.4 Sound absorption coefficient	48

2.1.5 Impedance tube	49
2.1.6 Methodology	49
2.1.7 Solution of computational analysis	51
2.1.8 Experimental analysis	53
2.1.9 Conclusion of noise reduction inside aircraft	59
2.2 Noise reduction outside aircraft	59
2.2.1 Objective of the project	59
2.2.2 Development of the master geometry of the winglet	59
2.2.3 Methodology	65
2.2.4 Comparison between winglets	71
2.2.5 Results	78
2.2.6 Conclusions	78
3 ECONOMIC SECTION	79
3.1 Competitive advantages of the designed aircraft and assessment of its possible volumes of its implementation in the sales markets	79
3.1.1 Characteristic of tactical and economic indexes of the designed long-range passenger aircraft as a commodity product	79
3.1.2 Consumer qualities of the aircraft, affecting the competitive advantages and economic costs when designing aircraft structures in the Design Bureau	79
3.2 Initial data for the calculation of technical and economic performance indicators for the creation of an aircraft	82
3.2.1 Data for calculating costs in the experimental design bureau	82
3.2.2 Data for calculating the costs of mass production of aircraft ...	82
3.3 Calculation of the main technical and economic indicators of design and production of aircraft	82
3.3.1 Calculation of costs of the experimental design bureau	82
3.3.2 Calculation of mass production costs	84
3.4 Evaluation of aircraft production efficiency depending on their sales volumes on sales markets	87
3.4.1 Break-even point determination	87

3.5 Economic conclusion88
CONCLUSIONS89
REFERENCES90
APPENDIX A91

1 DESIGN SECTION

1.1 Automated formation of an airplane view

1.1.1 Development of the concept of creating a projected aircraft and a scientific and technical program to achieve its characteristics

The creation of a new generation of medium-range aircraft for 120 passengers is due to the needs of the world passenger air transportation market. It is also necessary to replace the aging McDonnell Douglas MD 90 and Tupolev TU 204-24 aircrafts.

The design of a medium-range jet aircraft with a passenger capacity of up to 120 people is carried out in order to:

- creation of highly economical medium-range jet aircraft of a new generation, fully complying with modern and future airworthiness standards;
- replacement of the fleet of outdated medium-range jet aircraft;
- providing airlines and other customers with a new international competitive medium-range jet aircraft
- creation of medium-range jet aircraft with high levels of fuel efficiency, environmental friendliness, reliability, increased comfort and safety for passengers as well as with low operating costs;
- creation of medium-range jet passenger aircraft with a significantly expanded range of operating conditions in comparison with the range of operating conditions available in modern analogues;
- further development of scientific and industrial potential, as well as the creation of jobs in high-tech industries in world;

Achieving these goals is possible under the following conditions.

From aerodynamics: to provide aerodynamic quality of the plane on a cruising mode not less than 15; reduce takeoff and landing distances through the use of flaps, occupying up to 70% of the wingspan, as well as the use of a screen effect that increases the lift during takeoff; to develop the aerodynamic scheme of the plane that allows to reduce essentially aerodynamic resistance of the plane and resistance of interference in comparison with the reached level; achieve a reduction in the probability of falling at critical angle of attack. If the crash occurs – to ensure the independent exit of the aircraft from it without the participation of the pilot, apply modern wing airfoils.

From the design: perform the design of the passenger aircraft so that the total mass return reached 50 – 60%. This task is realized by application of modern methods of calculation on durability, use of modern composite materials, materials with the increased mechanical properties (2024, 7075, 1420, B95AT, 1161T, 1933T3, D16AT), tight high-resource fastening.

Management: it is necessary that the aircraft was stable and controllable in all flight modes. Use of the classical scheme of the aircraft and the presence of controls, such as ailerons, flaps, rudder altitude and direction, makes it possible to ensure high stability and controllability of the designed aircraft in all flight modes.

From the equipment: on the plane it is necessary to use modern digital equipment that has less mass than analog and increases the ease of reading information by the crew by outputting data to liquid crystal displays with high image quality.

From durability and resource: at the set lifecycle, the design of the passenger aircraft should provide not less than 60,000 flight hours.

From operational manufacturability and repair: it is necessary that the layout of the aircraft carried out a convenient and fast boarding and disembarking of passengers by using a removable step. The design of the aircraft will allow for a quick inspection and preparation for the flight without additional maintenance personnel.

From the range of functionalities: The designed aircraft must have the widest possible range of functionalities in terms of range and speed of flight, comfort of passengers and crew when operating in different climatic conditions, nomenclature of transported cargo, autonomy of operation and variability of aerodrome network.

1.1.2 Purpose, tactical and technical requirements for the aircraft, the conditions for its production and operation, restrictions imposed by aviation regulations in the design of the aircraft

The projected aircraft is being created as a base for passenger aircraft with a passenger capacity of up to 120 people, with two turbofan engines.

This aircraft must provide:

- the possibility of using various options for the types of application (trunk, administrative, regional) and equipment configuration (foreign or domestic avionics and equipment);

- full compliance with the AP-25, CS-25, FAR-25 airworthiness standards used today, environmental requirements and quality standards;

- high level operational and technical excellence;

- a wide range of speed, range, comfort;

- comprehensive in terms of foreign analogues;

- high fuel efficiency;

- the ability to fly adverse weather conditions.

The projected aircraft is designed to carry passengers, cargo, mail, baggage on local and international airlines.

The aircraft, all its equipment, components, engines as well as documentation must comply with:

- this technical assignment;

- aviation rules AP-25;

- auxiliary power unit (APU) – aviation regulations AR-AE «Airworthiness standards for aircraft auxiliary engines» (АП-ВД «Нормы летной годности вспомогательных двигателей воздушных судов»);

- engines-aviation regulations AP-33 «Airworthiness standards for aircraft engines» (АП-33 «Нормы летной годности двигателей воздушных судов»).

In terms of noise, the aircraft should not violate the requirements of the 4th chapter of the international standards the aircraft should not violate the requirements of the 4th

chapter of the international standards «Environmental protection» («Охрана окружающей среды») and the requirements of AP-36 (АП-36).

The aircraft must be designed according to the principle of "damage-safe".

The aircraft, equipment and systems, engines should be operated no more than the assigned resource.

The aircraft must provide flights:

- at different times of the day (night and day)
- in difficult and simple weather conditions;
- planted (seas and oceans) by space;
- over mountainous, hilly and flat terrain;

The design and location of cargo hatches must ensure the departure and access of ground vehicles for loading and unloading operations.

The cleanliness of the hydraulic system fluid should be controlled by filtration means (onboard).

The design of the hydraulic system must allow for the possibility of dismantling the units and filters, have a shorter resource than the corresponding resources of the airframe, without draining the fluid.

During the entire flight, the air temperature in the aircraft cabins must be maintained within 18...25°C. These temperatures must be obtained no more than 25 minutes after take-off.

Individual ventilation means must be provided for each passenger and crew members.

The design of the airframe of the aircraft must allow the installation of other similar engines, including foreign ones.

The fuel system must be free from the possibility of accumulation of contaminants in the fuel delivery elements and in the fuel tanks.

Means must be provided to ensure the survivability of the power plant in the event of a fire on the engine, as well as to protect the structure from fire.

In accordance with the requirements on board the aircraft, there must be provided and equipped places for placing a first-aid kit.

The design of the functional systems of the aircraft must ensure:

- certain goods for various types of control (visual, optical, organoleptic)
- easily removable and easy to connect connecting devices;
- the possibility of combining control objects with external control means.

Ground maintenance facilities must perform high-performance, high-quality maintenance, elimination of various kinds of malfunctions and search for problems, and efficiently carry out unloading and loading operations.

Ground refuelling facilities must exclude the possibility of contamination of the fuel, oil hydraulic systems.

The aircraft refuelling system should be linked to the characteristics of foreign refuelling systems.

The location of sensors and various external devices should not interfere with the joining of ladders of foreign designs.

The paints and varnishes used in the construction must allow the use of foreign liquids to remove icing from the surface of the aircraft.

1.1.3 Collection, processing and analysis of statistical data. Selection of the basic relative initial parameters of the aircraft.

Collection and processing of statistical data during aircraft design allows:

- to get a visual idea of the current level of development of aircraft construction of passenger aircraft and their flight performance;
- to determine the trends and development prospects of the type of aircraft being developed, quantitative and qualitative changes in the tactical and technical requirements to the aircraft, the conditions of production and operation.
- determine a number of aircraft parameters.

To collect statistical daytime data, it is necessary to use data from aircraft similar to those designed and have similar flight performance and operating conditions.

The following aircraft were taken as analogues aircraft: Airbus A220-100 (Figure 1.1); McDonnell Douglas MD 90 (Figure 1.2); Tupolev Tu 204-24 (Figure 1.3); Embraer E190-E2 (Figure 1.4).

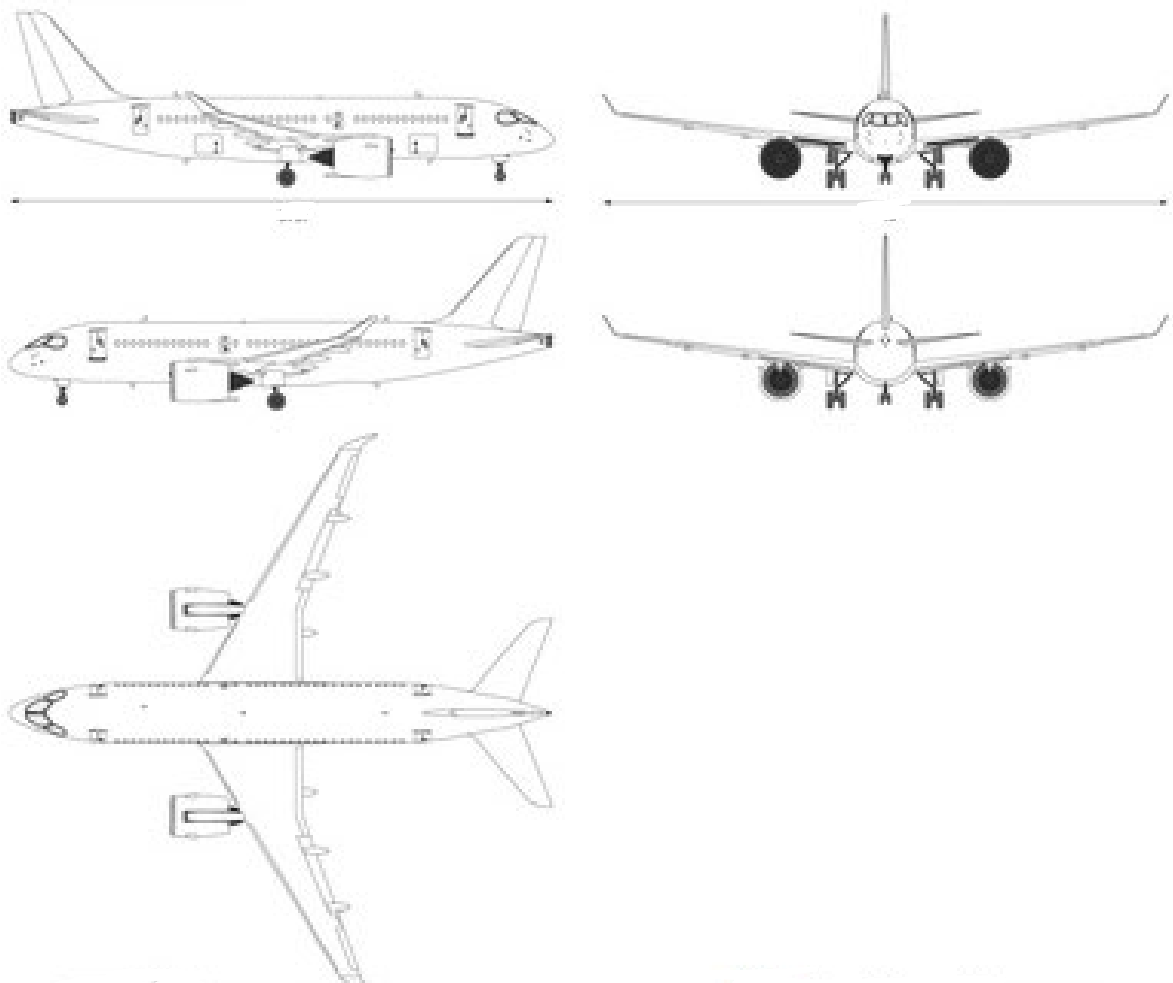


Figure 1.1 – Scheme of the Airbus A220-100

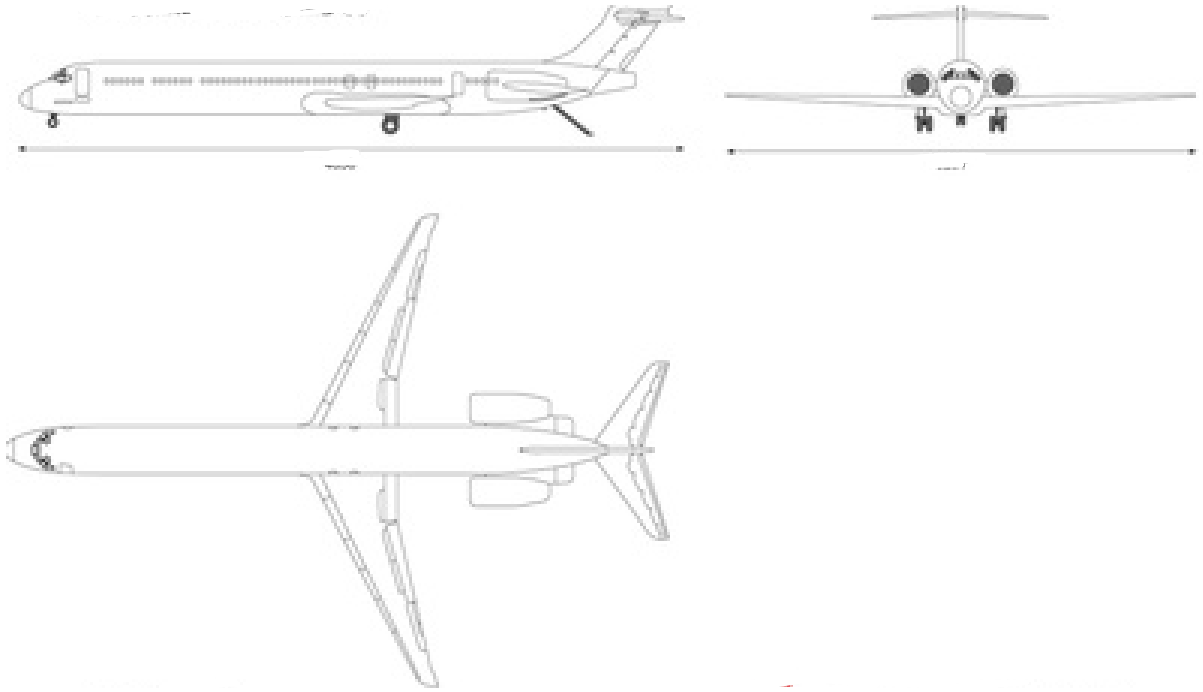


Figure 1.2 – Scheme of the McDonnell Douglas MD 90

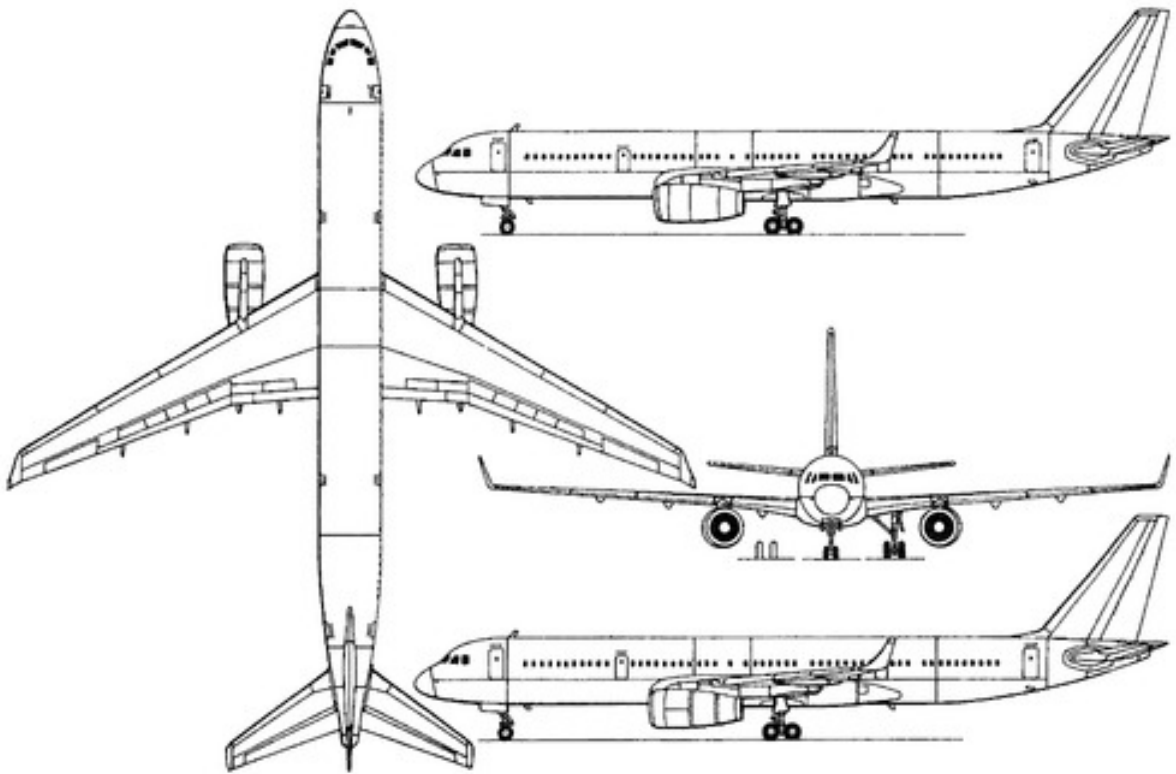


Figure 1.3 – Scheme of the Tupolev Tu 204-24



Figure 1.4 – Embraer E190-E2

Statistical data of analog aircraft are entered in table 1.1.

Table 1.1 – Statistics of similar aircraft and requirements for the designed aircraft

Parameters	The name of the aircraft				
	Airbus A220-100	McDonnell Douglas MD 90	Tupolev Tu 204-24	Embraer E190-E2	Projected Aircraft
Flight data					
V_{max} , km/h	870	940	900	880	870
H_{clg} , m	12000	11000	12000	12000	12000
V_{cruise} , km/h	840	860	850	830	840
H_{cruise} , m	12000	11300	12100	12000	12000
L , km	6400	3860	4340	5280	6400
L_{TO} , m	1500	2130	2030	1480	1500

End of table 1.1

Mass Characteristics					
$m_0(m_{TO}), \text{kg}$	50770	60390	78080	43080	
m_{0max}, kg	63100	70760	110750	56400	
m_e, kg	35300	40000	59000	33000	
m_f, kg	21800	17750	35700	13500	
m_{pl}, kg	15000	19000	25200	13700	
n_{pass}	120	155	200	110	120
n_{crew}	2	2	3	2	2
Power plant data					
Number, type, model of engines	2·Turbofan PW1500G	2·Turbofan IAEV2525-D5	2·Turbofan RB211-535E4B	2·Turbofan PW1919G	2·Turbofan
P_{0en}, kN	95	110	160	85	
m_{en}, kg	2800	2600	3700	2180	
Geometric data					
S, m^2	112	112	185	103	130
l, m	35	32	40	33	40
$\chi_{1/4}, \text{deg}$	30	30	30	30	30
λ	11	10	9	12	10
η	4	4	5	4	4
L_f, m	35	46	46	36	40
D_f, m	3.5	4	4.1	3.5	4

While planning another airplane, the issue emerges of picking its general plan. This is basically the underlying stage in the combination of an airplane plan. It is absurd to expect to formalize the choices made on this issue in full.

In any case, inside the system of currently carried out or proposed arrangements, sorting out a proper quest for the best arrangement as far as the assessment measure and the fulfilment of the undertaking of strategic and specialized prerequisites and specialized specifications is conceivable.

The decision of the general plan of the airplane implies not just the selection of its streamlined plan, in spite of the fact that it is conclusive in the execution of the standard of activity of the airplane, yet additionally the plan of the power plant, departure and landing gadgets, the situation of the team and the objective burden, and so forth.

The last decision of the general plan is produced using various contending choices in light of the streamlining of every one of them and further thorough examination. As an assessment rule for an airplane, we take its departure mass and as constraints - flight execution, determined strategic and specialized necessities and specialized details.

Subsequent to gathering measurable information, we continue to the advancement of strategic and specialized necessities. This stage will be done based on the examination of measurable materials, supplementing the predefined strategic and specialized necessities of the planned airplane. The Airbus A220 - 100 was taken as the prototype.

With crew member $n_{crew} = 2$ pers and flight range $L = 6400$ km. assign the run length $L_{TO} = 1500$ m.

The tactical and technical requirements are listed below in table 1.2.

Table 1.2 – Tactical and Technical Requirements of Projected Aircraft.

V_{max} (km/h)	V_{cruise} (km/h)	H_{clg} (m)	L (km)	L_{to} (m)	n_{pass}	n_{crew}
870	840	12000	6400	1500	120	5

1.1.4 Selection and justification of the scheme of the aircraft

Based on the tactical and technical assignment for the designed aircraft and the analysis of the statistical data, select (from all existing schemes) an aircraft of the classical scheme with a low swept wing, The tail of the normal scheme, located in the fuselage and consists of a single-fin vertical tail with a rudder and a horizontal tail with an elevator.

Justification of the selected aerodynamic design of the aircraft

After careful study of all aircraft selected to collect statistics, a normal aerodynamic scheme was chosen for the designed aircraft, as it provides the following advantages [1]:

- there are no parts in front of the wing that could obscure it when the position of the aircraft changes or disturb the air flow, disrupting the smooth flow around the wing and reducing its carrying capacity;
- placement of the tail of the wing allows you to shorten the nose of the fuselage, which improves visibility and reduces the area of the vertical tail;
- horizontal tail does not shade the wing.
- crew has better observation of the front semi-sphere.

Justification of the chosen wing location relative to the fuselage

The choice of wing location relative to the fuselage is primarily related to layout considerations. It is a low-wing monoplane. This arrangement has several advantages:

- during an emergency landing with the landing gear not extended, the impact is taken up mainly by the wing structure, protecting passenger and crew;
- during an emergency landing on water, the wing acts as a pontoon, together with the fuselage, ensuring the buoyancy of the aircraft;
- landing gear legs can be made short and as a result more durable and light mass; easier cleaning and release;
- when the engines are located on the wing, it is easier to access them, which makes it convenient to maintain the engines during operation.

The wing is swept, which has a number of advantages:

- the speed at which the wave crisis occurs increases and as a consequence less drag at transonic speeds compared to a straight wing;
- slow increase in lift depending on the angle of attack, which means better resistance to atmospheric turbulence.

For passenger aircraft, the most commonly used are two tail unit schemes: normal and T-shaped. The powerful accompanying flow from the propulsion system adversely affects the conventional low-lying horizontal tail assembly and may impair the stability of the aircraft in some flight modes.

Selecting the central tail structure as the engines are located in the middle of the fuselage, Thus, it is the most widespread wing. The elevator is in unperturbed airflow and remains stable in most flight modes.

Justification of the chosen power plant

It is advisable to install two engines for this aircraft. The refusal from one engine is explained by the fact that there are great difficulties with its scheme and also one engine does not satisfy flight safety. The use of three or more engines will weigh and complicate the design as a result of this the cost of the aircraft will increase.

The aircraft is equipped with two turbofan engine which are located on the rear fuselage. This arrangement has several advantages:

- easy maintenance of the engine and its replacement;
- provides less noise from engines in the passenger compartment;
- improving fire safety.

Justification of the chosen scheme of takeoff and landing devices

The main landing gear is located behind the aircraft's center of gravity, the additional strut is in the nose section. Since the spatial position of the aircraft on the ground and in the air is all the same, the jet stream from the engines is parallel to the ground, which protects the runway surface from damage [1]. Besides:

- lower risk of overturning (nosing) during heavy braking;
- lower risk of aircraft skidding due to inaccurate taxiing and crosswind;

- the aircraft is less prone to bouncing as the center of gravity is in front of the rear landing gear forces the aircraft to take a more horizontal position as a result of which the angle of attack and the lift acting on the aircraft are reduced;
- the view from the cockpit is better and the boarding and disembarkation of passengers and cargo handling is more convenient and safer.

According to statistical data, the main parameters of the wing are determined relative flap chord, flap deflection angles, relative aileron area, fuselage parameters, horizontal tail, vertical tail are listed below in table 1.3 [1]

Table 1.3 – Parameters of the airplane

λ	χ	η	λ_f	D_f	L_f	λ_{HS}	χ_{HS}	η_{HS}	λ_{VS}	χ_{VS}	η_{VS}
10	30	4	10	4	40	4	32	4	2	32	2

Based on the prototype's parameters, selected the following scheme for the projected medium-range jet aircraft with two turbofan engines (Figure 1.5).

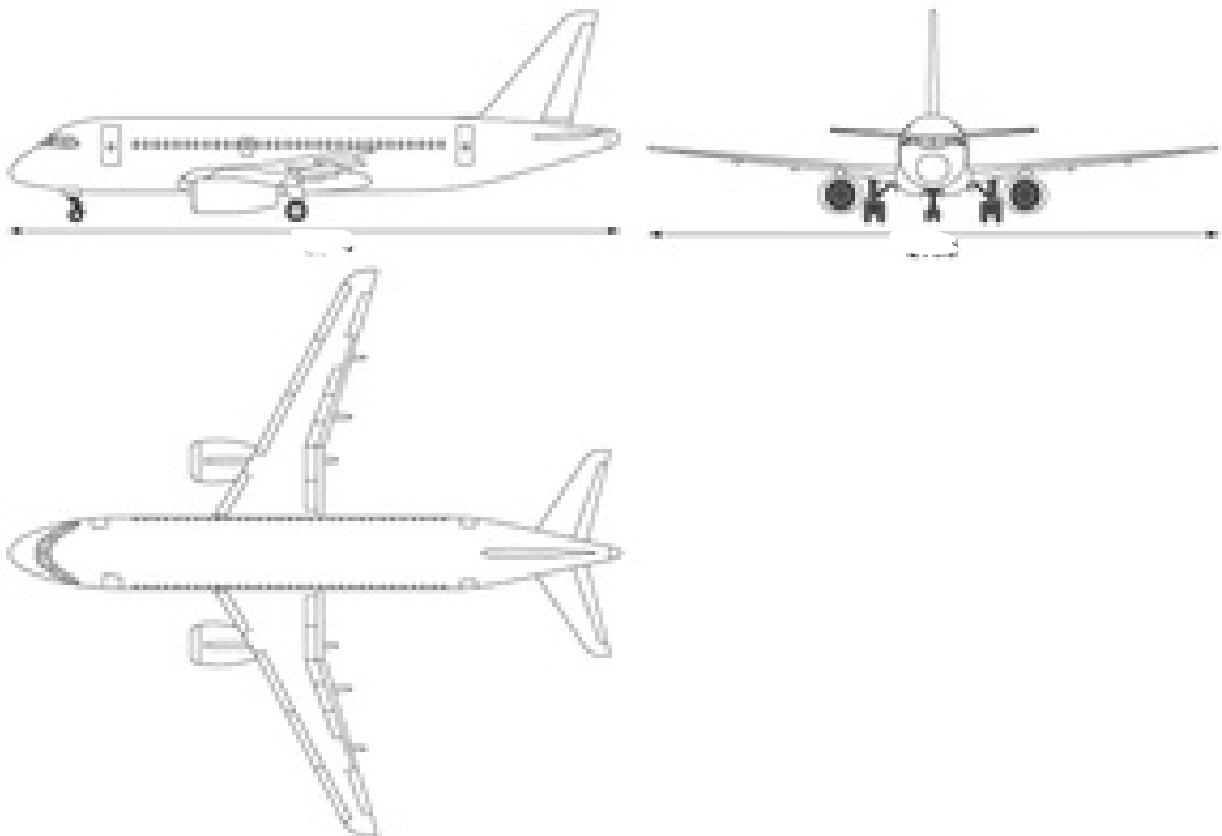


Figure 1.5 – Scheme of the designed aircraft

1.1.5 Calculation of aircraft mass in three approximations

1.1.5.1 Calculation of aircraft zero approximation mass

The takeoff mass of the aircraft in the zero approximation is determined after the choice of the aircraft scheme and is calculated by the formula [1].

$$m_0 = (m_{pl} + m_{crew}) / \left[1 - (\bar{m}_{airfrm} + \bar{m}_{pow.pl.} + \bar{m}_{fuel} + \bar{m}_{ctl.sys}) \right],$$

where m_{pl} – payload mass;

m_{crew} – mass of crew;

\bar{m}_{st} – relative structure mass;

\bar{m}_{PP} – relative power plant mass;

\bar{m}_{fuel} – relative fuel mass;

\bar{m}_{eq} – relative equipment mass.

The commercial load for a passenger aircraft will be determined from the condition that 150 kg of mass per passenger is required:

$$m_{pl} = 150 \cdot n_{pass} = 100 \cdot 120 = 18000 \text{ kg.}$$

The mass of the crew based on the condition that 100 kg of mass per crew member is required:

$$m_{crew} = 500 \text{ kg,}$$

The value of \bar{m}_{fuel} is determined by the formula:

$$\bar{m}_{fuel} = a + b \frac{L}{V_{CR}} = 0.26$$

where L – flight range, km; V_{CR} – cruising speed of the flight km/h.

Relative masses \bar{m}_{st} , \bar{m}_{PP} , \bar{m}_{eq} , for medium-range jet aircraft are in the following ranges of values:

Taking into account the range and purpose of the aircraft and assigning the following values of relative masses $\bar{m}_{st} = 0.28$; $\bar{m}_{PP} = 0.10$; $\bar{m}_{eq} = 0.10$.

The takeoff mass of the aircraft :

$$m_0 = (m_{pl} + m_{crew}) / \left[1 - (\bar{m}_{airfrm} + \bar{m}_{pow.pl.} + \bar{m}_{fuel} + \bar{m}_{ctl.sys}) \right],$$

$$m_0 = \frac{2280 + 504}{1 - (0.28 + 0.10 + 0.26 + 0.10)}$$

$$m_0 = 70000 \text{ kg.}$$

1.1.5.2 Calculation of structural mass of the main aircraft assemblies, power plant mass, fuel mass, mass of the equipment and control

Known the takeoff mass of the aircraft and the relative masses of the structure, power plant, fuel, equipment and control, find the masses:

- aircraft structure mass:

$$m_{st} = 19600 \text{ kg;}$$

- wing mass;

$$m_{wing} = 27370 \text{ kg};$$

- fuselage mass;

$$m_{fus} = 24990 \text{ kg};$$

- tail unit mass;

$$m_{TU} = 4970 \text{ kg};$$

- landing gear mass;

$$m_{LG} = 12670 \text{ kg};$$

- fuel mass;

$$m_{fuel} = 18200 \text{ kg};$$

- power plant mass;

$$m_{pp} = 7000 \text{ kg};$$

- equipment mass;

$$m_{eq} = 2700 \text{ kg}.$$

All values of masses are entered in table 1.4.

Table 1.4 – Masses of the aircraft parts and units

m_0 (kg)	m_{pl} (kg)	m_{crew} (kg)	m_{airfr} (kg)	m_{wing} (kg)	m_{fus} (kg)	m_{tail} (kg)	$m_{L/G}$ (kg)	m_{fuel} (kg)	m_{pp} (kg)	m_{eng} (kg)
70000	18000	500	19600	27370	24990	4970	12670	18200	7000	2700

There should be an approximation separation. Since it is not clear which calculations will be performed further.

1.1.5.3 Determination of takeoff mass of the aircraft in the first approximation.

Investigation of the influence of wing aspect ratio on the aerodynamic and mass characteristics of the aircraft.

The main difference between this calculation and the calculation m_0^0 is based on the dependency of \bar{m}_c , \bar{m}_{fuel} , \bar{m}_{eq} from the takeoff mass of the aircraft, wing parameters

and other parts of the aircraft from the flight mode. Because of \bar{m}_c rather difficult depends on the takeoff mass, then it has to be calculated \bar{m}_0^1 apply either a graphical method of solving the equilibrium mass balance of the aircraft, or sequentially approach the solution and find it using a computer.

Table 1.5 – Initial Data for the Calculation

№	Relative parameter	Name	Marking	Size
Wing high-lift device				
1	C_y increases by lift devices	DCY	$\Delta \bar{C}_{y l. dev}$	2.2
2	Flap relative span	LZ	\bar{l}_{fl}	0.7
3	Flat relative chord	BZ	\bar{b}_{fl}	0.35
4	Flap relative chord (Table)		$\bar{b}_{fl, tab}$	0.3
5	Flap quality factor	KZ	k_{fl}	0.15
6	Flap takeoff deflection angle	DZB	$\delta_{fl, TO, deg}$	25
7	Flap takeoff deflection angle (table)		$\delta_{fl, TO, Tabl, deg}$	45
Initial data				
1	Airfoil relative thickness	C	$\bar{c}, \%$	12
2	Takeoff angle of attack	AOT	$\alpha_{TO, deg}$	12
3	Load on middle	KMI	$K_{mid}, daN / m^2$	3000
4	Relative height of the wing (B_{mac})	HOT	\bar{h}	0.8
5	Wing aspect ratio	LKR	λ_w	10
6	Takeoff mach number	MOT	M_{TO}	0.18
7	Wing interference coefficient	KIN	$k_{int, w}$	0.65
8	Relative wingspan	LOT	\bar{l}	7
9	Wing taper ratio	TK	η	4
10	Fuselage diameter	DF	d_{fus}, m	4
11	Wing sweep on the leading edge	XP	χ_{le}, deg	30
12	Fuselage fineness ratio	LF	λ_{fus}	10
13	Payload ratio	KOTD	k_{pl}	0.25
Engine				
1	Engine type	TIP		Turbofan
2	Number of engines	ND	$n_{eng, itm}$	2
3	Air intakes thrust decrease	ZW	ζ_{int}	0.98
4	Mach number at cruising speed	MX	M_{cr}	0.85
5	Engine mode in cruise flight	ZD	$\zeta_{tr, cr}$	0.6
6	Engine mode at takeoff	ZDO	$\zeta_{tr, TO}$	0.95
7	Initial cruising altitude	HN	H_{init}, km	12
8	Final cruising altitude	HK	H_{fin}, km	12
9	Engine bypass ratio	DM	y	8

Effect of aspect ratio of the wing on lift coefficient and lift quality

The lift coefficient at takeoff is determined by the formula [2]:

$$C_{y_{t.off}} = C_{y_w}^{t.off} \left(1 + \Delta \bar{C}_y \frac{\delta_{flap.t.off}}{\delta_{flap.tab}} \cdot \frac{\bar{b}_{flap}}{\bar{b}_{flap.tab}} \cdot \bar{S}_{mech}^{t.off} \cdot \cos^2 \chi_{0,75} \right) + \Delta C_{y_{land}} + \Delta C_{y_{oda}},$$

where $C_{y_w}^{t.off}$ – the lift coefficient of the wing during takeoff without use of mechanization;

$\Delta \bar{C}_y$ – increase in lift factor dur to use of mechanization of the wing;

$\delta_{flap, t.off}$ - angle of deviation of flap at takeoff;

$\delta_{flap, tab}$ - relative chord of flap;

$\bar{b}_{flap.tab}$ - relative chord of flap;

\bar{b}_{flap} – relative chord flap;

$\bar{S}_{mech}^{t.off}$ - the relative area of the console serviced by mechanizations;

$\chi_{0.75}$ – sweep of 0.75 chords in the area of mechanization;

$\Delta C_{y_{land}}$ – an increase in the lift coefficient due to the impact of the earth.

The increase in lift due to the impact of the earth can be estimated by the formula [2]:

$$\Delta C_{y_{land}} = 0.313 - 0.237\bar{h} + 0.0572(\bar{h})^2.$$

The derivative of the lift coefficient for the angle of attack for the aircraft in the flight configuration is determined by:

$$C_y^\alpha = \frac{0.11 - 0.029\sqrt[4]{\bar{c}}}{\frac{0.0775}{\cos \chi_{0.25}} + \lambda},$$

where \bar{c} – relative thickness of the profile;

$\chi_{0.25}$ – wing sweep angle of 25%chord;

λ – aspect ratio of the wing.

According to the results of calculation, graphs were constructed.

The initial data for the calculation from university program:

According to the results of the calculation, the graphs of the dependences of the lift coefficient on aspect ratio of the wing (Figure 1.6) and the quality of the aircraft

from the specific load on the wing (Figure 1.7) are constructed for the wings, which are the most suitable according to the collected statistics of analog aircrafts.

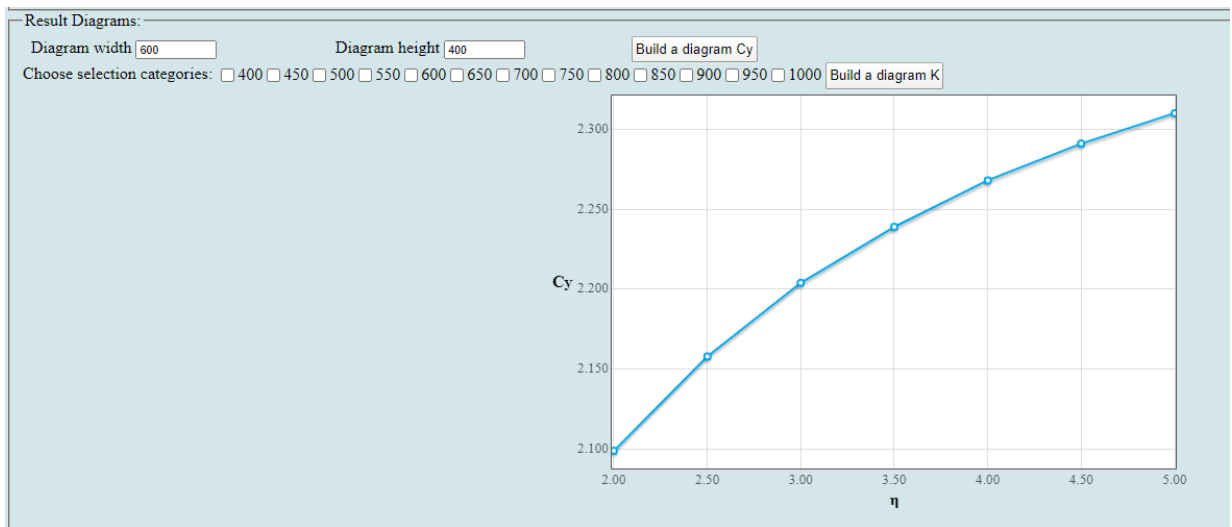


Figure 1.6 – Dependence of lift coefficient on aspect ratio of the wing

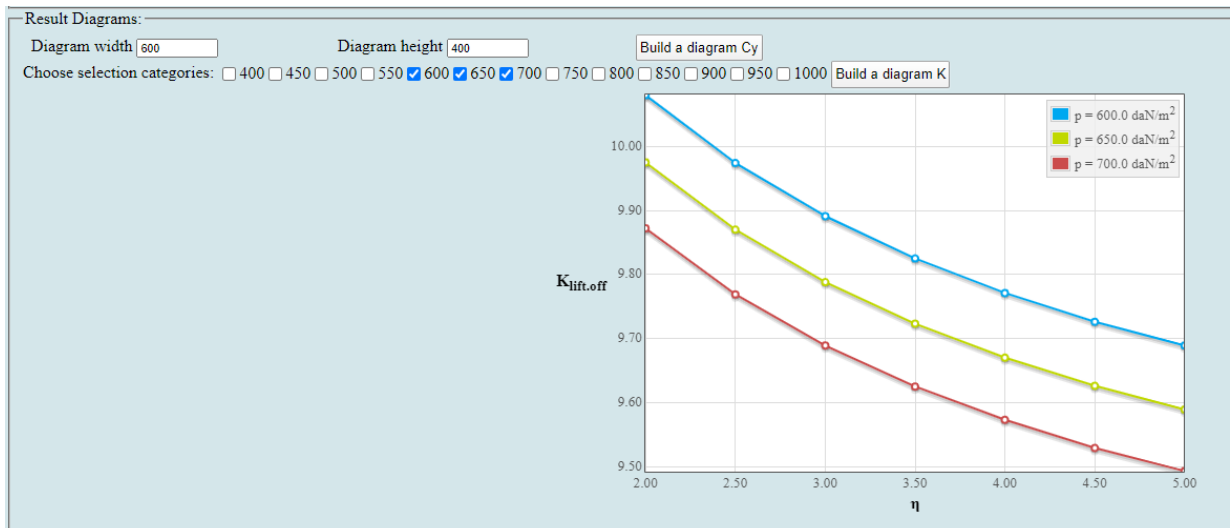


Figure 1.7 – Dependence of takeoff quality on specific wing loading for different values of aspect ratio of the wing

As the wing lengthens, the lift coefficient increases, when the value of aspect ratio of wing exceeds 6, the growth rate of the lift coefficient slows down and gradually approaches the limit. As the wing load increases, the quality decreases, and there is a linear dependence between specific wing loading and aerodynamic quality during lift-off. But with higher aspect ratio, the quality is relatively higher.

Investigation of the effect of aspect ratio of the wing on the magnitude of thrust-weight ratio

To study the effect of wing aspect ratio on arms draft, use the following dependencies:

$$t_{0cruise} = \frac{0.933 p_H M_{cruise}^2}{\xi_{cruise}} \left(\frac{F_1}{p} + F_2 \right);$$

$$t_{0t.off} = \frac{1}{\xi_{t.off}} \left(\frac{0.832p}{C_{yt.off} L_{rol}} + \frac{1}{3} \left(\frac{1}{K_{t.off}} + 2f \right) \right);$$

$$t_0 = \frac{n_{eng}}{\xi_{t.off} (n_{eng} - 1)} \left(\frac{1}{K_{t.off}} + tg(\theta_{flap}) \right),$$

where p_H – pressure at cruise altitude;

F_1, F_2 – coefficient changes in traction, windshield resistance and plumage, fuselage windshield and nacelle [3].

According to the results of the calculation, the graphs of the dependences of the starting thrust-to-weight ratio, determined by the take-off run, take off safety and cruising flight speed at aspect ratio of the wing are constructed (Figure 1.8).

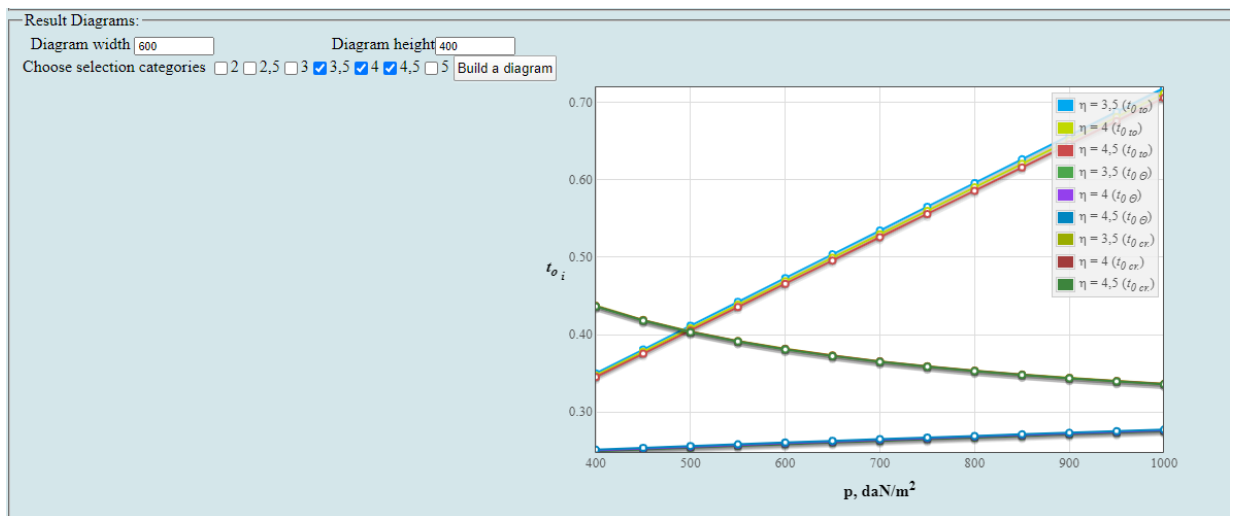


Figure 1.8 – The thrust-to-weight ratio acting on wing and high lift devices.

As the specific load on the wing increases, the starting thrust-to-weight ratio is provided, which provides the lifting capacity, the runway length, the given angle of climb, and the energy due to the cruise speed of flight – decreases. As the wing lengthens, the starting energy, determined by the cruise speed, increases in all other modes.

Determination of the influence of wing aspect ratio on the value of the relative mass of the power plant

The relative mass of the power plant determined by the formula [1]:

$$\bar{m}_{pp} = R\gamma_{eng}t_{max},$$

where R – coefficient of increase in mass of power plant compared to the mass of the engine;

γ_{eng} - specific mass of the engine;

t_{max} – the highest starting value thrust-to-weight ratio.

According to the results of the calculation, the graphs of the dependences of the starting thrust-to-weight ratio (Figure 1.9) and the relative mass of the power plant (Figure 1.10) on the specific load of the wing are constructed.

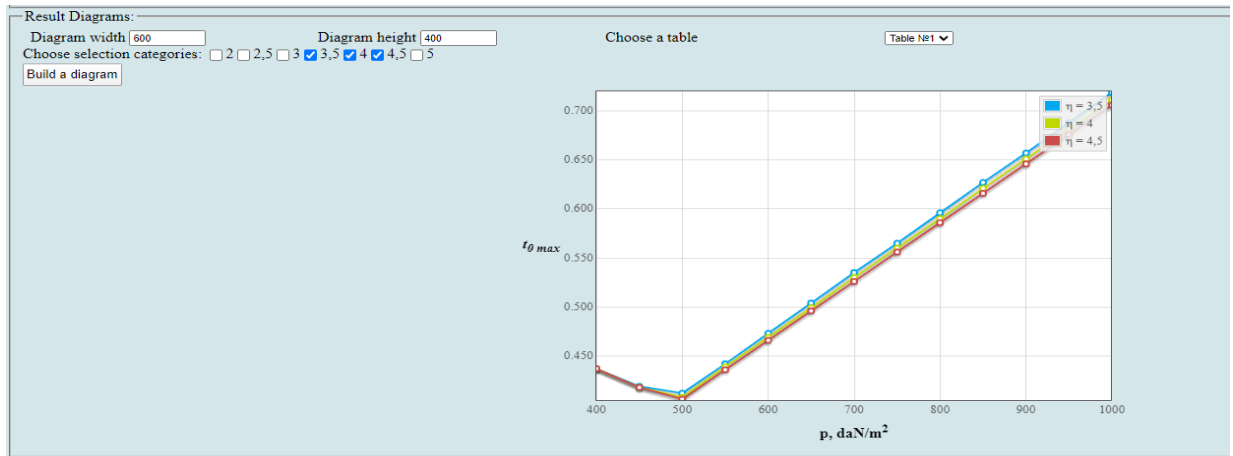


Figure 1.9 – Dependence of the starting thrust-to-weight ratio on the specific load of the wing for different values of the wing aspect ratio

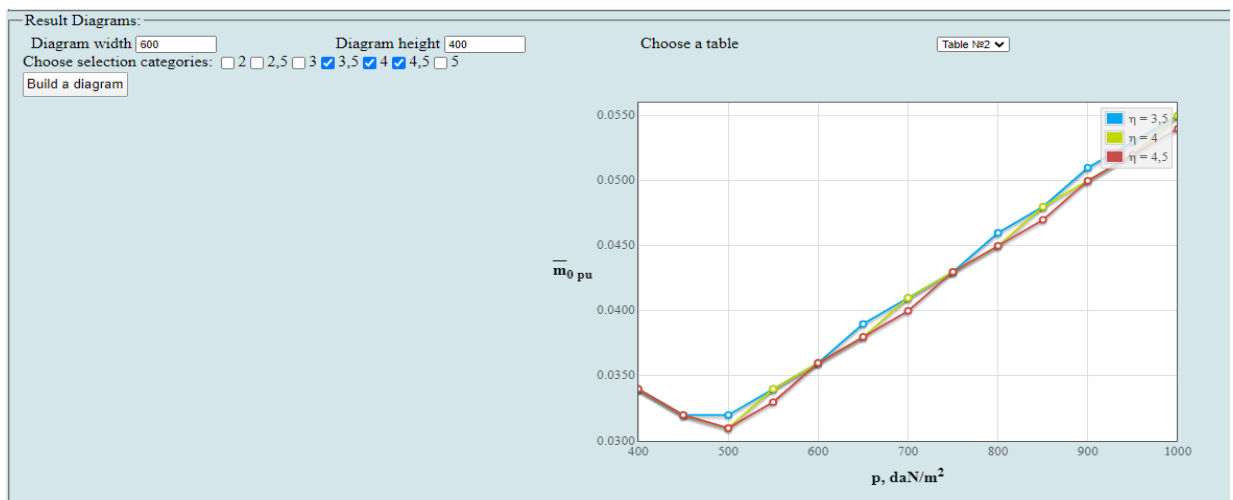


Figure 1.10 – Graph of the dependence of the relative mass of the power plant on the specific load on the wing for different values of the wing aspect ratio

The graphs show that the thrust-to-weight ratio and the relative mass of the power plant basically remain unchanged, as the load increases, thus the most favourable values of the specific load, that they increase with the load and has a linear relationship.

Effect of wing aspect ratio on the value of the relative mass of fuel

The graph of the dependence of the relative fuel mass on the value of the specific wing loading and wing aspect ratio is shown in Figure 1.11.

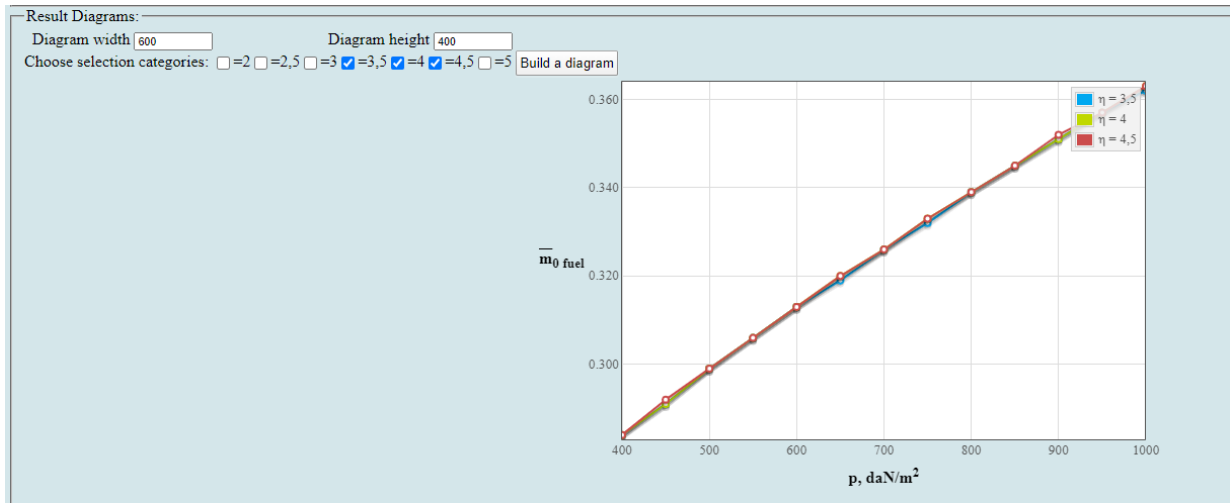


Figure 1.11 – Dependence of the relative fuel mass on the specific load and relative wing aspect ratio

Relative mass of the fuel increases with the increase in the specific load on the wing, and there is a linear dependence between specific wing loading and relative fuel mass. As the lengthening increases, the relative mass of the fuel decreases.

Effect of wing aspect ratio on the relative mass of the wing

The graph of the Effect of wing aspect ratio on the relative mass of the wing is shown in Figure 1.12.

According to the results of the calculation, the graph of the dependences of the relative mass of wing (Figure 1.12) on the specific load of the wing at aspect ratio of the wing are constructed.

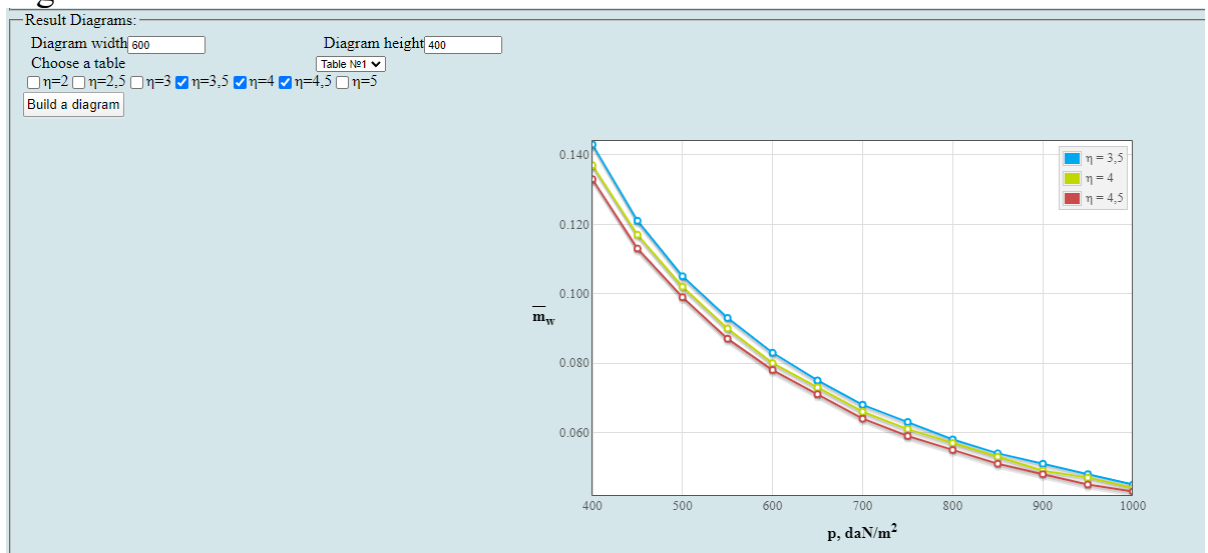


Figure 1.12 – Dependence of the relative wing mass on the specific load on the wing and the relative wing aspect ratio

With an increase in the specific loading on the wing, the relative wing mass decreases, the rate of decrease of the wing relative mass gradually tends to be slope. With an increase in aspect ratio, the relative mass of the wing increases.

Effect of fuselage aspect ratio and diameter on the mass of the fuselage

The graph of the effect of fuselage aspect ratio and diameter on the mass of the fuselage is shown in Figure 1.13.

According to the results of the calculation, the graphs of the dependences of the relative mass of the fuselage on its diameter and aspect ratio (Figure 1.13) are constructed.

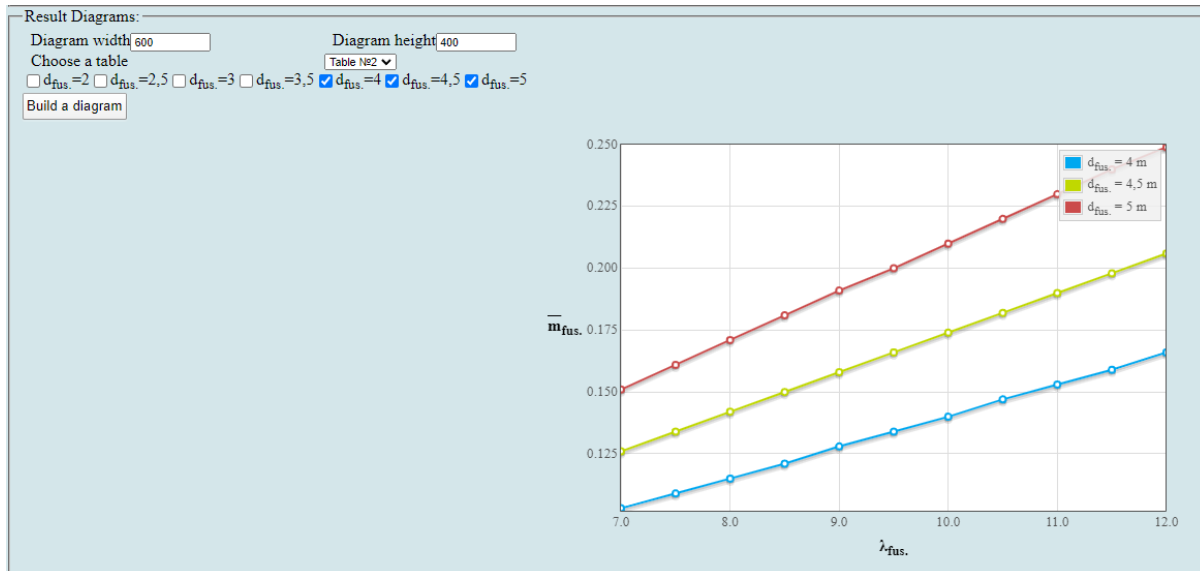


Figure 1.13 – Dependence of the relative mass of the fuselage on its diameter and aspect ratio

With an increase in the fuselage aspect ratio, the relative mass of fuselage decreases, and there is a linear relationship between the fuselage aspect ratio and the relative mass of fuselage. As the fuselage diameter increases, the relative mass of the fuselage increases.

Dependences of the relative mass of the tail unit on the specific load on the wing

The graph of the relative mass of the tail unit on the specific load on the wing is shown in Figure 1.14.

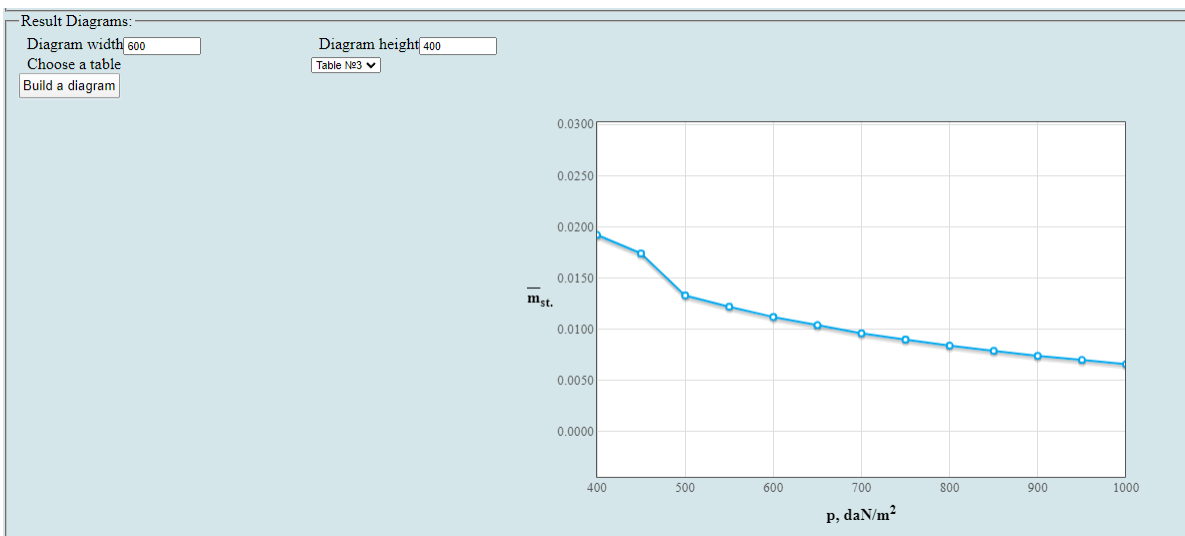


Figure 1.14 – Dependence of the relative mass of the tail unit on the specific load on the wing

As the specific load on the wing increases, the relative mass of the tail unit decreases, and the rate of decrease in relative mass of tail unit gradually tends to be flat.

Calculation of the relative mass of the landing gear

The relative mass of the landing gear is determined by Fadeev's formula [4]:

$$\bar{m}_{LG} = k_{LG} \cdot k_{FD} \cdot \frac{m_{p.load}/k_{pl} + 204000}{m_{p.load}/k_{pl} + 79000},$$

where $k_{FD} = 0.02728$ – coefficient taking into account the influence of fuselage diameter and engine type on the weight of the landing gear;

$k_{LG} = 1$ – coefficient taking into account the number of main landing gear posts;

$k_{pl} = 0.25$ – the return ratio coefficient.

$$\bar{m}_{LG} = 0.049$$

Determination of crew mass, equipment and commercial load

The mass of the crew is determined by its number, depending on the type of aircraft. The mass of one crew member is 100 kg.

So:

$$m_{crew} = 100 \cdot n_{crew},$$

where n_{crew} – the number of crew members, including the flight attendants.

$$m_{equip} = 100 \cdot n_{pas} \cdot (5 \cdot 10^{-5} \cdot L_{tech} = 0.66)$$

where technical range is defined in kilometers:

$$L_{tech} = (L+700)$$

Given $L = 6400$ km, $n_{pas} = 120$ then

$$m_{equip} = 11571 \text{ kg};$$

Total mass of the airplane load

$$m_{c.e.p} = 23971 \text{ kg}$$

<p>Calculation results:</p> <p>$m_{cr.} = 400(\text{kg}); m_{eq.} = 11571(\text{kg}); \text{Total mass of airplane load} - m_{c.e.p} = 23971(\text{kg})$</p>

Figure 1.15 – Total mass of airplane load

Further, the value is used in the calculations of the take-off mass of the aircraft as one of the initial.

1.1.5.13 Take-off mass of the aircraft in the first and second approximation

The take-off mass of the aircraft in the first approximation is determined by the formula obtained from the equation of relative masses:

$$m_0^1 = \frac{m_{crew} + m_{equip} + m_{p.load}}{1 - (\bar{m}_{str} + \bar{m}_{p.pl} + \bar{m}_{fuel})}$$

where $m_{c.e.p} = m_{crew} + m_{equip} + m_{pl}$ - total mass of crew, equipment and commercial load

\bar{m}_{str} , $\bar{m}_{p.pl}$, \bar{m}_{fuel} - relative mass of the structure, power plant and fuel.

The dependency of takeoff mass on specific wing load and wing aspect ratio was presented in Figure 1.16.

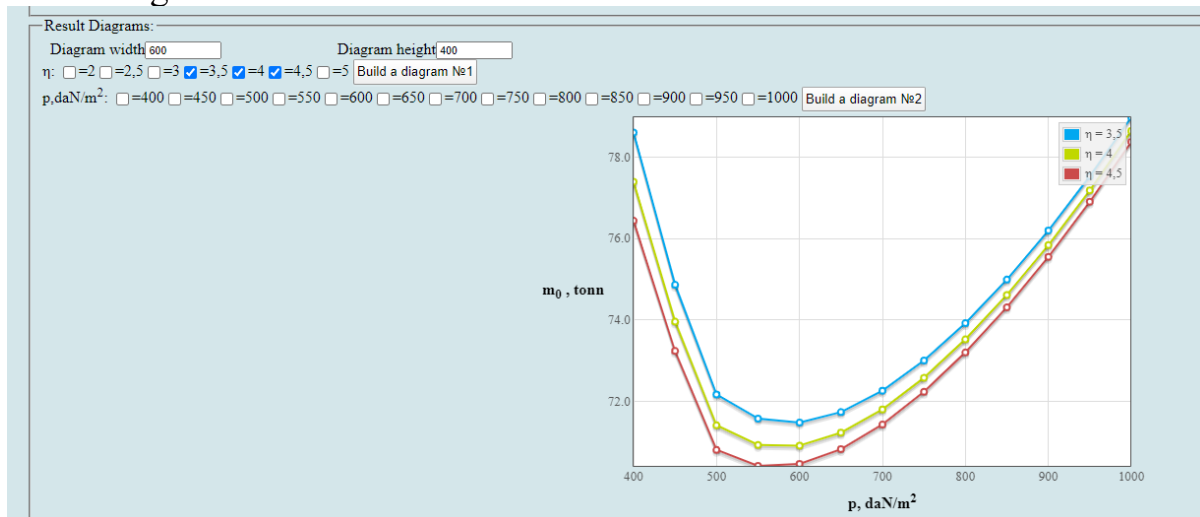


Figure 1.16 - Dependence of the take-off mass of the aircraft in the first approximation

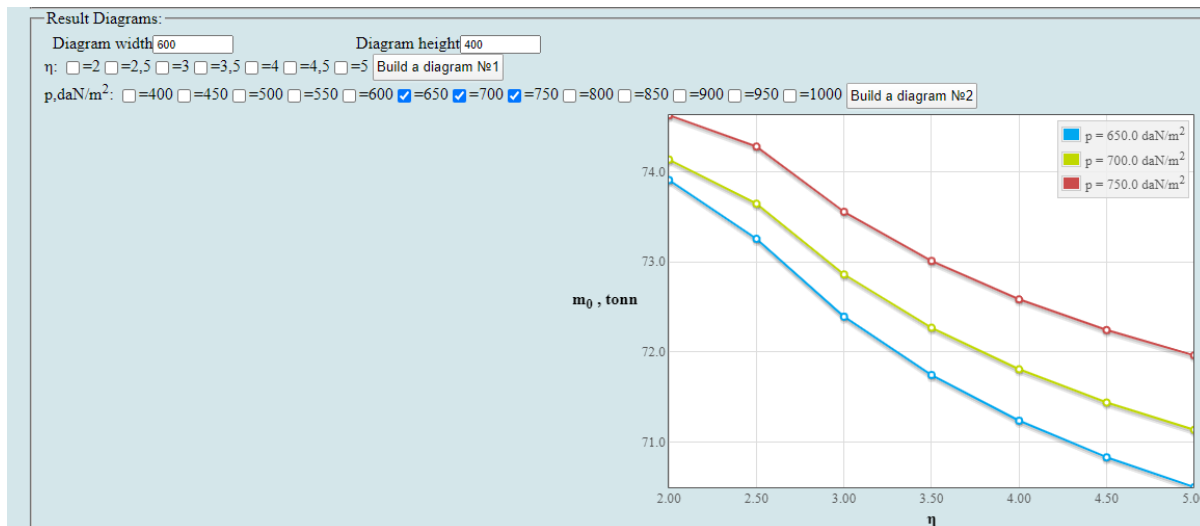


Figure 1.17 - Graphs of the dependence of the take-off mass of the aircraft from the specific load on the wing for various aspect ratio

Restrictions on specific load and determine the mass

To accept the minimum mass m_0 and P_{opt} it is necessary to limit the specific load on the wing at landing speed P_{lim}^{vland} and the magnitude of normal overload when flying in a turbulent atmosphere P_{lim}^{ny} .

Limitations can be defined by the formula [7]:

$$P_{lim}^{V_{land}} = \frac{V_{land}^2 \cdot C_{y,land}}{180(1-0.8 \cdot \bar{m}_{fuel})}$$

where $V_{land} = 250$ km/h; $\bar{m}_{fuel} = 0.26$; $C_{y,land} = 2.2$; then

$$P_{lim}^{V_{land}} = 250^2 \cdot 2.2 / 180(1-0.8 \cdot 0.26)$$

$$P_{lim}^{V_{land}} = 964.506 \text{ daN} / \text{m}^2;$$

Specific load limitation on the value of normal load when flying in a turbulent atmosphere P_{lim}^{ny} is calculated by the formula:

$$P_{lim}^{ny} = 3.6 C_y^\alpha \cdot V \cdot W$$

where C_y^α – the derivative of the lift coefficient on the angle of attack is determined by the formula.

$$C_y^\alpha = \frac{0.11 - 0.029 \sqrt[4]{c}}{\frac{0.0775}{\cos \chi_{0.25}} + \lambda}$$

V – ground speed = 360 km/hr; W – upstream speed = 15 m/s.

$$C_y^\alpha = \frac{0.11 - 0.029 \cdot \sqrt[4]{12}}{\frac{0.775}{\cos(35)} + \frac{2}{10}} = 0.049$$

$$P_{lim}^{ny} = 3.6 \cdot 0.049 \cdot 100 \cdot 15 = 264 \text{ daN} / \text{m}^2$$

For the designed aircraft, the preferable wind load is 500 daN/m² when the wing aspect ratio value is 10, since such values of the wing load and wing aspect ratio give the aircraft the smallest takeoff mass of 41900 kg.

1.1.5.4 Determination of mass of the power plant

To determine the mass of the power plant uses the formula [1]:

$$m_{p.pl}''' = R \cdot m_{eng} \cdot n_{eng}$$

where n_{eng} – number of engines installed on the aircraft; m_{eng} – the mass of the engine indicated on his passport, kg; R – factor taking into account the increase in the mass of the power plant compared to the mass of the engine;

$$R = K_1 \left(1 + k_{rev.noise} \frac{n_{eng.revers}}{n_{eng}} \right) \left[k_{afterburn} + \frac{k_{air-int}}{Y_{eng}} (1.2 + 0.275y^{0.75})^2 \right]$$

where $k_1 = 0.95$ – a factor that takes into account the number of engines and the location of their installation on the aircraft; $k_{rev.noise} = 0.15$ – coefficient accounting presence of thrust reverser and noise suppression; $n_{eng.revers} = 2$ – number of engines with thrust reverse; $k_{afterburn} = 1$ – coefficient accounting afterburning of engines; $k_{air-int} = 0.0236$ – coefficient taking into account the type of air collectors and engine pipe; $\gamma_{eng} = 0.238$ – passport specific weight of the engine; $y = 8$ – a measure of the double contour of the engine specified in its passport;

$$m'''_{pp} = 4.93 \cdot 1350 \cdot 2 = 13311 \text{ kg}$$

Determination of fuel mass

The mass of the fuel is determined by the formula[1]:

$$m'''_{fuel} = m''_0 \bar{m}'''_{fuel},$$

here m'''_{fuel} – the take-off mass of the aircraft in the second approximation; \bar{m}'''_{fuel} – the relative mass of the fuel in the third approximation, which is defined below;

$$\bar{m}'''_{fuel} = \bar{m}_{fuel-climb} + \bar{m}_{fuel-cruis} + \bar{m}_{fuel-reserv} + \bar{m}_{fuel-land} + \bar{m}_{fuel-remain}$$

where $\bar{m}_{fuel-climb}$ – the relative mass of fuel consumed by climbing; $\bar{m}_{fuel-cruis}$ – the relative mass of fuel consumed in a cruise flight; $\bar{m}_{fuel-reserv}$ – the relative mass of the navigation stock of the fuel; $\bar{m}_{fuel-land}$ – the relative mass of fuel consumed for reduction and landing; $\bar{m}_{fuel-remain}$ – relative mass of other unaccounted fuel reserves; $\bar{m}_{fuel-remain} = 0.006$;

$$\bar{m}_{fuel-climb} = \frac{0.0035 H_{init} (1 - 0.03y)}{1 - 0.004 H_{init}}$$

$$\bar{m}_{fuel-land} = 0.002 H_{end} (1 - 0.03y) (1 - 0.023 H_{end}),$$

here $H_{init} = 12$ – starting cruising altitude, km; $H_{end} = 13$ – end altitude of cruise flight, km; $y = 3$ – bypass ratio;

The relative mass of fuel for cruise flight and navigation reserve is determined by formula:

$$\bar{m}_{fuel-cruis} = 1 - \exp \left[- \frac{(L - L_{climb-desc}) C_{pcruis} \sqrt{AC_{x_0}}}{1.8(a_H M_{cruis} - 0.28W)} \right]$$

$$\bar{m}_{fuel-reserv} = 1.8 C_{pcruis} \sqrt{AC_{x_0}},$$

Here L – flight range in km, specified in performance requirements; $L_{climb-desc}$ – horizontal flight range during climbing, accelerating and descending, km, $L_{climb-desc} = 40H_{over}$, H_{over} – cruising averaged altitude, $H_{over} = (H_{init} + H_{end})/2$, km; M_{cruis} – cruising Mach number M , corresponding to cruising speed, the longest flight range and flight duration; W – head wind speed: H is in 10...12, km, $W=70$ km/h; C_{pcruis} – fuel specific consumption of selected engine at cruising altitude and flight speed (ratings), kg/daN; A – polar curve coefficient; C_{x0} – drag coefficient at zero lift.

The mass of the fuel in the third approximation:

$$m_{fuel}''' = 41900 \cdot 0.472 = 19776.8 \text{ kg}$$

1.1.5.5 Determination of the takeoff mass of the aircraft in the third approximation

The takeoff mass of the aircraft in the third approximation determined by the following equation[4]:

$$m_0''' = m_w'' + m_{fus}'' + m_{TU}'' + m_{LG}'' + m_{crew} + m_{eq.ctl}'' + m_{p.pl}''' + m_{fuel}''' + m_{p.load}''$$

where $m_w'' + m_{fus}'' + m_{TU}'' + m_{LG}''$ – respectively the mass of the wing, fuselage, plumage, chassis taken as a result of the calculation of the second approximation; $m_w'' = 27370$ kg; $m_{fus}'' = 24990$ kg; $m_{TU}'' = 4970$ kg; $m_{LG}'' = 12670$ kg;

m_{crew} – mass of the crew = 500 kg;

m_{eq}''' – mass of the equipment = 2700 kg;

m_{pp}''' – mass of the power plant = 7000 kg;

m_{fuel}''' – mass of the fuel = 19776.8 kg;

m_{pl} – mass of the commercial load = 18000 kg.

$$m_0''' = 27370 + 24990 + 4970 + 12670 + 500 + 2700 + 7000 + 19776.8 + 18000 = 117977 \text{ kg.}$$

1.1.6 Selection of engines and checking of run length

Based on the graphs, when the wing aspect ratio value is 10, the value of the wing load is 500 daN / m², obtained the smallest takeoff mass of the aircraft, which is 41900 kg.

$$P_{0dem} = \frac{g \cdot m_0'' \cdot t_{0opt}}{10 \cdot n_{eng}}$$

where $m_0'' = 41900$ kg – aircraft takeoff mass; $t_{0opt} = 0.29$ – starting thrust-to-weight ratio; $n_{eng} = 2$ – number of engines.

$$P_{0dem} = 93.53 \text{ kN}$$

According to the catalog, the turbofan engine Rolls-Royce BR.183 Tay without afterburning configuration is selected, which has the following characteristics:

$P_0 = 95 \text{ kN}$ – nominal maximum thrust;

$m_{\text{eng}} = 1400 \text{ kg}$ – engine dry weight;

$L_{\text{eng}} = 3184 \text{ mm}$ – engine length;

$D_{\text{eng}} = 2006 \text{ mm}$ – engine diameter;

$y = 12 : 1$ – bypass ratio;

Calculation of the required takeoff length before takeoff:

$$L_{t.off} = \frac{0.832 \cdot p_{opt}}{C_{yt.off} [\xi_{t.off} t_0 - \frac{1}{3} (\frac{1}{K_{t.off}} + 2f)]}$$

where $\xi_{t.off} = \xi_V \xi_H \xi_{air} \xi_{rest}$ – coefficient taking into account the dependence of engine thrust on speed and altitude - $\xi_V = 0.86$, $\xi_H = 1$; traction drops due to pressure loss in the air intakes - $\xi_{air} = 0.96$, engine operating mode $\xi_{rest} = 0.95$; pneumatic friction coefficient $f = 0.02$; the optimal wing load $p_{opt} = 500 \text{ daN/m}^2$; the lift – to – drag ratio at takeoff $K_{t.off} = 8.47$ and lift coefficient at takeoff $C_{yt.off} = 1.13$, thrust-to-weight ratio at takeoff $t_0 = 0.29$, then

$$L_{t.off} = 1971 \text{ m}$$

Given, $L_{t.off.calc} < L_{t.off.nom}$, this engine provides a given takeoff run length, which is 1500 m.

1.1.7 Determination and optimization of design parameters of the aircraft and its units

1.1.7.1 Determination of the geometric parameters of the wing

The area of the wing is determined by the formula [1];

$$S = m_0 \cdot g / 10 \cdot p_0 = 130 \text{ m}^2$$

Wingspan :

$$l = \sqrt{\lambda \cdot S} = \sqrt{10 \cdot 130} = 36.05 \text{ m.}$$

Root b_0 and b_{tip} end chords of the wing determined based on the values η , l , S . $\eta = 4$ - wing taper ratio.

$$b_0 = 2\eta \hat{S}_{wing} / L_{wing} (\eta + 1);$$

$$b_0 = 5.2 \text{ m}$$

$$b_{\text{tip}} = b_0/\eta.$$

$$b_{\text{tip}} = 1.3 \text{ m}$$

The mean aerodynamic chord (MAC) is calculated:

$$b_A = \frac{2}{3} \cdot b_0 \cdot \frac{\eta^2 + \eta + 1}{(\eta + 1) \cdot \eta}$$

$$b_A = 3.64 \text{ m}$$

Determine the coordinate of the MAC by the wingspan:

$$Z_A = \frac{l}{6} \cdot \frac{\eta + 2}{\eta + 1}$$

$$Z_A = 7.21 \text{ m}$$

The coordinate of the beginning of the MAC along the axis OX is determined:

$$X_A = \frac{l}{6} \cdot \frac{\eta + 2}{\eta + 1} \cdot \text{tg} \chi_{l,e}$$

$$X_A = 4.15 \text{ m.}$$

1.1.7.2 Determination of geometric parameters of the fuselage

Fuselage length:

$$L_f = \lambda_f \cdot d_f = 40 \text{ m.}$$

Fuselage nose length:

$$L_{np} = \lambda_{np} \cdot d_{nf} = 6.5 \text{ m}$$

Fuselage tail length:

$$L_{tp} = \lambda_{tp} \cdot d_{af} = 13.5 \text{ m}$$

1.1.7.3 Determination of the geometric parameters of the horizontal tail (HT)

HT area:

$$S_{HS} = S_{HS} S .$$

$$S_{HS} = 33 \text{ m}^2$$

HT span:

$$L_{HS} = \sqrt{\lambda_{HS} S_{HS}} .$$

$$L_{HS} = 12.5 \text{ m}$$

HT root chord:

$$b_{OHS} = \frac{2S_{HS}}{L_{HS}} \frac{\eta_{HS}}{\eta_{HS} + 1} .$$

$$b_{OHS} = 4.24 \text{ m}$$

HT tip chord:

$$b_{KHS} = b_{OHS} / \eta_{HS} .$$

$$b_{KHS} = 1.056 \text{ m}$$

HT MAC:

$$b_{AHT} = \frac{2}{3} \cdot b_{root.HT} \cdot \frac{\eta_{HT}^2 + \eta_{HT} + 1}{(\eta_{HT} + 1) \cdot \eta_{HT}}$$

$$b_{AHT} = 5.936 \text{ m}$$

MAC coordinate along HT span:

$$Z_{AHT} = \frac{L_{HT}}{6} \cdot \frac{\eta_{HT} + 2}{\eta_{HT} + 1}$$

$$Z_{AHT} = 2.5 \text{ m}$$

MAC coordinate along the OX axis:

$$X_{AHT} = Z_{AHT} \cdot \text{tg} \chi_{HT}$$

$$X_{AHT} = 1.56 \text{ m}$$

1.1.7.4 Determination of the geometric parameters of the vertical tail (VT):

VT area:

$$S_{VS} = \bar{S}_{VS} S .$$

$$S_{VT} = 24 \text{ m}^2$$

VT span;

$$L_{VS} = \sqrt{\lambda_{VS} S_{VS}} .$$

$$L_{VS} = 6 \text{ m}$$

VT root chord:

$$b_{OVS} = \frac{2S_{VS}}{L_{VS}} \cdot \frac{\eta_{VS}}{\eta_{VS} + 1} .$$

$$b_{OVS} = 5.3 \text{ m}$$

VT tip chord:

$$b_{RVS} = b_{OVS} / \eta_{VS} .$$

$$b_{RVS} = 2.65 \text{ m}$$

VT MAC:

$$b_{AVT} = \frac{2}{3} \cdot b_{root.VT} \frac{\eta_{VT}^2 + \eta_{VT} + 1}{(\eta_{VT} + 1) \cdot \eta_{VT}}$$

$$b_{AVT} = 4.12 \text{ m}$$

MAC coordinate along the VT span:

$$Y_{AVT} = \frac{L_{VT}}{3} \cdot \frac{\eta_{VT} + 2}{\eta_{VT} + 1} .$$

$$Y_{AVT} = 2.66 \text{ m}$$

MAC coordinate along the OX axis:

$$X_{AVT} = Y_{AVT} \cdot \text{tg} \chi_{VT}$$

$$X_{AVT} = 1.66 \text{ m}$$

1.1.7.5 Determination of the geometric parameters of the landing gear

For a tricycle landing gear with a nose strut, the main parameters are:

1) b – landing gear base – the distance between the axles of the main and front supports. The base should ensure good operational quality of the aircraft when manoeuvring at the airfield. According to statistics, accept:

$$b = 0.3 \cdot 40 = 12 \text{ m}$$

2) B – landing gear track – the distance between the planes of symmetry of the main supports.

$$B = \frac{2 H b \mu}{\sqrt{a^2 - H^2 \mu^2}}$$

$$B = 18.1 \text{ m}$$

3) e – extension of the main supports, that is, the distance between the vertical passing through the center of mass of the aircraft and the projection of the axis of the main supports on the reference plane of the aircraft.

$$e = 0.06 \cdot 12 = 0.72 \text{ m}$$

4) a – extension of the front support, that is, the distance between the vertical passing through the center of mass of the aircraft and the axis of the front wheel:

$$a = 0.94 \cdot 12 = 11.28 \text{ m}$$

5) $H_{C.G}$ – aircraft center of mass height;

$$H_{C.G} = 4.8 \text{ m}$$

6) φ – rollover angle (angle of contact of the fuselage tail or its safety support of the runway surface. In this case, the ventral fin):

$$\varphi = 12^\circ$$

The angle of the main supports relative to the center of mass of the aircraft:

$$\gamma = 13^\circ$$

1.1.8 Calculation of the center of gravity of the aircraft

Taking the fuselage beginning as the origin of coordinates, and the OX axis is combined with the building horizontal of the fuselage.

The coordinate of the center of mass along the OX axis is determined by the formula [5]:

$$x_T = \frac{\sum m_i \cdot g \cdot x_i}{\sum m_i \cdot g};$$

and the centering value

$$\bar{x}_T = \frac{x_T - x_A}{b_A}.$$

here, x_A – the distance from origin of coordinates to b_A nose.

Wing

The center of mass of the wing is determined by the formula:

$$x_{T_w} = 0.5 \cdot 3.64 + x_A = 1.82 + 11.28 = 13.1 \text{ m}$$

Tail unit

The center of mass of the horizontal and vertical tail is taken to lie at 0.5 HT and VT MAC. I. e.

$$x_{T_{HT}} = 29.6 \text{ m},$$

$$x_{T_{VT}} = 20.3 \text{ m}.$$

Fuselage

The center of mass of the fuselage and fuselage cargo is approximately taken at half the length of the fuselage:

$$x_{T_f} = 0.5 \cdot L_f = 20 \text{ m}$$

Landing gear

Since determining the position of the center of mass only along the longitudinal axis, and take the center of mass of the chassis as the distance from the origin of the adopted coordinate system to the point of contact of the wheels with the surface of the runway. Then the center of mass of the nose landing gear $x_{T_{NLG}} = 4.25 \text{ m}$, and the center of mass of the main landing gear $x_{T_{MLG}} = 15.3 \text{ m}$

Power plant

It is assumed that the center of mass of each engine nacelle is located at 0.6 of its length.

So:

$$x_{T_{eng}} = 21.5 \text{ m}$$

Fuel system and fuel

The center of mass of the fuel and the fuel system is assumed to be located in the centers of mass of the areas of the wing fuel compartments. Then the center of mass of the internal fuel compartments $x_{T_{eng}} = 15.25 \text{ m}$

Equipment and controls

The center of mass of the equipment and control is taken at the center of mass of the fuselage, that is, at about half of its length.

So:

$$x_{T_{eq.cont}} = 15.05 \text{ m}$$

Based on the obtained mass of aircraft units, the list of center of gravity position is showed (Table 1.6)

Table 1.6 – List of centers of gravity positions

Name of the aircraft unit	$m_i \cdot g$	x_i	$m_i \cdot g \cdot x_i$
	daN	m	daN · m
Wing	27370	13.1	358547
Fuselage	24990	20	499800
Horizontal tail	3000	29.6	88800
Vertical tail	1970	20.3	39991
Nose landing gear	4670	4.25	19847
Main landing gear	8000	15.3	122400
Power plant	7000	21.5	150500
fuel	19776	15.25	301584
Equipment and controls	2700	15.05	40635
Commercial load	18000	15.23	274140
Σ	117476		1896244

Substitute the numerical values obtained from the list to the formula:

$$x_T = 16.142 \text{ m}$$

To obtain the position of the center of mass in the MAC shares of the wing, we substitute x_T to the formula:

$$\bar{x}_T = 16.142 - 11.28 / 3.64 = 1.336$$

1.1.9 Conclusion

The calculation of the take-off mass of the projected aircraft in three approximations has been performed. As a result, the take-off mass in the third approximation is 117977 kg, wing mass – 27370 kg; fuselage mass – 24990 kg; tail mass – 4970 kg; power plant mass – 7000 kg; landing gear mass – 12670 kg; as well as fuel mass – 19776 kg. The basic geometric parameters of the projected aircraft have been determined: $S = 130 \text{ m}^2$, $\eta = 4$, $\lambda = 10$, $b_A = 3.64 \text{ m}$, $L_f = 40 \text{ m}$. After obtained the updated data, the geometric parameters of the projected aircraft were calculated and the centering position was determined. The centering position in lobes of the mean aerodynamic chord is 1.33.

1.2 Analysis of optimized aircraft design parameters influence on its aerodynamic and mass characteristics

1.2.1 Determination of the drag of the designed aircraft

Profile resistance found by the sum of the resistances of its isolated units, taking

End of table 1.7

Profile Resistance VT in the Aircraft System							
0	0.00099	0.00093	0.00089	0.00085	0.00082	0.0008	0.00077
12	0.00118	0.0011	0.00105	0.00101	0.00097	0.00094	0.00091
Profile Resistance of Nacelles in the Aircraft System							
0	0.00371	0.00369	0.00373	0.00378	0.00384	0.0039	0.00396
12	0.00447	0.00442	0.00445	0.0045	0.00456	0.00462	0.00469
Drag Coefficient of the Aircraft at $C_{ya} = 0$							
0	0.02212	0.0215	0.02113	0.02086	0.02065	0.02048	0.02032
12	0.02502	0.0242	0.02321	0.02252	0.02231	0.02152	0.02142

Based on the results from table 1.7, plotted the dependences of the profile resistance of aircraft parts: the fuselage, wing, HT, VT, engine nacelles and profile interference resistance of the wing + fuselage, HT + fuselage systems. Also plotted is the dependence of the total profile resistance of the aircraft (Figure 1.18).

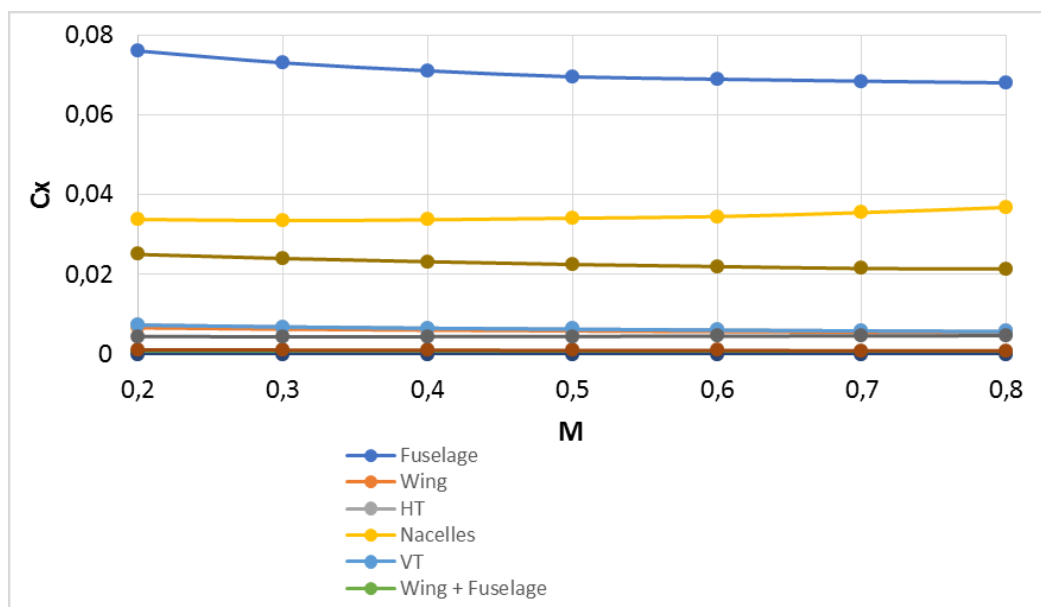


Figure 1.18 – Graphs of the dependence of the resistance coefficients on the Mach number

1.2.2 Lift force, inductance, aircraft polar, aerodynamic quality of the aircraft, aircraft polarities in take-off and landing configurations

The expression for calculating the polar has the form [2]:

$$C_{Xa} = C_{X0} + AC_{Ya}^2 + \sum \Delta C_{Xi}$$

where $A = \frac{1+\delta}{\pi \lambda_w} \cdot \frac{\gamma_{HT}}{m_w}$ – polar blade coefficient; – wing lengthening;

γ_{HT} – takes into account the contribution of horizontal tail to inductive reactance;
 m_w – depends on the shape of the cross section of the wing-fuselage system;

$\Sigma \Delta C_{xi}$ – increment of inductive resistance due to an increase in the angle of attack and additional resistance due to the appearance of local shock waves at values C_{Ya}^2 , going beyond the range of subsonic speeds.

In accordance with the calculated shape and size of the aircraft, the aircraft polar was calculated in the flight configuration and speed coordinate system for a number of values $M = 0,2; 0,3; 0,4; 0,5; 0,6; 0,7; 0,8$. The aerodynamic coefficients at the nodal points of the polar and the maximum quality of the aircraft given in table 1.7 and table 1.8. Graphs of polar and maximum aircraft quality built on Figure 1.19 and Figure 1.20.

Table 1.8 – Airplane drag coefficients

$M \backslash C_{Ya}$	0.2	0.3	0.4	0.5	0.6	0.7	0.8
0,0	0.02225	0.0217	0.02111	0.02095	0.02101	0.02046	0.02021
0,2	0.02424	0.02363	0.02326	0.023	0.02279	0.02362	0.02347
0,4	0.03077	0.03019	0.02985	0.02962	0.02947	0.02935	0.02927
0,6	0.042	0.0415	0.04125	0.04115	0.04114	0.04121	0.04136
0,8	0.05834	0.05804	0.05804	0.05825	0.05865	0.05926	0.06216
1,0	0.08073	0.08098	0.08174	0.08303	0.08514	0.08904	–
1,2	0.1139	0.12028	–	–	–	–	–
$C_{Xa.max}$	0.14313	0.1377	0.13241	0.12716	0.12193	0.1167	0.13766

Table 1.9 – Coefficient of maximum lifting force and maximum quality at take-off

M	0.2	0.3	0.4	0.5	0.6	0.7	0.8
$C_{Ya.max}$	1.24815	1.21064	1.17121	1.12987	1.08661	1.04144	0.99436
K_{max}	14.888	15.359	15.59	15.68	15.699	15.638	15.577

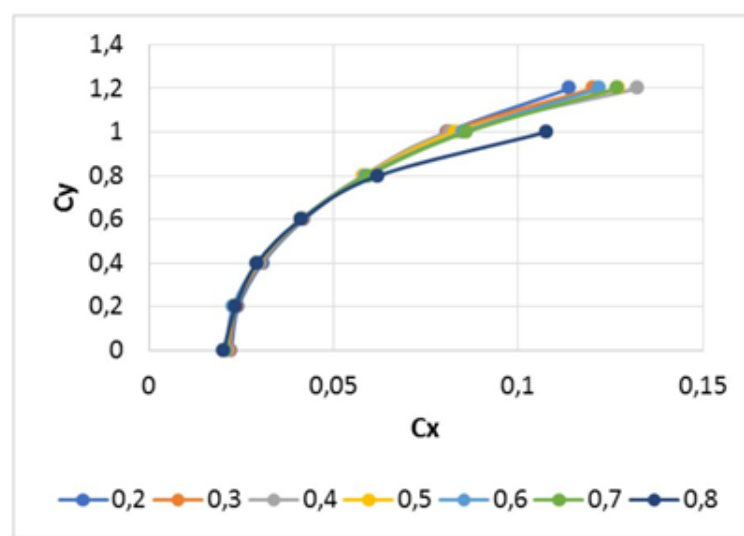


Figure 1.19 – Aircraft polars

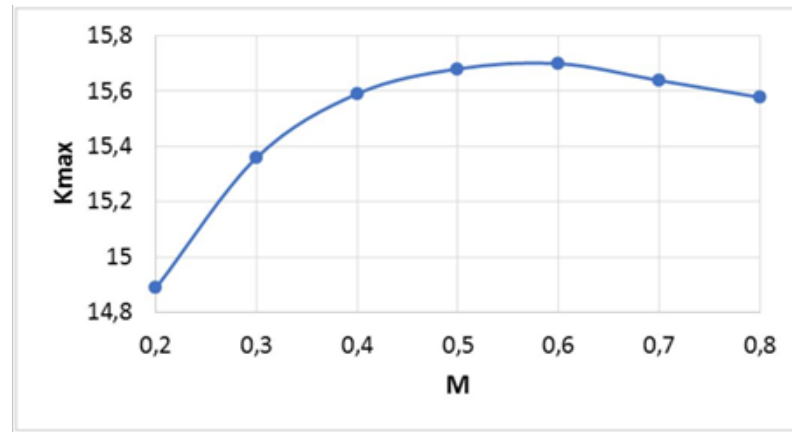


Figure 1.20 – Maximum Aircraft Quality

When calculating the take-off and landing characteristics of an aircraft, it is necessary to build polars with taking into account the landing gear, wing mechanization, braking devices, etc. for an approximate calculation, use statistical materials regarding the influence of landing gear and wing mechanization on the polar and dependence $C_{ya} = f(\alpha)$ for flight configuration with low subsonic numbers M .

The mechanization of the wing on takeoff and landing increases C_{xa} at $\Delta C_{xa} m$, and C_{ya} at $\Delta C_{ya} m$. With the release of mechanization, the value shifts to the negative region α_0 at $\Delta \alpha_0$, leading to an increase $C_{ya} max$, moreover $C_{ya} max$ achieved at approximately the same angles α , as without mechanization. Thus, the polarities on takeoff and landing can be obtained by shifting the initial polar for the flight configuration to the right by $\Delta C_{xa} = \Delta C_{xa} LG + \Delta C_{xa} m$ and up at ΔC_{ya} .

The calculation of the polar in the take-off configuration for each i -th point performed according to the formulas [2]:

$$C_{ya\ t.off} = (C_{ya})_i + 0,25;$$

$$C_{xa\ t.off} = (C_{xa})_i + (0,6 + 0,5) \cdot C_{xa0}.$$

Similarly, the aircraft polar calculated in the landing configuration

$$C_{ya\ land} = (C_{ya})_i + 0,45;$$

$$C_{xa\ land} = (C_{xa})_i + (0,6 + 1,4) \cdot C_{xa0}.$$

The calculated values of the lift and drag coefficients are listed in table 1.9.

Table 1.10 – Lift and drag coefficients for different flight modes

Flight		Takeoff		Landing	
C_y	C_x	C_y	C_x	C_y	C_x
0.0	0.02221	0.25	0.046389	0.7	0.090851
0.2	0.02432	0.45	0.048456	0.9	0.092854

End of Table 1.10

0.4	0.03181	0.65	0.055322	1.1	0.099224
0.6	0.04221	0.85	0.066455	1.3	0.110613
0.8	0.05835	1.05	0.082871	1.5	0.126952
1.0	0.08235	1.25	0.105112	1.7	0.149354
1.2	0.11398	1.45	0.138323	1.9	0.182546
1.24815	0.14365	1.49821	0.167235	1.94901	0.211923

According to the results, graphs of the polars during flight, take-off, landing, were built on Figure 1.21.

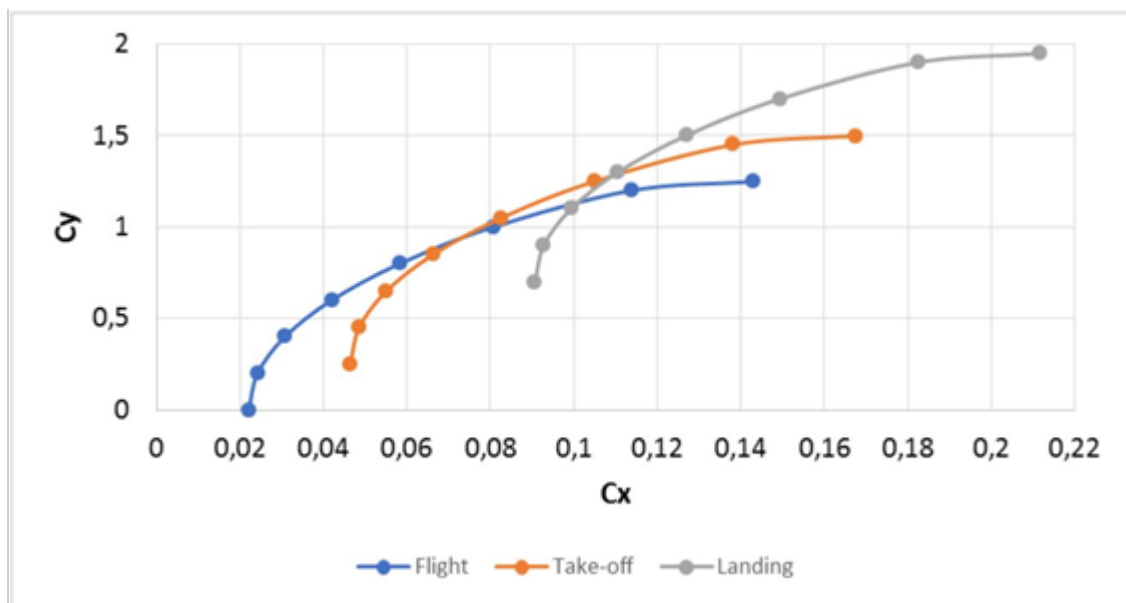


Figure 1.21 – Polars during flight, takeoff and landing

1.2.3 The longitudinal moment and the location of the aerodynamic focus of the aircraft

The longitudinal moment, like other aerodynamic characteristics, is determined by the sum of the moments of the individual units of the aircraft. The moment coefficient expressed as follows [3]:

$$m_z = m_{z0} + \left(\frac{m_z^\alpha}{C_{ya}^\alpha} \right) C_{ya}^\alpha$$

where $m_z^\alpha = m_{z \text{ without HT}}^\alpha + m_{zHT}^\alpha$.

The position of the aerodynamic focus of the aircraft as a whole and the aircraft without GO relative to the nose of the fuselage in fractions of its length determined by the following relationships:

$$\bar{X}_F = -\frac{m_z^\alpha}{C_{ya}^\alpha};$$

$$\bar{X}_{F \text{ without HT}} = -\frac{m_z^\alpha \text{ without HT}}{C_{ya}^\alpha \text{ without HT}},$$

In the problems of flight dynamics, the values of the focus position relative to the nose of the MAC of the wing are used. New values of the longitudinal moment are found by the formulas:

$$\bar{X}_{FA} = [\bar{X}_F - (\bar{X}_K + \bar{X}_A)] \frac{l_{fus}}{b_A};$$

$$\bar{X}_{FA \text{ without HT}} = [\bar{X}_{F \text{ without HT}} - (\bar{X}_K + \bar{X}_A)] \frac{l_{fus}}{b_A},$$

where b_A and \bar{X}_A – MAC wing length and distance from the MAC nose to the leading edge of the airborne chord.

The moment coefficient at zero lifting force determined by the following formula:

$$m_{z0} = m_{z0}^* + m_{z0f} + m_{z0w} + m_{e.n} + m_{z0HT},$$

where m_{z0f} , m_{z0w} , $m_{e.n}$, m_{z0HT} – longitudinal moments at zero lifting force of the fuselage, wing, engine nacelles and HU in the aircraft system, respectively; m_{z0}^* – increment of longitudinal moment at zero lifting force of the ventral fuselage.

The calculated data are entered in the table 1.10.

Table 1.11 – Coefficient of the longitudinal moment of the aircraft

Longitudinal moment of the aircraft without horizontal tail							
$M \backslash C_y$	0.2	0.3	0.4	0.5	0.6	0.7	0.8
0	-0.1344	-0.1342	-0.1338	-0.1332	-0.1325	-0.1314	-0.1299
0.2	-0.0729	-0.0734	-0.074	-0.0748	-0.0759	-0.0771	-0.0784
0.4	-0.0114	-0.0125	-0.0142	-0.0164	-0.0192	-0.0227	-0.027
0.6	0.0502	0.0483	0.0456	0.042	0.0374	0.0316	0.0244
0.8	0.1117	0.1091	0.1053	0.1004	0.094	0.086	0.0759
1.0	0.1732	0.1699	1.1651	0.1588	0.1506	0.1403	
1.2	0.2347	0.2307					
Longitudinal moment of the aircraft with horizontal tail							
0	0.0985	0.102	0.1074	0.1148	0.1249	0.1389	0.1585
0.2	0.0448	0.0483	0.0535	0.0609	0.071	0.0852	0.1056

0.4	-0.0089	-0.0055	-0.0004	0.0069	0.0171	0.0316	0.0527
0.6	-0.0626	-0.0593	-0.0542	-0.047	-0.0367	-0.0221	-0.0003

End of table 1.11

0.8	-0.1163	-0.1131	-0.1081	-0.1009	-0.0906	-0.0757	-0.0532
1.0	-0.17	-0.1668	-0.162	-0.1549	-0.1445	-0.1294	
1.2	-0.2237	-0.2206					

Xf HT

	-0.2348	-0.2312	-0.226	-0.2191	-0.2102	-0.1989	-0.1843
--	---------	---------	--------	---------	---------	---------	---------

Xf

	0.3413	0.3418	0.3422	0.3425	0.3424	0.3411	0.3376
--	--------	--------	--------	--------	--------	--------	--------

According to table 1.11, the graphs of the dependence of the longitudinal moment on the lift of the aircraft with and without HT for $M = 0,8$ and the graph of the position of the aircraft focus relative to the MAC with and without HT were constructed (Figures 1.22 and 1.23).

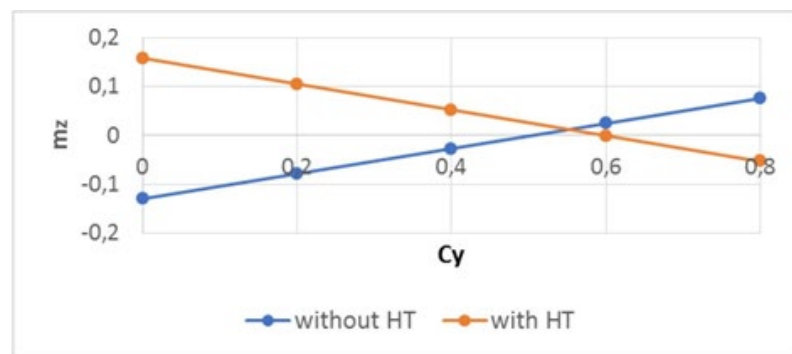


Figure 1.22 – Dependence of m_z (C_y) aircraft with and without HT

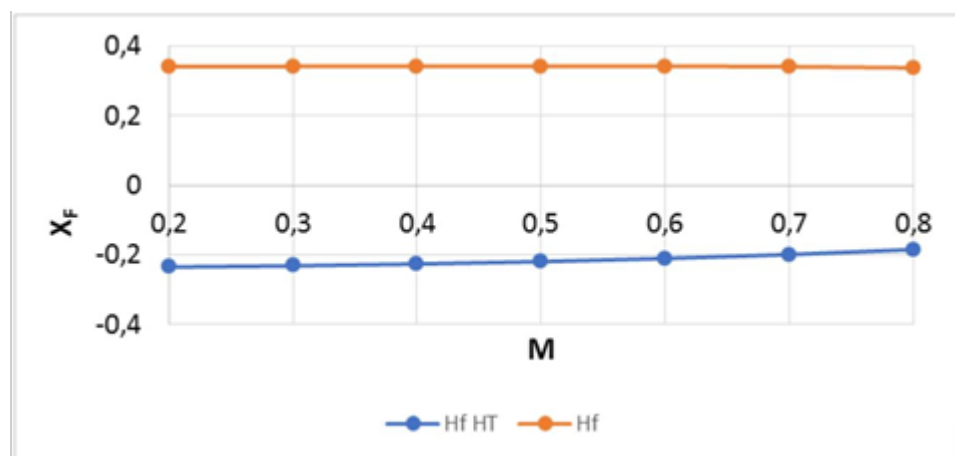


Figure 1.23 – X_f (M) dependence of aircraft with and without HT

1.2.4 Conclusions

The values of the coefficients of the lifting force and the force of the frontal resistance are determined. Polars were built during cruise flight, takeoff and landing.

It was determined that the maximum aerodynamic quality=lift-to-drag ratio is 15.7 units.

2 RESEARCH SECTION

2.1 Integrated design and noise reduction inside aircraft

2.1.1 Objective of the project

The overall idea of this project is to reduce the noise in commercial aircraft cabins which provides comfort to humans. The main objective of the project is to design a composite using natural fibers which satisfies the following needs,

- Sound Proof
- Light Weight
- Abundant
- Biodegradable
- Cost efficient
- Eco-friendly
- Fire Resistant

2.1.2 Application of sound absorbing material

The improvement of the human quality of life and the continuous growth in population in developing and developed societies, have exacerbated the environmental and financial issues. Some of these problems are noise and the different types of human and industrial wastes. Many natural products have been recently developed and tested for acoustic applications. Sound absorbing materials absorb most of the sound energy striking them and reflect very little. Therefore, sound absorbing materials have been founded very useful for the control of room noise. In this study, sound absorption technology as an effective noise reduction technology building using sustainable acoustic absorbers, will be discussed. Sound absorptive materials may also be used to control the response of artistic performance spaces to steady and transient sound sources, thereby affecting the character of the aural environment, the intelligibility of unreinforced speech and the quality of unreinforced musical sound. Combining absorptive materials with barriers produces composite products that can be used to lag pipe or provide absorptive curtain assemblies. Due to their biodegradable, lightweight, cheaper, nontoxic, and nonabrasive qualities, natural fibers are receiving much attention in composites as a substitute for synthetic fibers for acoustic absorption purposes. The natural fibers with desirable physical and mechanical properties are exhibited as high-performance composites with environmental and economic advantages . Natural fibers reinforced composites are emerging very rapidly as the potential substitute to the metal or ceramic based materials in applications that also include automotive, aerospace, marine, sporting goods and electronic industries.

2.1.2.1 Properties of the natural fibers

- High specific strength

- High specific stiffness
- High density
- High modulus
- Bio - degradable
- UV, acid and alkali resistant
- Less carbon residue

2.1.2.2 Factors influencing sound absorption material

- **Fiber Size**
Thin fibers can move more easily than thick fibers on sound waves. Moreover, with fine denier fibers more fibers are required to reach equal volume density which results in a more tortuous path and higher air flow resistance. Fine fiber content increases sound absorption coefficient values due to an increase in airflow resistance by means of friction of viscosity through the vibration of the air.
- **Airflow Resistance**
One of the most important qualities that influence the sound absorbing characteristics of a fibrous material is the specific flow resistance per unit thickness of the material. The characteristic impedance and propagation constant, which describes the acoustical properties of porous materials, a great extent by flow resistance of the material.
- **Porosity**
Number, size and type of pores are the important factors that one should consider while studying sound absorption mechanism in porous materials. To allow sound dissipation by friction, the sound wave has to enter the porous material. This means, there should be enough pores on the surface of the material for the sound to pass through and get dampened.
- **Tortuosity**
Tortuosity is a measure of the elongation of the passageway through pores, compared to the thickness of the sample. Horoshenkov et al. (2001) stated that tortuosity mainly affects the location of the quarter wavelength peaks, whereas porosity and flow resistivity affect the height and width of the peaks. It has also been said that the value of tortuosity determines the high frequency behaviour of sound absorbing porous materials.
- **Thickness**
Numerous studies that dealt with sound absorption in porous materials have concluded that low frequency sound absorption has direct relationship with thickness. The rule of thumb that has been followed is the effective sound absorption of a porous absorber is achieved when the material thickness is about one tenth of the wavelength of the incident sound.
- **Density**
Density of a material is often considered to be the important factor that governs the sound absorption behaviour of the material. At the same time, cost of an acoustical material is directly related to its density.

- **Surface Impedance**

The higher the acoustic resistivity of a material, the higher is its dissipation, for a given layer of thickness. At the same time the surface impedance of the layer also increases with resistivity, resulting in a great number of reflections on the surface layer, giving a lower absorptive capability. Moreover, the whole process is frequency dependent, so that for lower frequency bands the necessary layer thickness increases as resistivity decreases.

- **Placement / Position of Sound Absorptive**

Placement / position of sound absorptive materials is a known absorption of a material depends also on the position and placement of that material. It has been reported by Alton Everest Alton, (2001), that if several types of absorbers are used, it is desirable to place some of each type on ends, sides and ceilings so that all three axial modes (longitudinal, transverse and vertical) will come under their influence.

2.1.3 Fiber selection and description

2.1.3.1 Fiber selection

The fibers studied for this project are

- Kenaf
- Jute
- Flax

2.1.3.1.1 Kenaf fiber

Kenaf fiber has emerged as an important plant cultivated worldwide and has been regarded as an industrial crop. It has a great potential for replacing synthetic fiber such as glass fiber. The use of kenaf fiber can provide mechanical properties, i.e. tensile strength, comparable to those of synthetic fiber with lower density than traditional materials, resulting in lightweight and eco-friendly polymer composites. The performance of kenaf reinforced polymer composites is affected by several factors such as chemical treatment, fiber content, the part of the kenaf fiber used, the form of fiber, and water uptake.



Figure 2.1 – Kenaf Fiber

2.1.3.1.2 Jute Fiber

Jute is a naturally occurring plant fiber and has been promoted as the most readily available, environmentally friendly, abundant, economic and renewable source. It is specifically cultivated in large quantities near large bodies of water in the eastern part of India and Bangladesh and are exported all over the world for various applications. Jute is a cellulose fiber that is composed primarily of the plant materials. Jute is used in various forms for noise control applications. It has excellent fire - retardant properties, high Noise Reduction Coefficient and Sound Absorption Coefficient. Jute based materials can also be engineered for good fire-retardant properties, structural strength and moisture proofing.



Figure 2.2 – Jute Fiber

2.1.3.1.3 Flax Fiber

In recent years, the use of flax fibres as reinforcement in composites has gained popularity due to an increasing requirement for developing sustainable materials. Flax fibres are co-effective and offer specific mechanical properties comparable to those of glass fibres. Composites made of flax fibres with thermoplastic, thermoset, and biodegradable matrices have exhibited good mechanical properties. This review presents a summary of recent developments of flax fibre and its composites. Firstly, the fiber structure, mechanical properties, cost, the effect of various parameters (i.e., relative humidity, various physical/chemical treatments, gauge length, fibre diameter, fibre location in a stem, oleaginous, mechanical defects such as kink bands) on tensile properties of flax fibre have been reviewed. Secondly, the effect of fibre configuration (i.e., in forms of fabric, mat, yarn, roving and monofilament), manufacturing processes, fibre volume, and fibre/matrix interface parameters on the mechanical properties flax fiber reinforced composites have been reviewed. Next, the studies of life cycle assessment and durability investigation of flax fibre reinforced composites have been reviewed. Flax is one of the most frequently used fibers. Among the various natural fibres, it has high mechanical properties comparable to glass fibres and high vibration absorption capability. Flax fibres also offer the excellent combination of low cost, light weight and high stiffness for applications such as infrastructures, auto mobiles and consumer products.



Figure 2.3 – Flax Fiber

2.1.4 Sound absorption coefficient

The sound absorption coefficient of a power absorbed by a surface to the incident sound power. It gives the relationship between the acoustic energy that is absorbed by a material and the total incident impinging upon it. The incident wave impacts the face of the material, reflecting some of its energy and sending the rest into the material. The energy in the material is either transmitted through the material or absorbed within the porous structure of the material. The sound absorption coefficient is the sum of the percentages of sound that were not reflected. Since some sound energy will be lost when waves travel through the material's structure, it is evident that the sound transmission coefficient will always be valued between zero and one. This coefficient is limited between 0 for non - absorbent materials and 1 for totally absorbent. The sound absorption coefficient can be measured using the formula

$$\alpha = |r|^2$$

α – sound absorption coefficient

r – is the complex sound reflection coefficient

$$r = \frac{Pr}{Pi}$$

Pr – reflected pressure

Pi – incident pressure

It can be shown that the sound absorption coefficient in terms of the real and imaginary parts of the impedance ratio is given by the formula:

$$\alpha = \frac{4R}{(R^2 + X^2) + 2R + 1} = 1 - |r|^2$$

In terms of a real (R is resistance) part and an imaginary (X is reactance) part, the specific acoustic impedance ratio can be calculated.

2.1.5 Impedance tube

Impedance tube technique is widely used for finding sound absorption properties of materials, where sound signals are generated from one end of the tube and samples to be tested are placed at another end. The method of testing materials using impedance tube is called as normal incident sound absorption or transmission loss testing because of the normally incident sound waves on to the surface of test sample in the tube. It is excited by plane wave source on the left side, while it is terminated with a complex impedance, Z , at the opposite end. Two pressure sensors (microphones) are used to determine the magnitude of the forward and backward traveling waves, from which the impedance, flow resistivity, and sound absorption coefficient may be determined. It is assumed that there are no losses along the length of the tube and that only plane waves propagate. The origin of the system is at the right end of the tube and the wave incident on the specimen will be traveling in a positive x direction.

2.1.6 Methodology

2.1.6.1 Numerical analysis

The most important acoustic parameter for porous materials is absorption coefficient. The sound absorption coefficient is calculated using two microphone techniques where the incident and reflected pressures are captured by two microphones. Finite Element Analysis has become a valuable engineering tool. FEM models are applicable when measurement equipment like impedance tubes is not available. Commercially available ANSYS, SDRC/IDEAS, NASTRAN/PATRAN, HYPERMMENS PLM NX, NISA, COMSOL, KEBIR, and so on. Here, ANSYS is used. ANSYS has its default quadratic acoustic elements called FLUID220. Finite Element Method is composed of nodes and elements and replaces the original engineering systems. Additionally, a complete FEM contains the boundary conditions of constraints and external loads of an engineering system.

2.1.6.2 Pre – processor

ANSYS has various analyses systems which serve different purposes. For acoustic analysis, it has a pre - processor called as harmonic acoustics. In this, the boundary conditions and the data of the materials are assigned.

2.1.6.3 Engineering data

The data of the natural composites are given manually in the engineering data column. For this acoustic analysis, some of the special parameters like, viscous and thermal characteristic length, tortuosity is given.

Table 2.1 – Engineering data of natural composites

Materials	Jute	Kenaf	Flax
Density (g/cm^3)	1.3 – 4.9	1.2	1.28 – 1.3
Tensile strength (MPa)	393 – 800	930	1500 – 1800
Young's Modulus (GPa)	13 – 26.5	7.13	60

End of table 2.1

Moisture absorption	12	17	10 – 12
Elongation of Failure(%)	1.8	1.6	2.7 – 3.5

2.1.6.4 Geometry

A 3D setup of the impedance tube should be modelled in the geometry. The dimensions of the tube should be assigned using the standards. Here, the ASTM E-1050 which is the standard test method for impedance and absorption of acoustic materials using a tube, two microphones and a digital frequency analysis system is used.

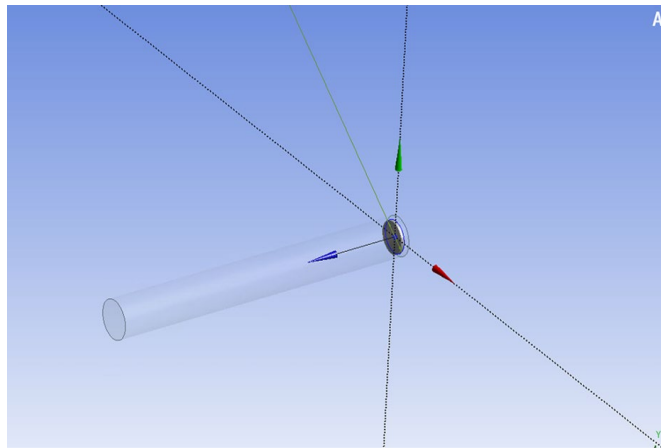


Figure 2.4 - Geometry

Table 2.2 – Parameters used in modelling impedance tube

Description	Value
Length	1 m
Width	0.1 m
Speed of sound	343.24 m/s
Density	1.2040 Kg/n
Mic 1 location (X1)	-0.4 m
Mic 2 location (X2)	-0.5 m

2.1.6.5 Mesh

The setup should be meshed. Mesh size is an important factor which deals with the accuracy of the results. The mesh element size of the model is 0.01 m.

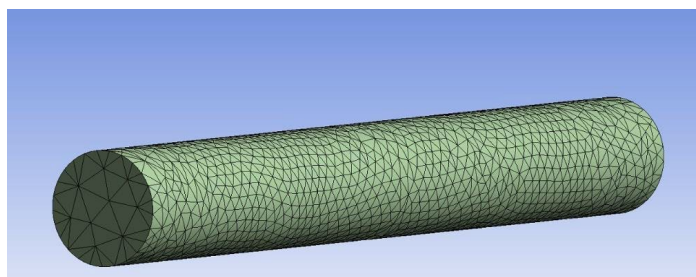


Figure 2.5 – Mesh element size distribution

2.1.6.6 Modelling

A 3D impedance tube test setup was modelled. It was by default quadratic acoustic elements FLUID220. The model was analyzed by Johnson - Champoux Allard. Absolute pressure was considered 1 (atm). The effect of humidity and temperature was considered the same as experimental test condition. The acoustic body is defined by giving speed of sound in air and volume density parameters. On the right side of the tube harmonic mass source is defined by giving amplitude of the mass source. On the left side of the tube, the tested specimen is spaced. At two different positions microphone are placed.

Details of "Acoustics Region"	
[-] Scope	
Scoping Method	Geometry Selection
Geometry	All Bodies
[-] Definition	
Structural	No
Acoustics	Yes
Suppressed	No
[-] Acoustic Domain Definition	
Artificially Matched Layers	Off
[-] Advanced Settings	

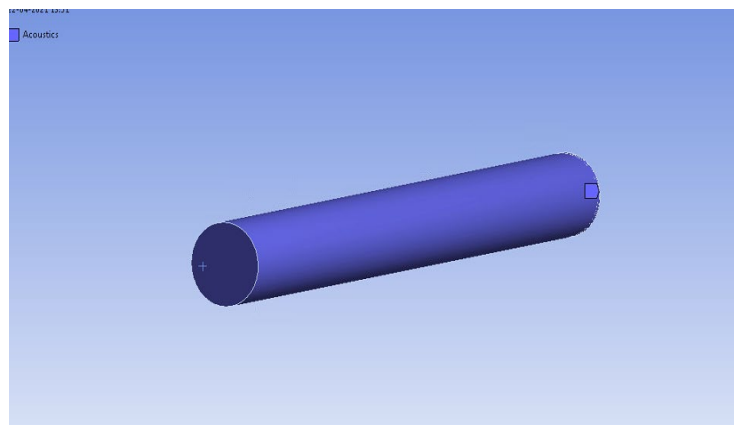


Figure 2.6 – Modelling

2.1.7 Solution of Computational Analysis

The frequency range should be given is 0 to 6300 Hz. The two-microphone method helps to get sound pressure levels of both microphone 1 and microphone 2 respectively. Since, we were able to find the reflected pressure level from microphone 1 and incident pressure from microphone 2.

2.1.7.1 Results

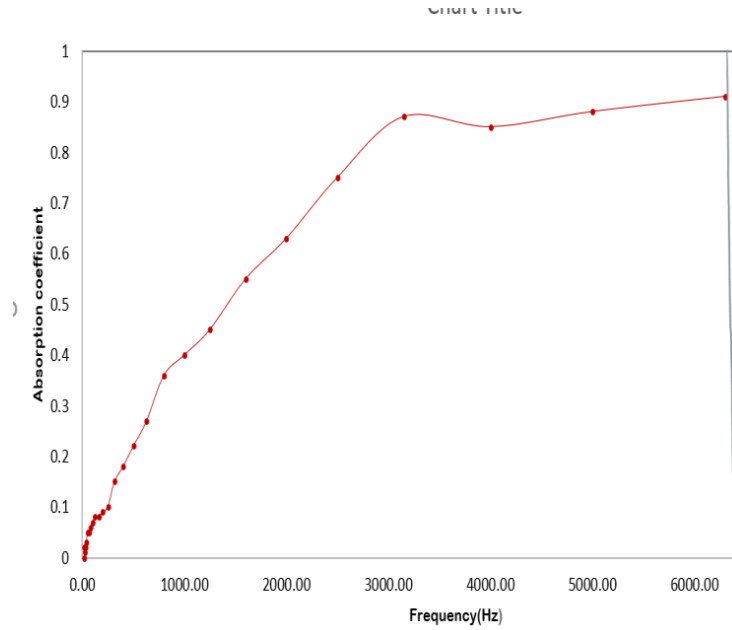


Figure 2.7 – Sound absorption coefficient plot of Jute

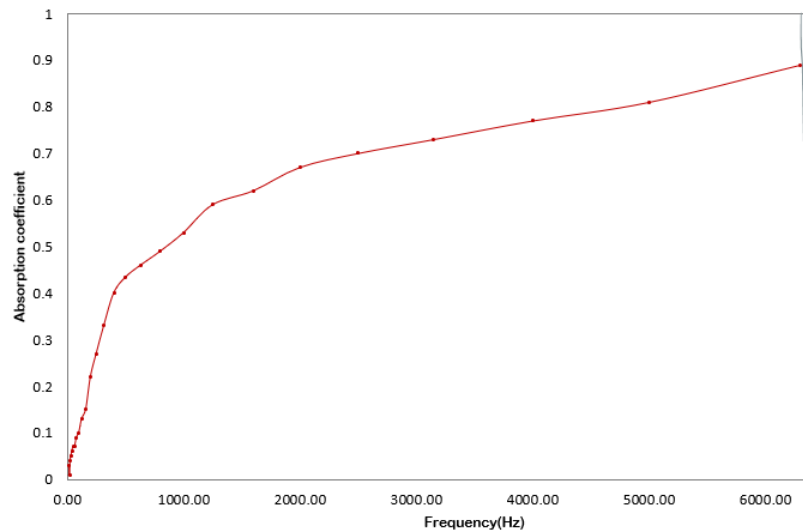


Figure 2.8 – Sound absorption coefficient plot of Kenaf

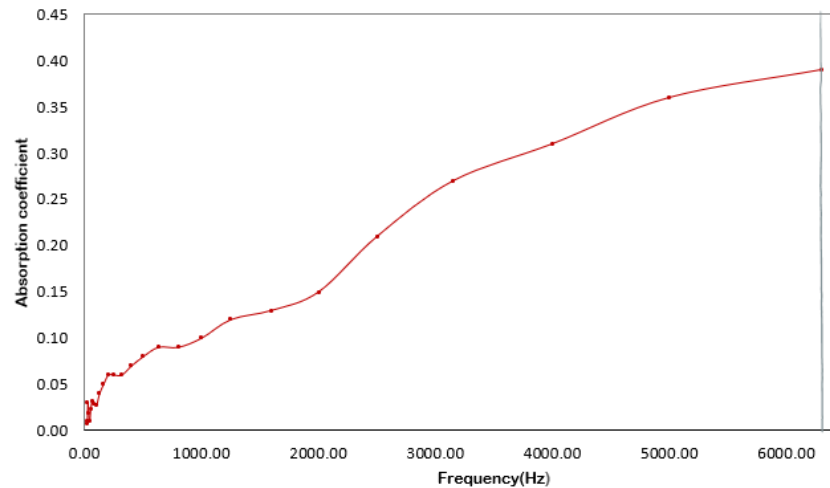


Figure 2.9 – Sound absorption coefficient plot of Flax

2.1.8 Experimental Analysis

Normal incidence sound absorption and transmission loss measurement can be found using an impedance tube. Unfortunately, this equipment's expensive. So, we have taken an effort to develop a cost-effective impedance tube for wider use especially for educational use. An impedance tube capable of measuring absorption coefficient has to be designed. We wanted to use a PVC tube, an inexpensive speaker, studio microphones and off-the-shelf materials for the construction of the tube. A laptop with integrated sound card was used for data acquisition and software with a Graphical User Interface (GUI) for data analysis and presentation.

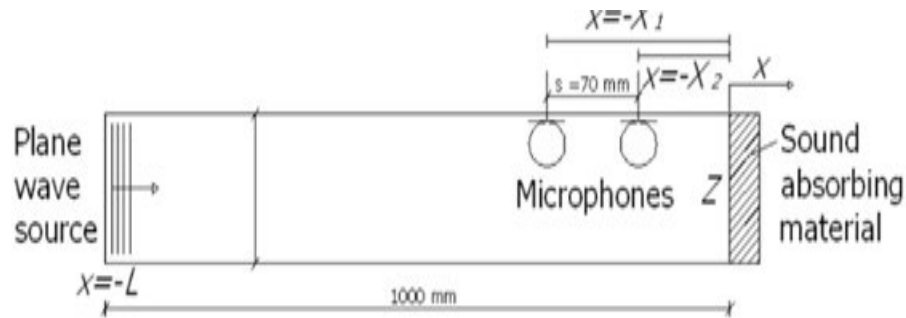


Figure 2.10 – Schematic view of the impedance tube

Test samples should be cut according to the given dimensions as 100mm from considerable distance from the fabric selvedge. The sample was fastened to the tube's left rigid wall by a sample hole waves of well-defined frequencies was attached to the right rigid wall. The analyzer generates a random signal which is then amplified. Finally, the analyzer measures the response of the two microphones and calculates the frequency response function between the two microphone channels. From this frequency response function, all test sample data will be calculated.

2.1.8.1 Fabric Production

Manufacturing processes of nonwoven fibre can be divided in three steps:

- Fiber opening
- Web Formation
- Web bonding
- Finishing

2.1.8.1.1 Web formation

Web formation is a process that arranges fibres or filaments into web form. The first step to prepare the fibers for web formation was carding. Producing a carded web starts with opening of bales of fibers.

2.1.8.1.2 Carding

Carding is the process of spinning which converts fed material into a uniform strand of fibres. The fibres tangle in this operation, thus it makes it possible to remove all types of impurities present. The carding, stripping and raising action take place during carding operation. In this way, continuous uniform fiber having parallel arrangement almost free of impurities is obtained. This method is commonly referred to as DRY - LAID. The fibers are combed into a web by a carding machine, which is

rotating drum or series of drums covered in fine wires or teeth. A carding machine brushes the loose fibers into rows that are joined as a soft sheet, or web. Fibres are conventionally carded to form a web, which then can be lapped to attain certain thickness and mass. The carding process was individually done for jute, kenaf, flax, each with a mixture of 10% of bamboo. Later the nonwoven fragments were weighed on an electronic balance. Then it was blended. The blended material was again fed into the carding machine twice for homogeneous mixture and for better evenness, orientation and successful web formation. The web formed is of PARALLEL LED WEB, that is the carded web in which the fibres are led parallel to each other. The fibres arranged in the direction of the machine, resulting in directional properties.



Figure 2.11 – Chopped Jute



Figure 2.12 – Carding of Jute



Figure 2.13 – Chopped Kenaf



Figure 2.14 – Carding of Kenaf



Figure 2.15 – Chopped Flax



Figure 2.16 – Carding of Flax

2.1.8.1.3 Needle punching of fibers

Needle punching is a nonwoven process by which the fibres are mechanically entangled to produce a nonwoven fabric by repeated penetration of barbed needles through a preformed dry fibrous web. The fibre web moves on a substrate between a metal bed plate and a stripper plate. The needles punch through the plates and the fibre web, reorienting the fibres so that mechanical interlocking or bonding occurs among the individual fibres. The substrate may be filaments, a scrim, or some other form .

These are the data given as an input,

- Number of punches per minute - 45
- Feed rate - 15 mm/stroke
- Punching done on both the sides of the fiber



Figure 2.17 – Needle punching of fibers



Figure 2.18 – Input data given to the machine

2.1.8.1.4 Sound absorption measurement

The impedance tube measurement obtains the normal incidence absorption coefficient of a layer of textiles with a small diameter (usually less than 10 cm). The results can be used to compare the basic absorption performance of a material and for acoustics simulations. The software used in the Impedance tube is holmarc wave analyser. The performance of sound absorbing materials in particular is evaluated by the sound absorption coefficient Alpha (α) is defined as the measure of the acoustical energy absorbed by the material upon incidence and is usually expressed as a decimal varying between 0 and 1.0. If 55 percent of the incident sound energy is absorbed, the absorption coefficient of that material is said to be 0.55. A material that absorbs all incident sound waves will have a sound absorption coefficient of 1.

Acoustical properties of nonwoven materials are measured by the impedance tube method according to ISO 105-23-41998 standard. The equipment used in this experiment consisted of a two-microphone impedance measurement tube type 7758 (PULSE Acoustic Material Testing Bruel & Kjaer and Computer System, Denmark). Test samples (28.5 cm and 99.5 cm) were cut randomly at a considerable distance from the fabric selvedge. The sample was fastened to the tubes left rigid wall by a sample holder, and a loudspeaker that can emit sound waves of well - defined frequencies was attached to the right rigid wall. The analyzer generates a random signal which is then amplified. Finally, the analyzer measures the response to the two microphones and calculates the frequency response function between the two microphone channels. From this frequency response function, all test sample data were calculated. The diameter of the tube d is smaller than the wavelength of the emitted sound wave

(typically $d = 99\text{mm}$ for $f < 1600\text{ Hz}$ and $d = 29\text{mm}$ for $f > 1600\text{ Hz}$), hence the wave can be thought of as a plane wave propagating along the axis of the tube. The value of the sound absorption coefficient is given from 0 to 1, which means sound absorption is zero at value of 0, reaching the maximum at a value of 1. The sound absorption coefficient indicates how much of the sound is absorbed in the materials. All sound absorption measurements were performed 4 times for each sample and the frequency analysis system was set from 100 to 6300 Hz.

2.1.8.1.5 Results using impedance tube

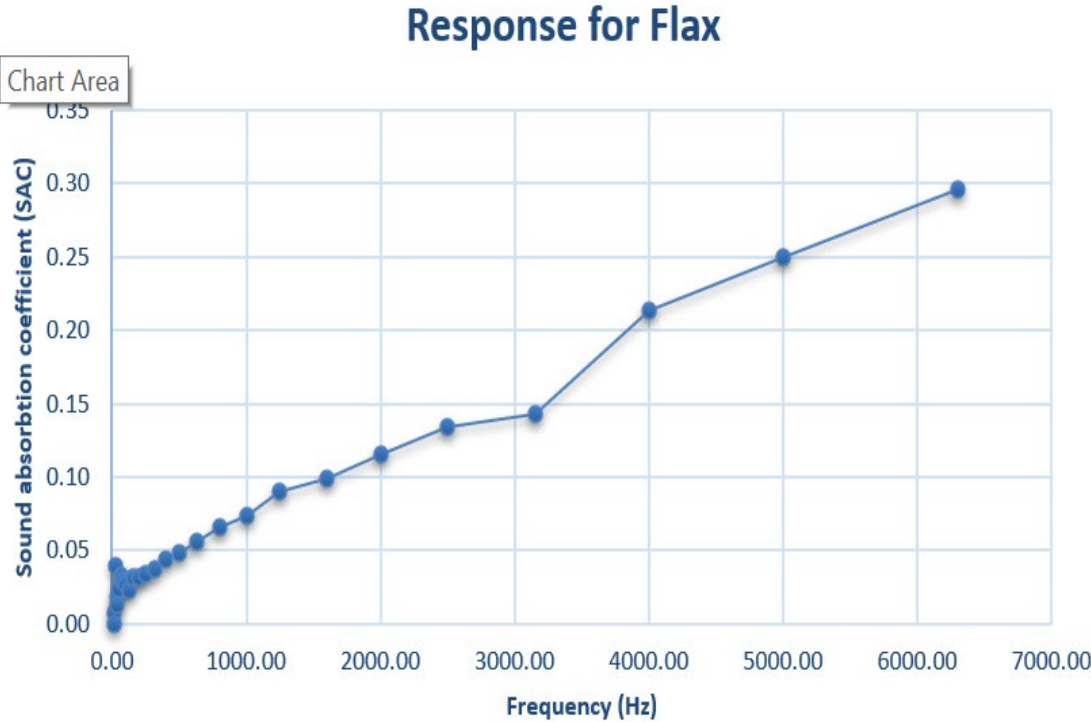


Figure 2.19 – Sound absorption coefficient of Flax

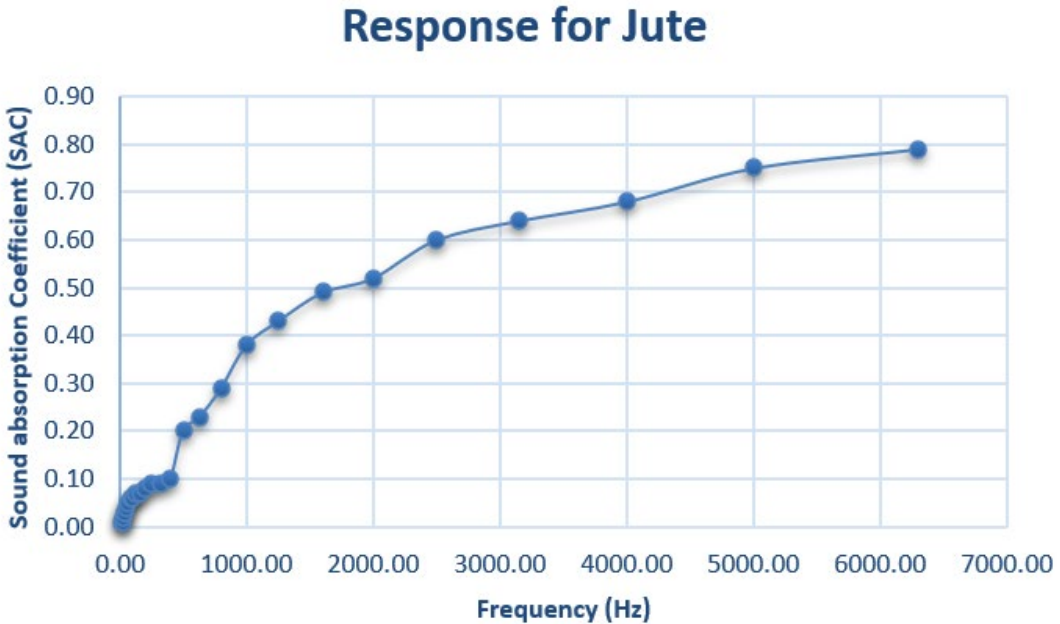


Figure 2.20 – Sound absorption coefficient of Jute

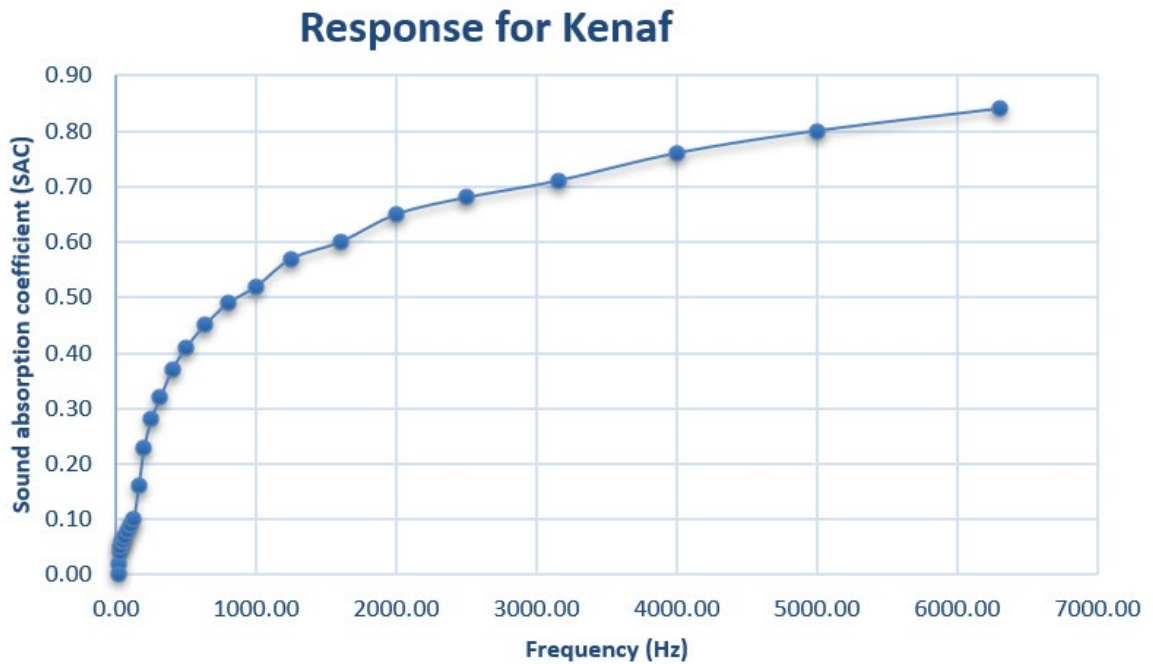


Figure 2.21 – Sound absorption coefficient of Kenaf

2.1.9 Conclusion of noise reduction inside aircraft

Natural fibers composites are renewable and cheaper substitute than synthetic fibers such as glass and carbon fiber reinforcements in making structural components.

Thus, from the analytical and experimental results, it is found that, kenaf has the highest sound absorption coefficient of 0.87 and to some extent jute also can be used in aircraft for sound absorption.

2.2 Noise reduction outside aircraft

2.2.1 Objective of the project

The main objective of the project is to reduce the noise outside the aircraft due to turbulences and engine noises. In this project, we are going to do comparative analysis of noise reduction in changing the design of the winglet.

Initial data for the winglet design.

- 1) The takeoff mass of the aircraft: 117977 kg;
- 2) Sweep angle $\chi = 30^\circ$;
- 3) Wing length $l = 20$ m;

To construct and analyse the designed winglet and use the integrated Computer – Aided Design system Siemens NX.

2.2.2 Development of the master geometry of the winglet

- 1) Starting the Siemens NX system and choose File → New → Model, assign the model name « Winglet Design »
- 2) To create expressions, Menu → Insert → Tools → Expression.

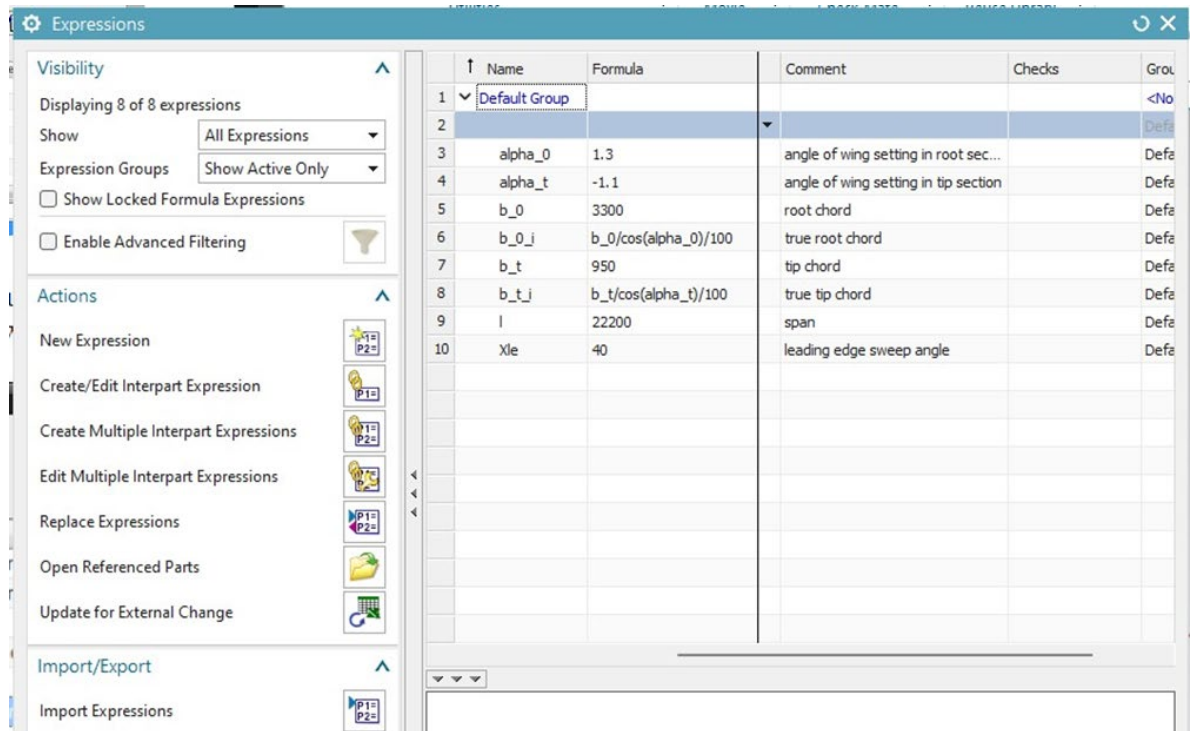


Figure 2.22 – Expression for creating wing planform

3) To create layers, Menu → Format → Layer Settings

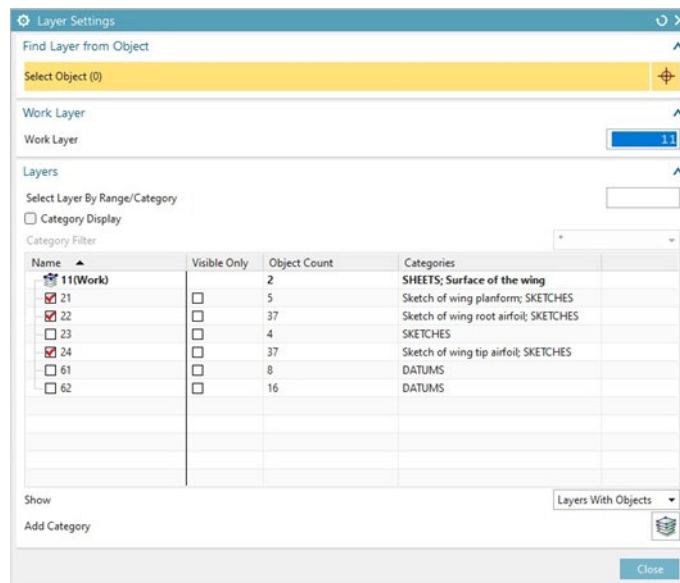


Figure 2.23 – Layer setting for aircraft wing

4) To create wing planform, Menu → Insert → Datum/Point → Datum CSYS,

5) Sketch of the wing planform, Menu → Insert → Sketch in task environment, Select XY plane for creating sketch. Disable Continuous Auto Dimensioning.

6) Select Line and create the outer sketch of the wing. Select Finish Sketch.

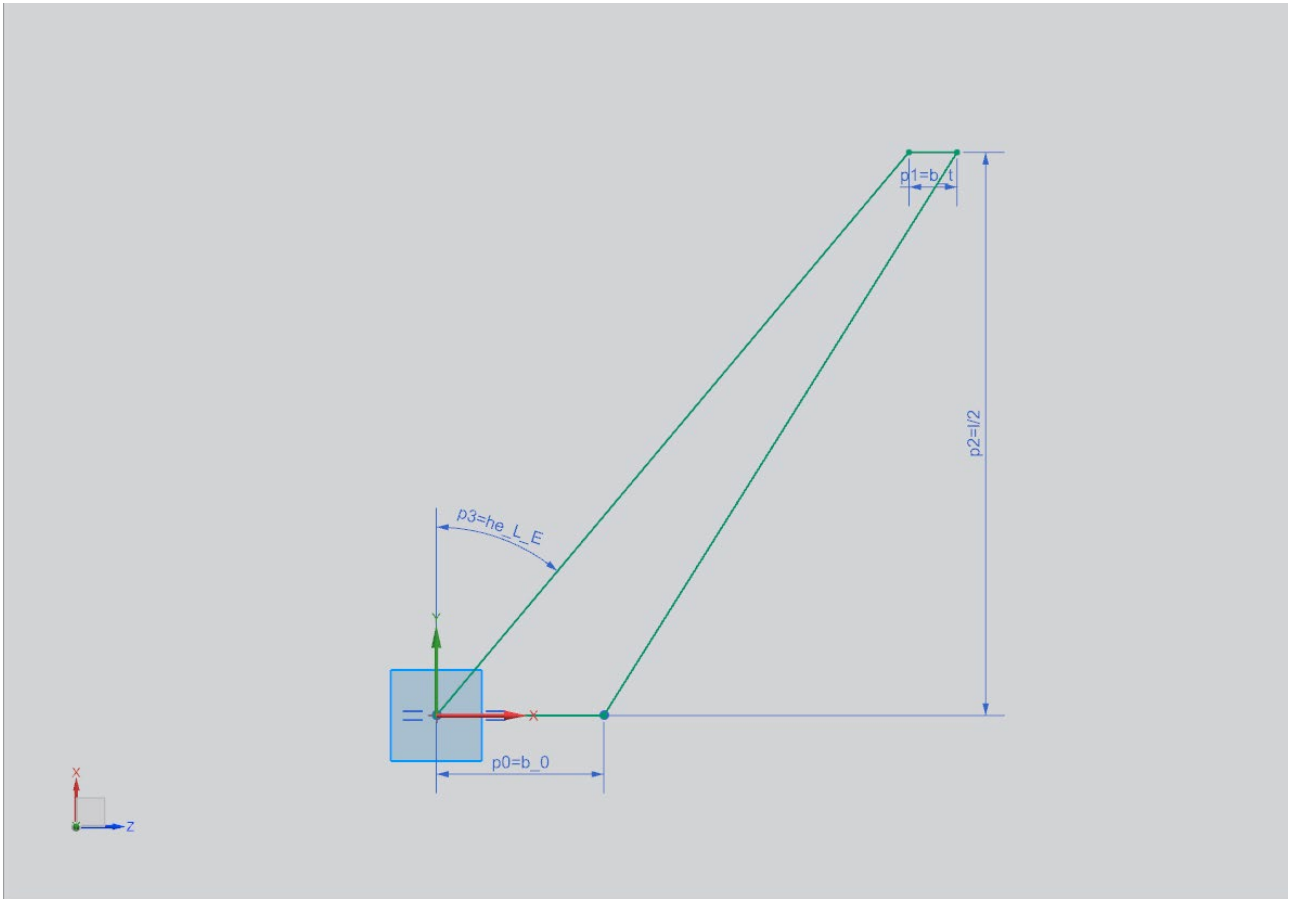


Figure 2.24 – Creating wing planform

7) Create Wing root airfoil, Menu → Insert → Sketch in task environment. Create airfoil perpendicular to wing planform. Select Finish Sketch.

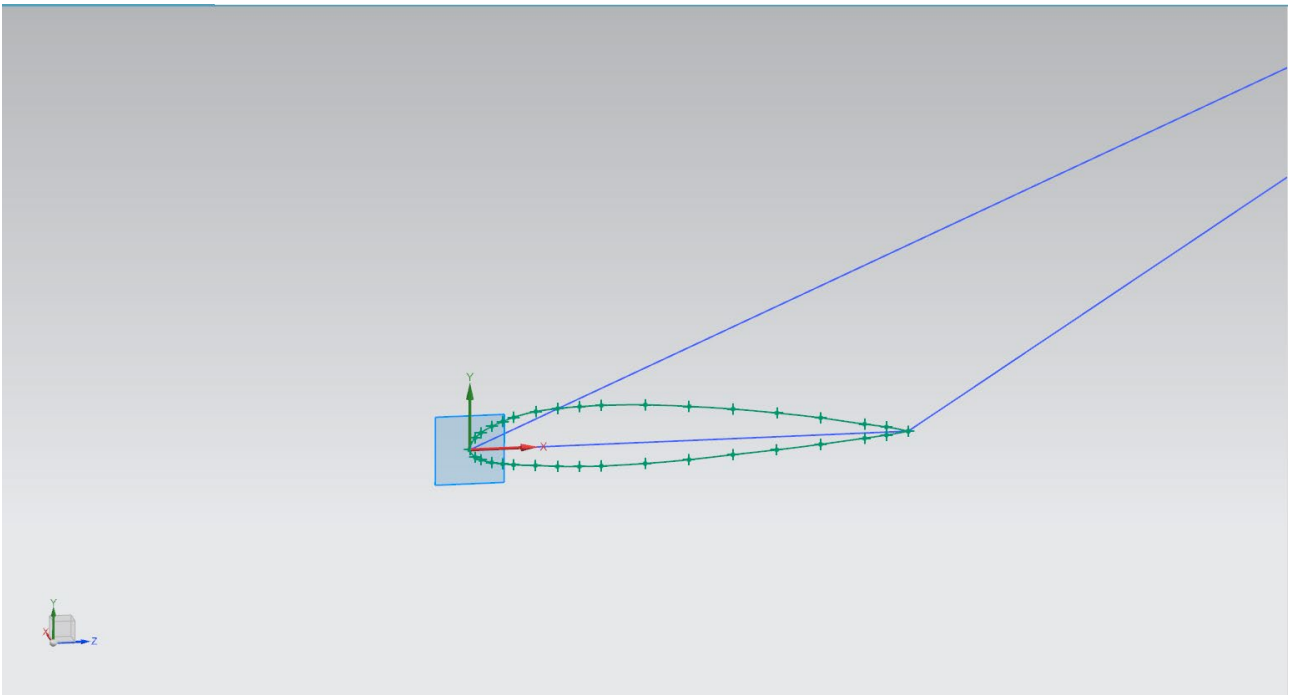


Figure 2.25 – Wing root airfoil

8) Create Wing tip airfoil, Menu → Insert → Sketch in task environment, Create airfoil at tip of the wing planform.

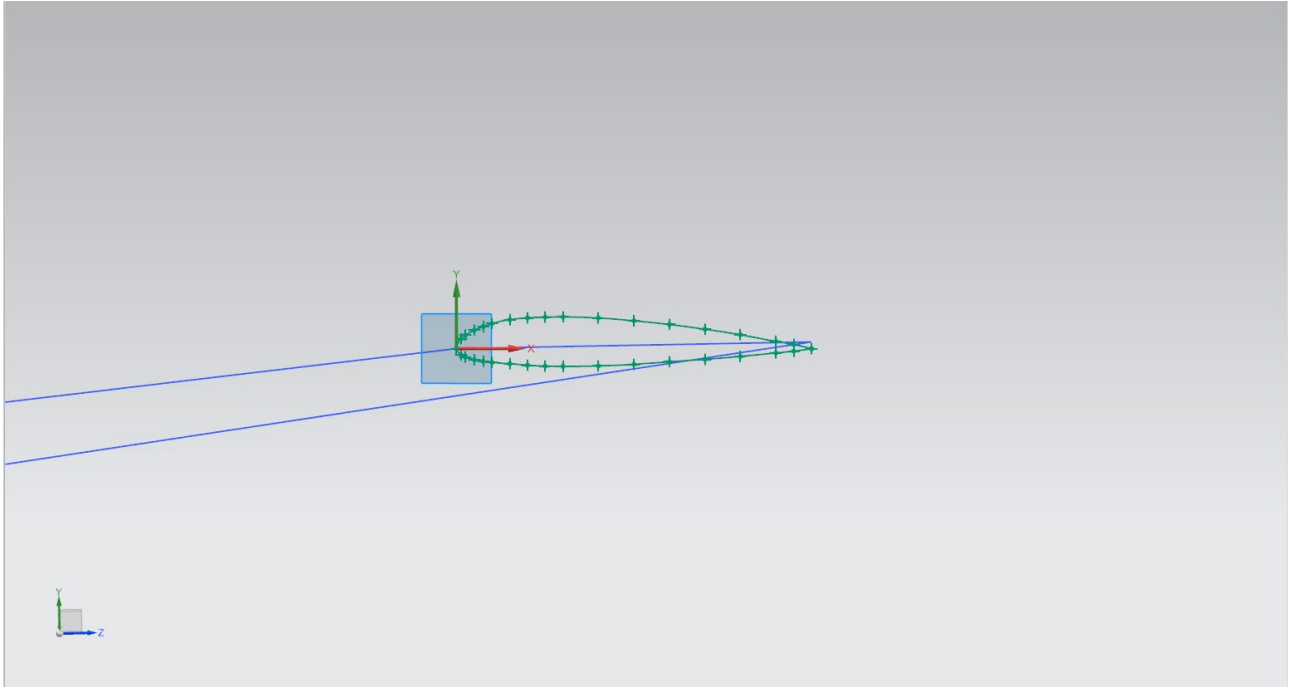


Figure 2.26 – Wing tip airfoil

9) Create upper surface, Menu → Insert → Mesh surface → Through curves.

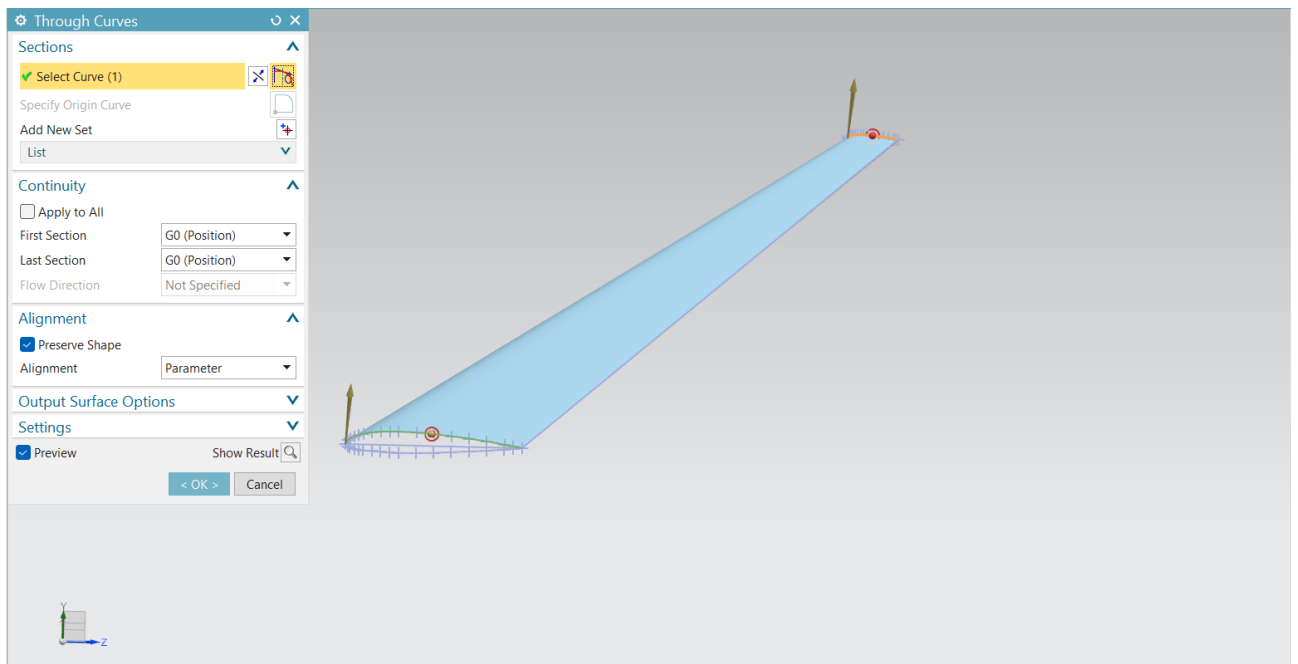


Figure 2.27 – Top surface of the wing

10) Create lower surface, Menu → Insert → Mesh surface → Through curves.

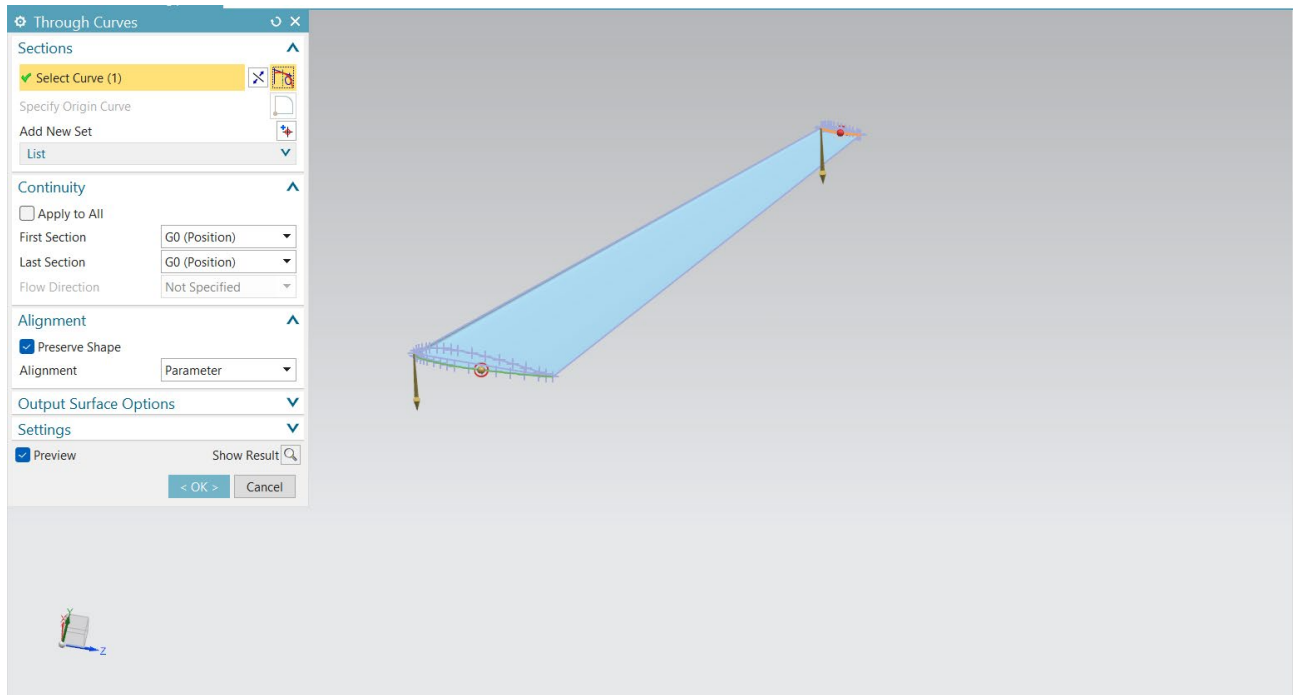


Figure 2.28 – Bottom surface of the wing

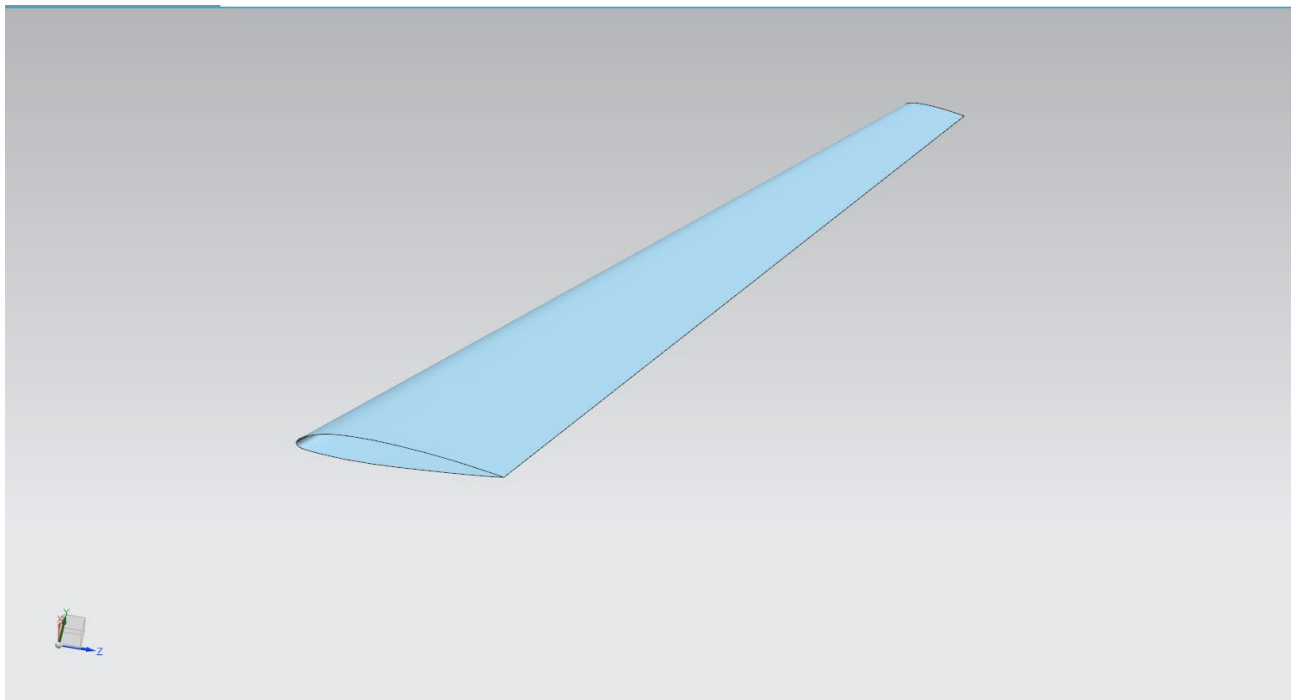


Figure 2.29 – 3-Dimensional model of the surface of the wing planform

11) Creating sketch for winglet, Menu → Insert → Sketch in task environment, creating sketch for winglet.

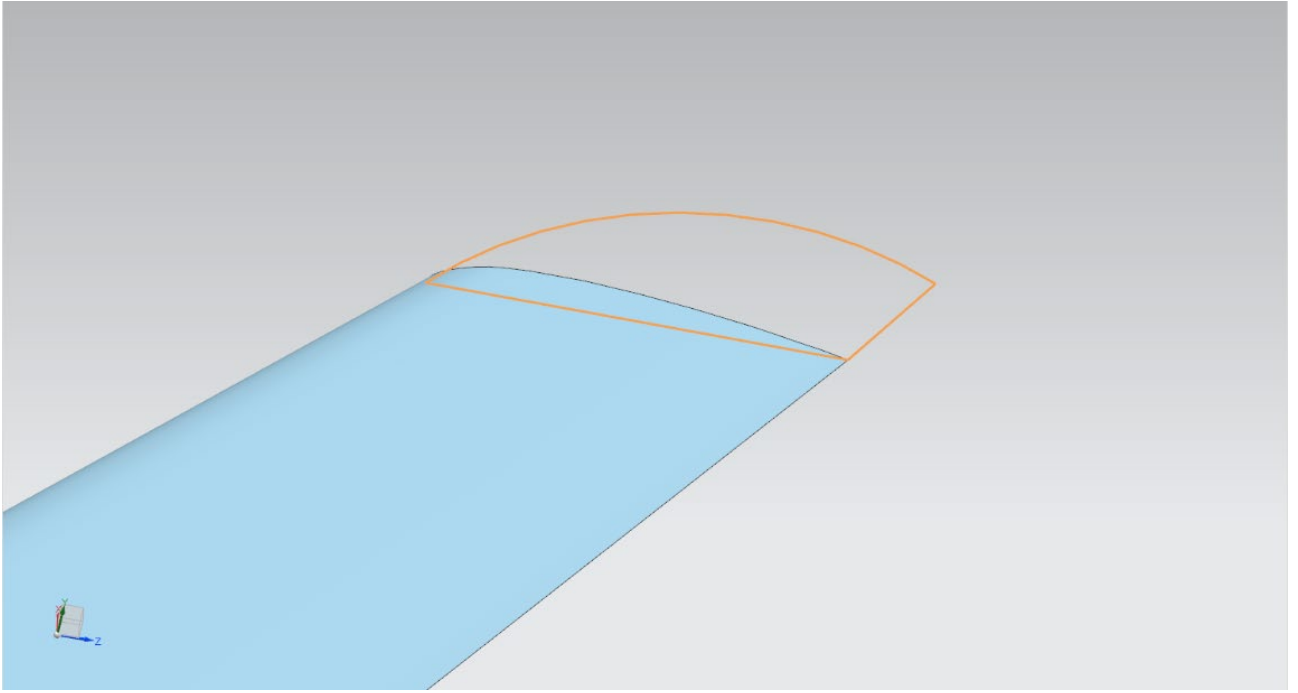


Figure 2.30 – Sketch of winglet

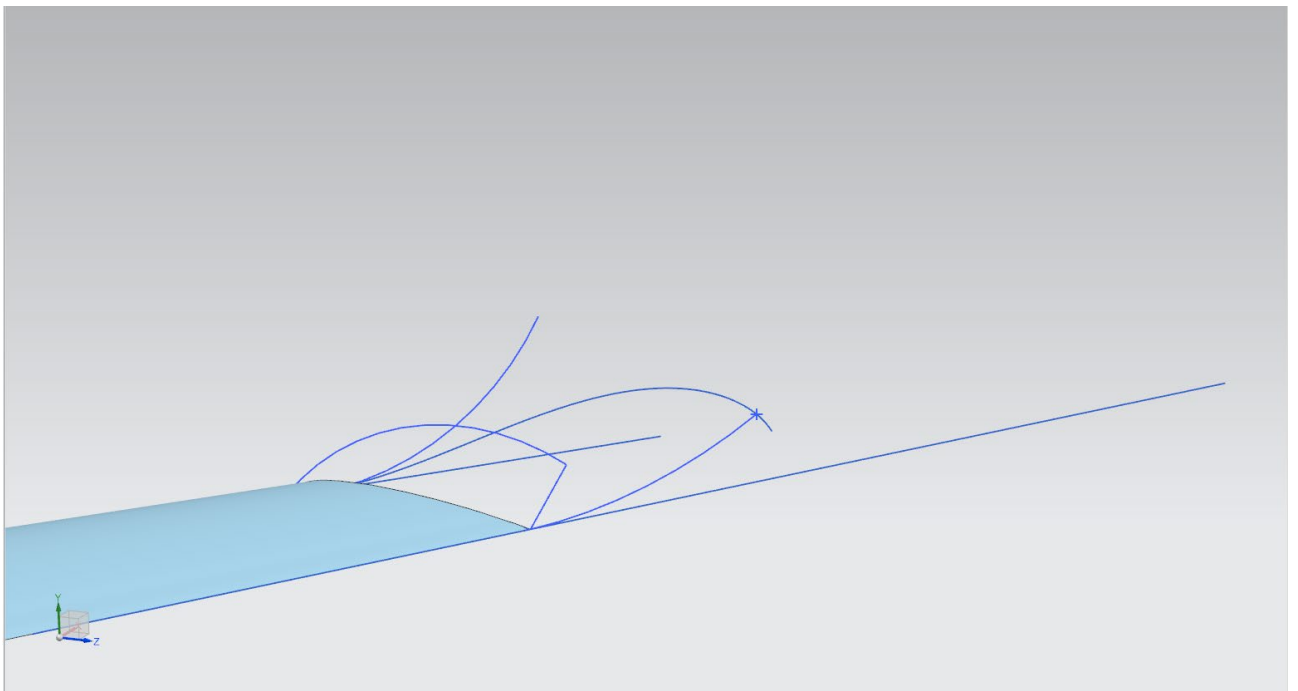


Figure 2.31 – Sketches of winglet using combined projection

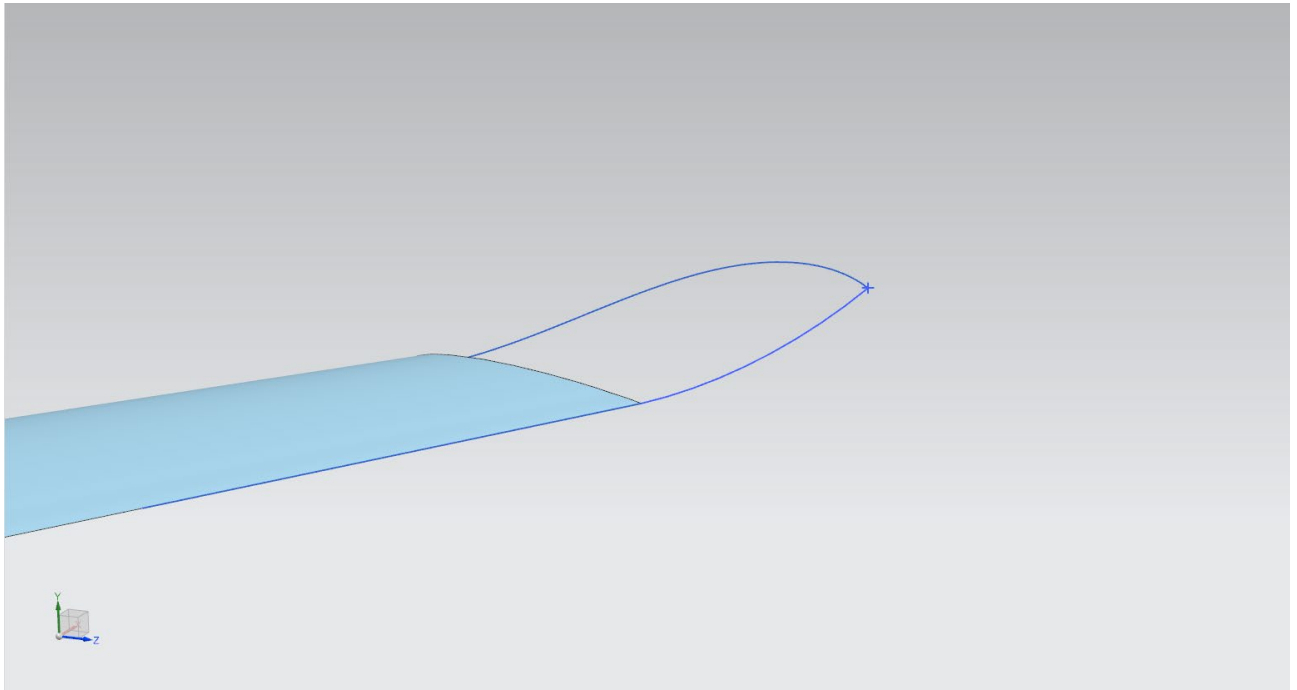


Figure 2.32 – Trimming the unwanted sketches

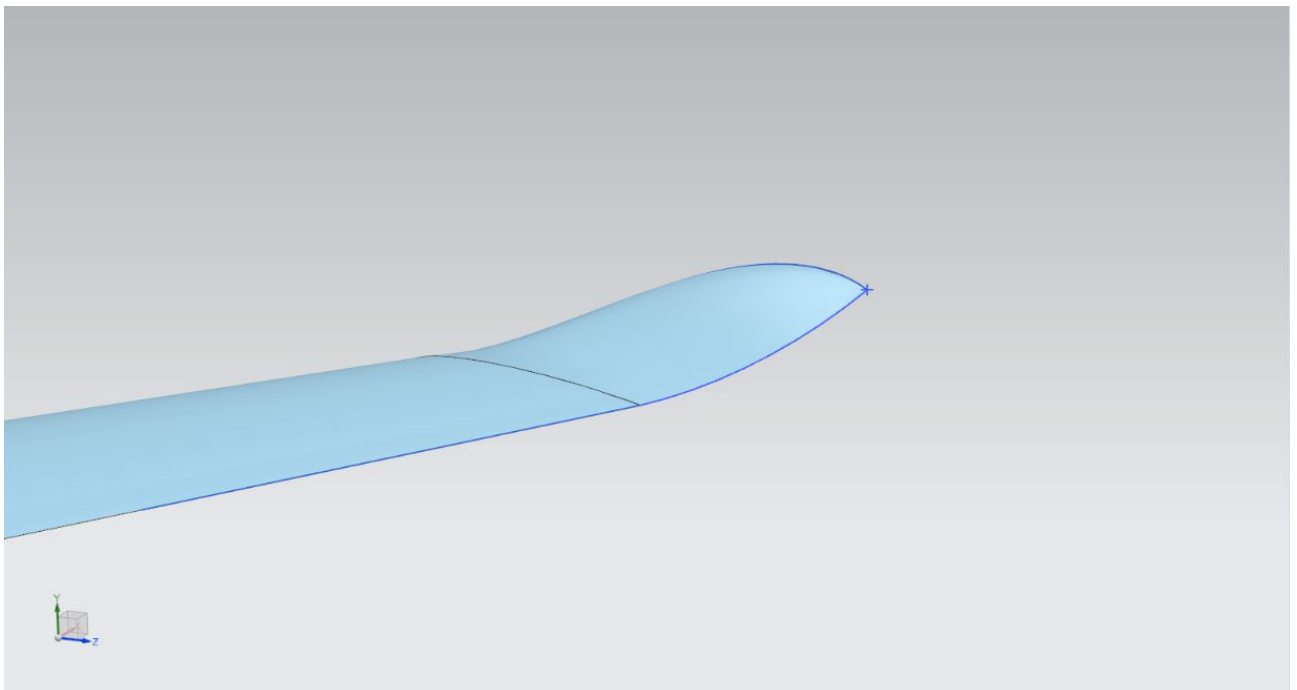


Figure 2.33 – Surface of the winglet

2.2.3 Methodology

In this stage, we are going to modify the winglet design to reduce the noise due to turbulence. The winglet design is modified and analysed in ANSYS Fluent. This software is used to analyze the results of the acoustic power produced by the wings.

In ANSYS, the modified geometry is imported and created the Enclosure and Boolean functions are given. The enclosure is created as cylinder and the radius of the

cylinder is 2.5 m and length of the cylinder is 8 m symmetrically. And meshing is done. The mesh size for this 0.25 m. Meshing is done for creating more accurate results.

In the setup settings, selects Models → Viscous → k – epsilon and in Near -wall treatment select enhanced wall treatment. Models → Acoustics → Broadband Noise Source.

After that select the Boundary Conditions → Select Inlet → Type → Velocity - inlet → Magnitude 75 m/s.

In Solutions select Methods → Scheme → Coupled, in Spatial Discretization the turbulent kinetic energy and turbulent dissipation rate is changed to Second Order Upwind.

In report definitions, determine the Lift and Drag coefficient settings. Then in Initialization → Hybrid Initialization → Initialize.

After initialization is done, select run calculations. Give the iterations up to 10000 and reporting interval 1 and update interval 1. Then select calculate. Then the model is analysed and when the model is converged the calculation is complete.

In result, select contours. In that select Acoustics in drop down list and click display. The result will be shown.

The result is now compared and analyzed. The suitable winglet is selected for aircraft wing.

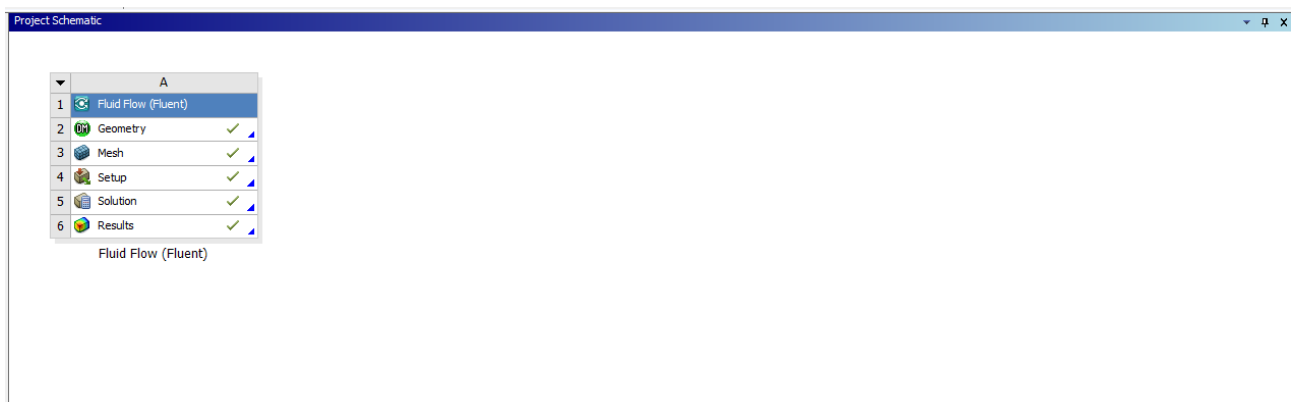


Figure 2.34

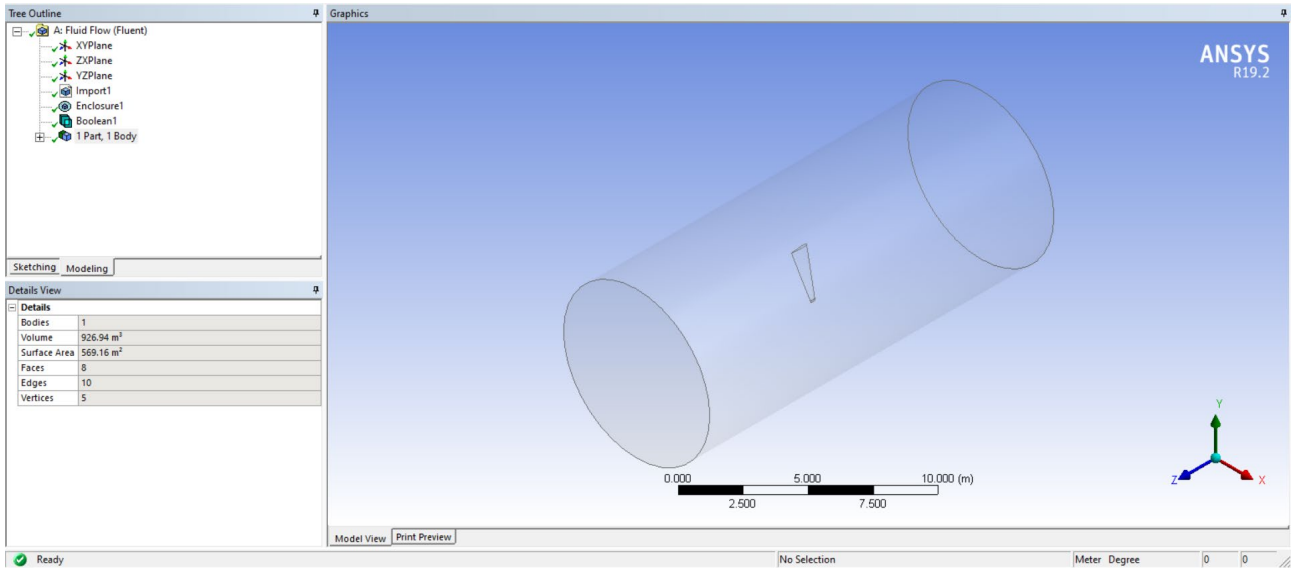


Figure 2.35

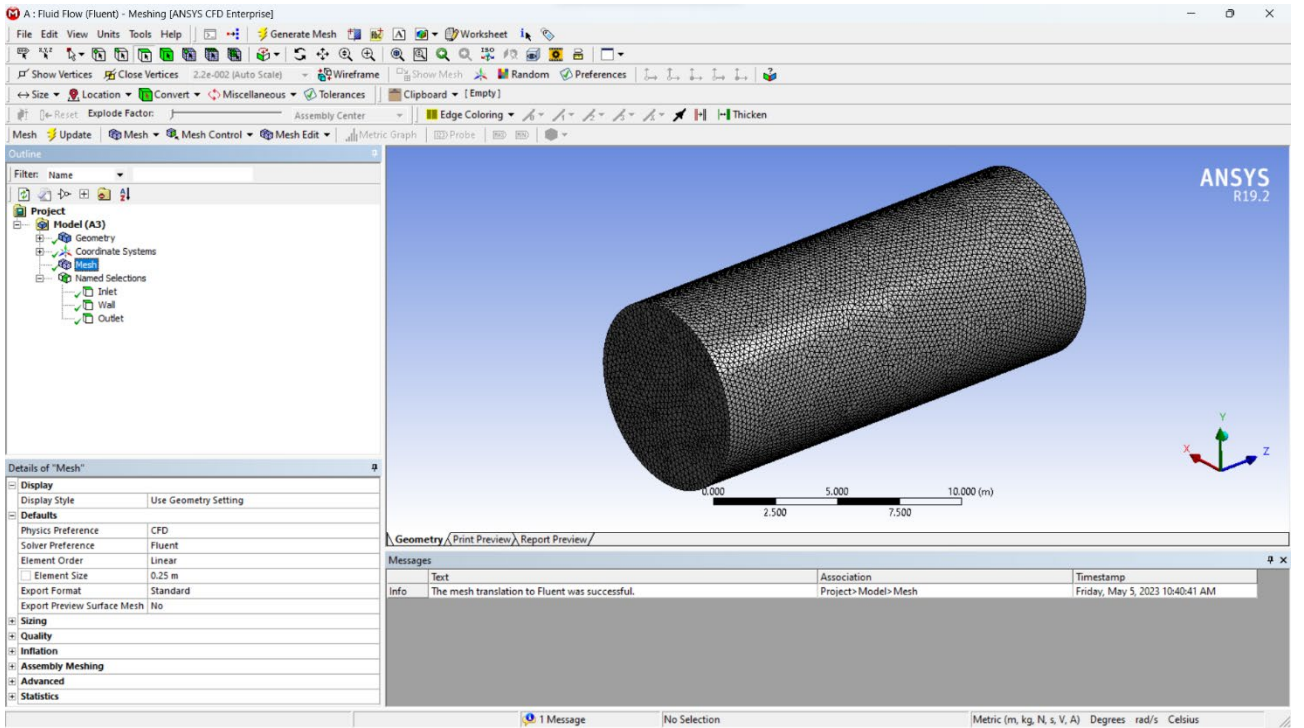


Figure 2.36

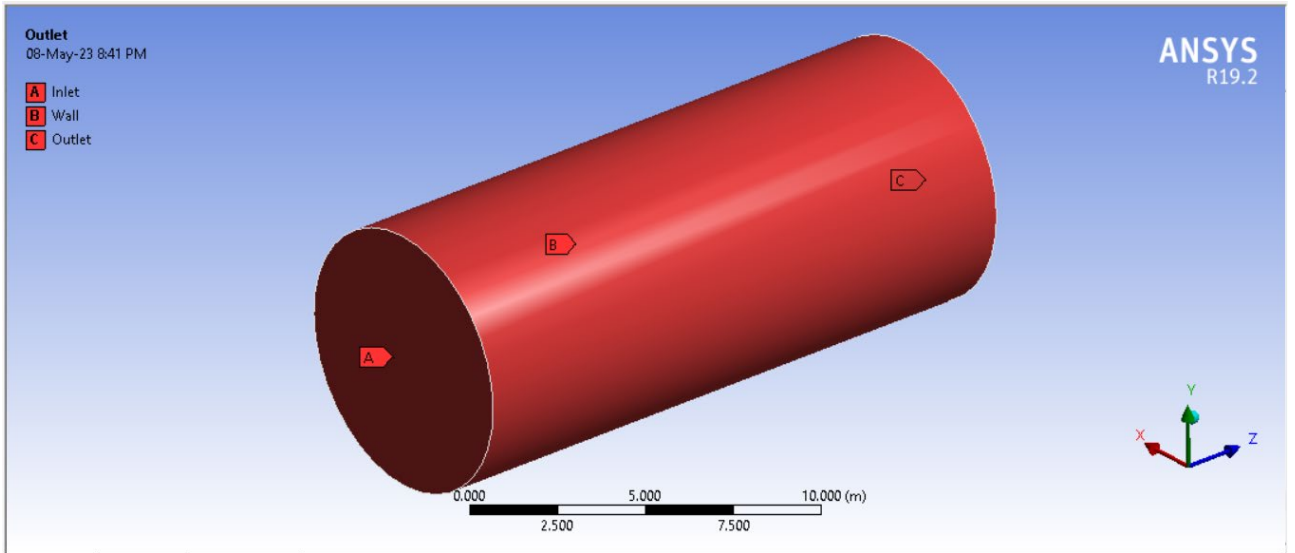


Figure 2.37

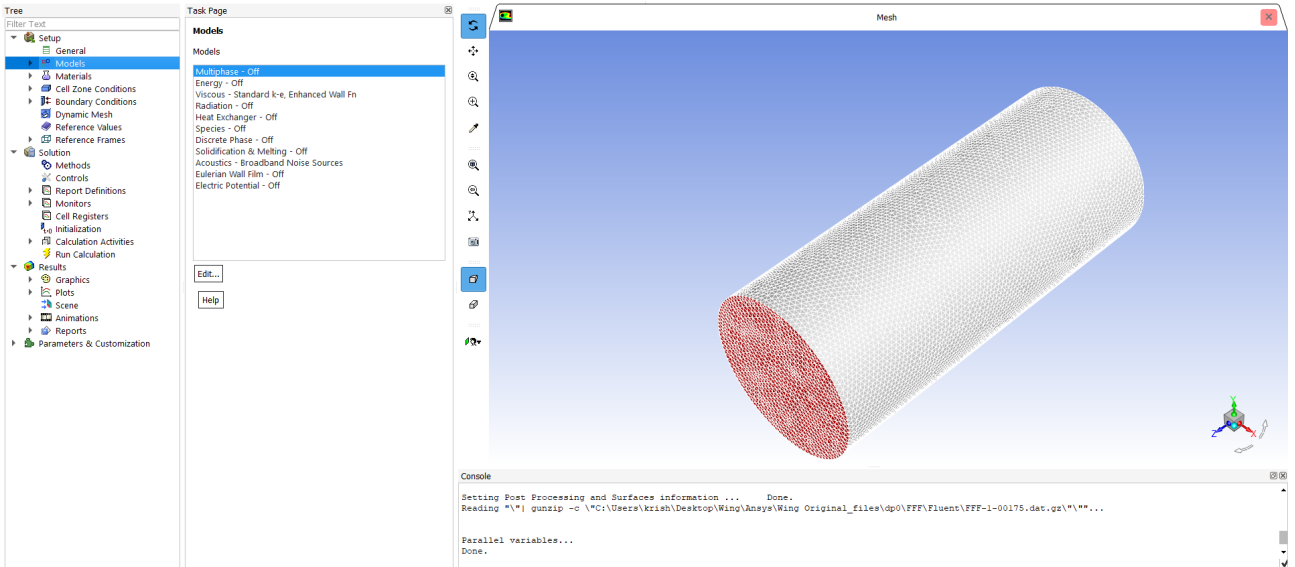


Figure 2.38

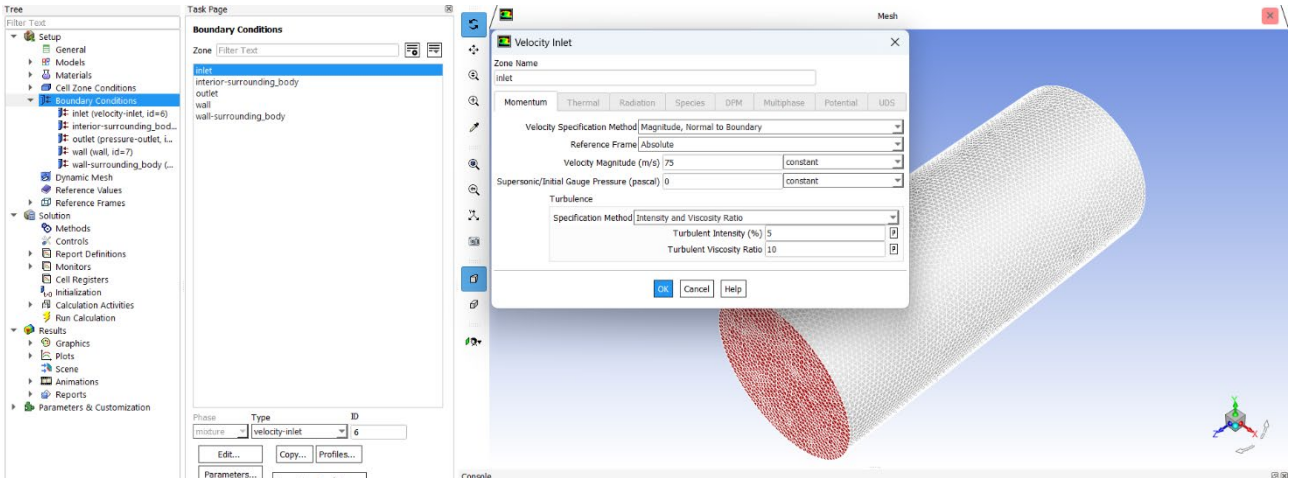


Figure 2.39

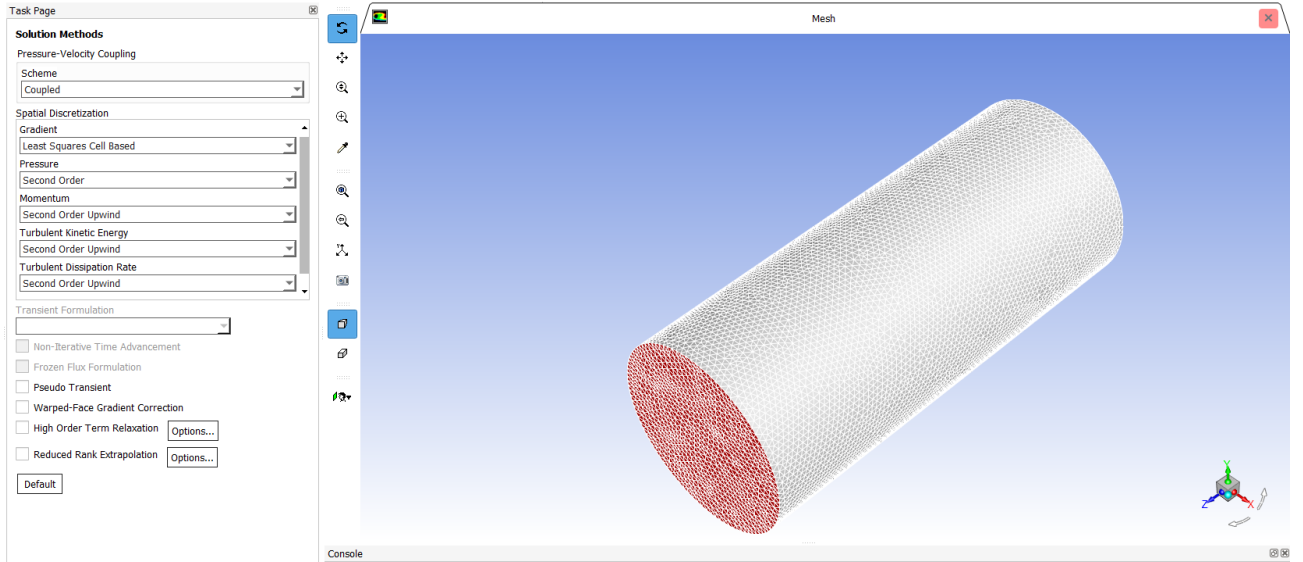


Figure 2.40

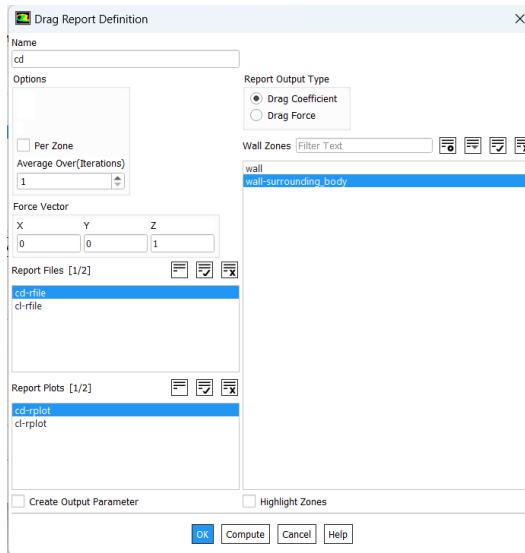


Figure 2.41

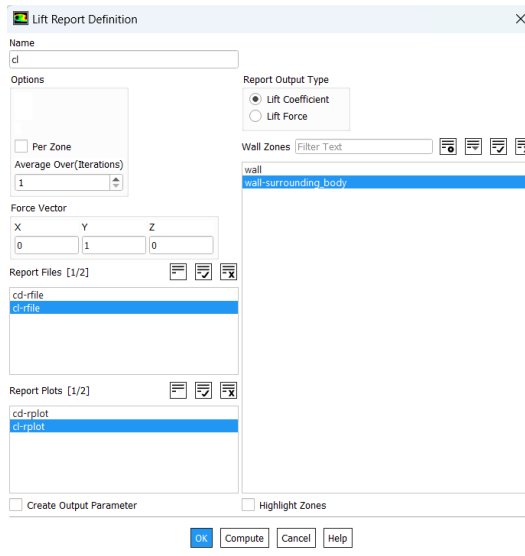


Figure 2.42

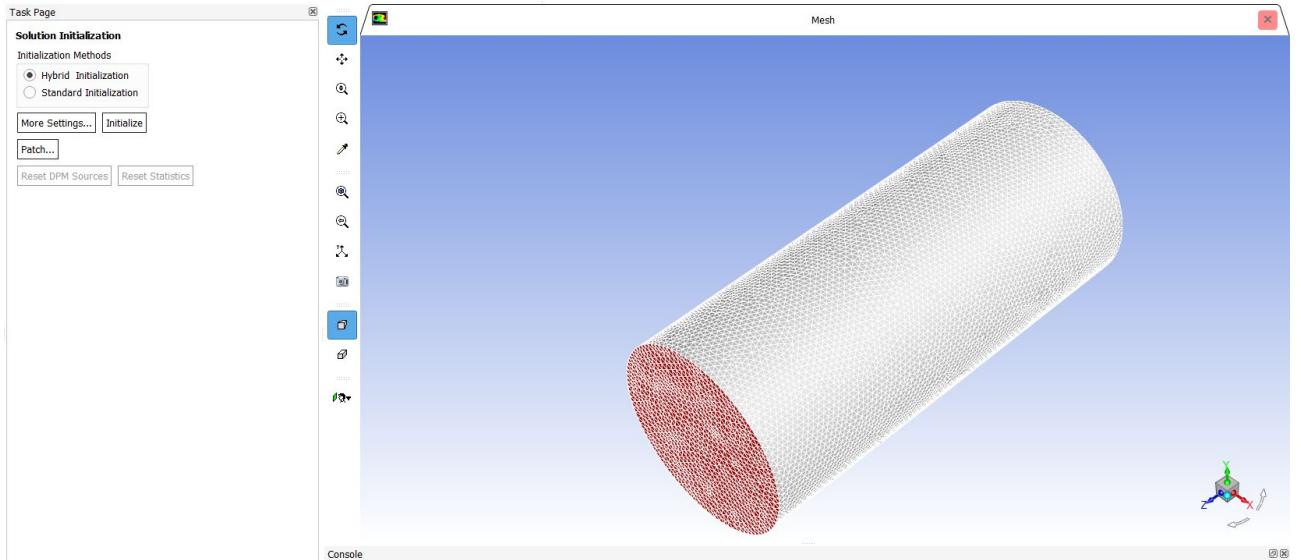


Figure 2.43

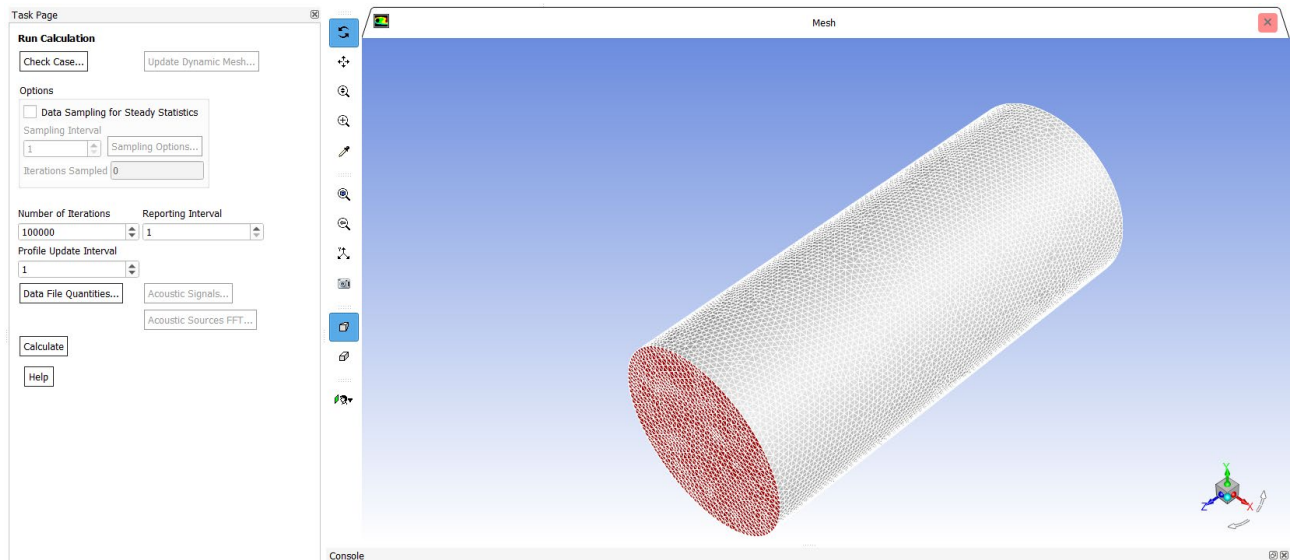


Figure 2.44

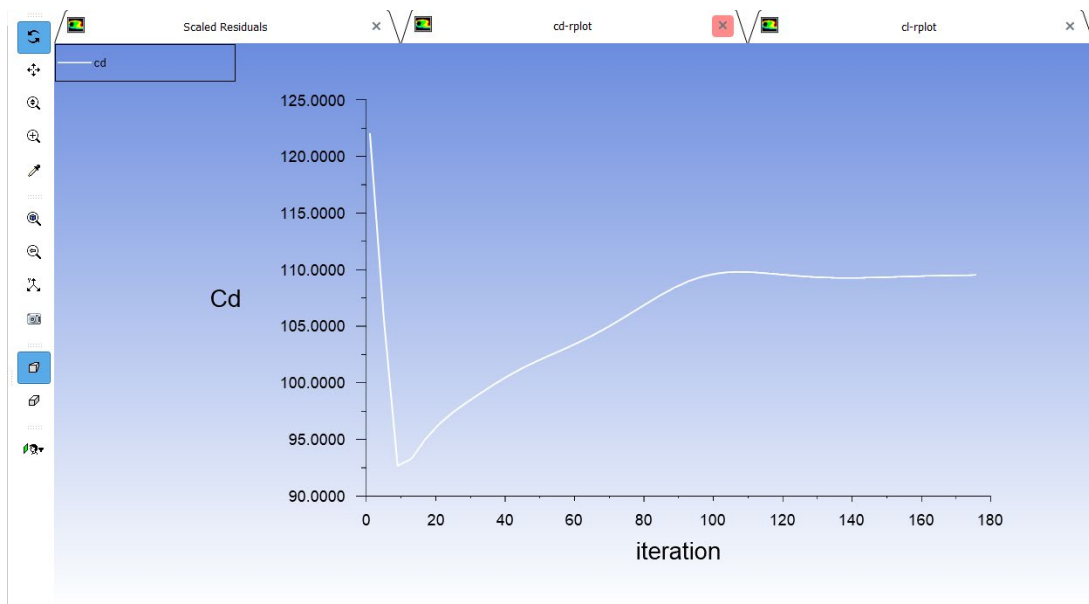


Figure 2.45

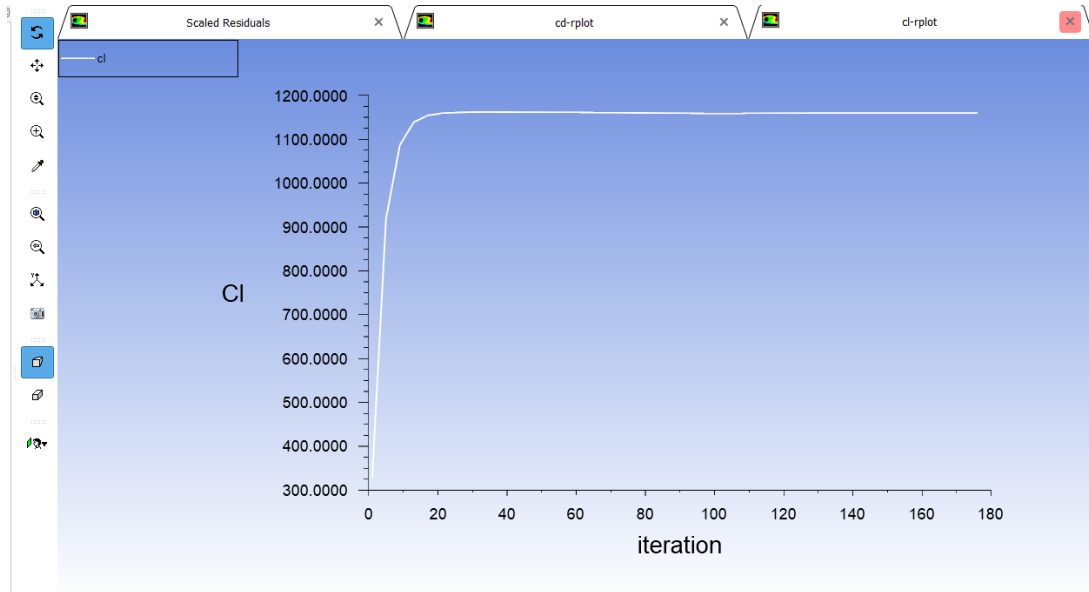


Figure 2.46

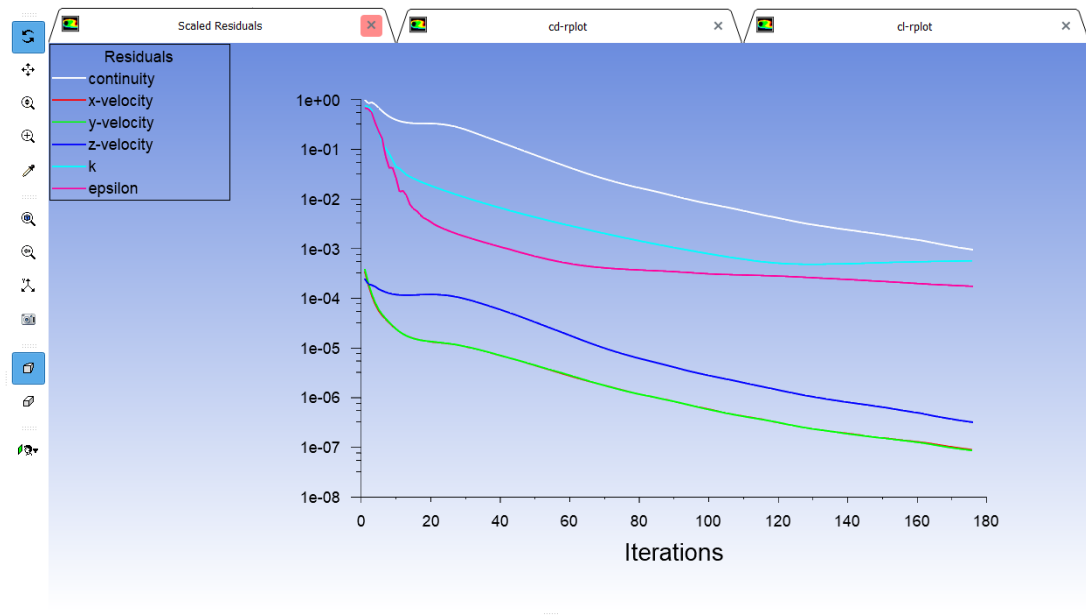


Figure 2.47

From Figure 2.34 to Figure 2.47 – Steps involved in doing the analysis

2.2.4 Comparison between Winglets

In this we are going to compare the result between the existing aircraft winglet design and modified winglets. In this we are going to scale down the model up to 0.25%, because the analysis result will take more time and the system configuration is important to run analysis.

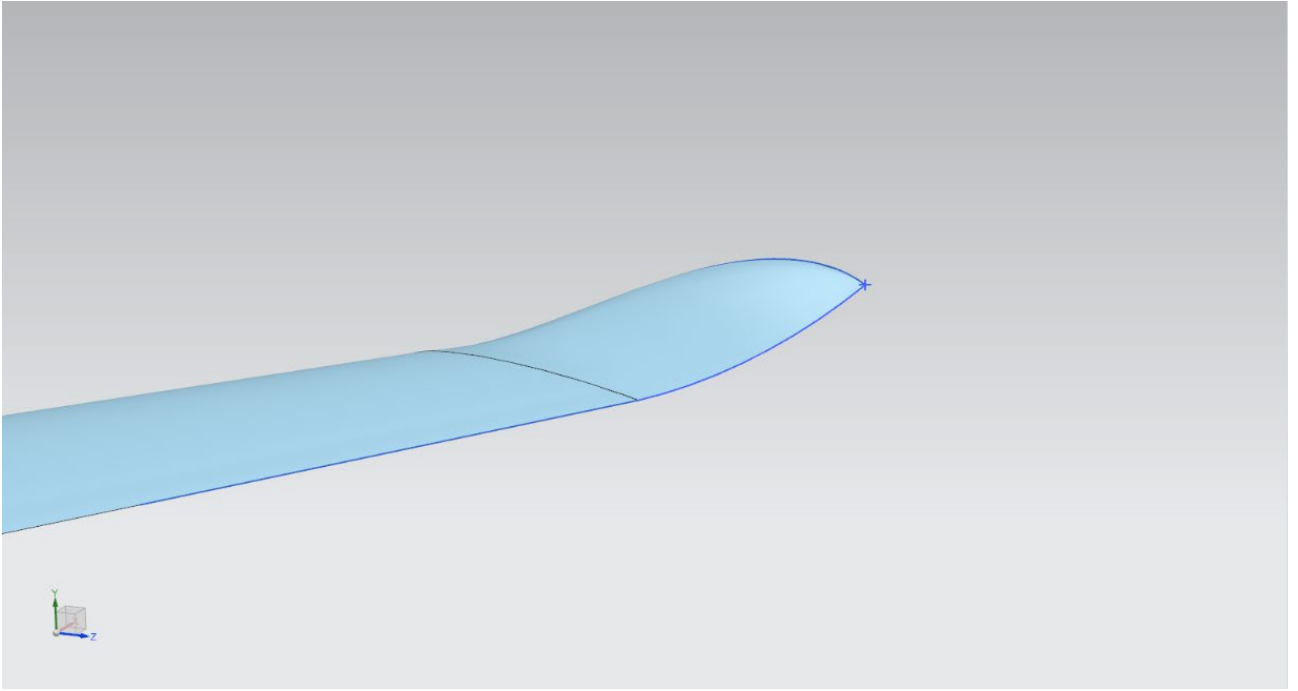


Figure 2.48 – Existing winglet design

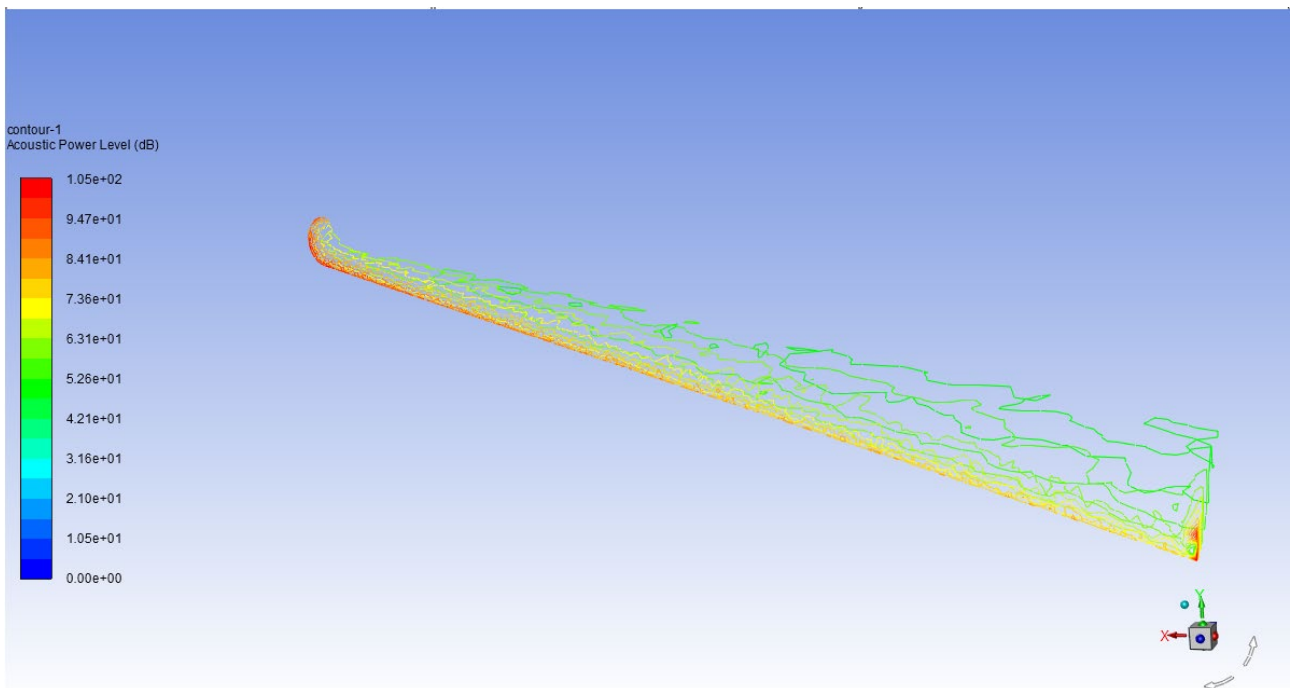


Figure 2.49 – Noise absorbed by existing winglets

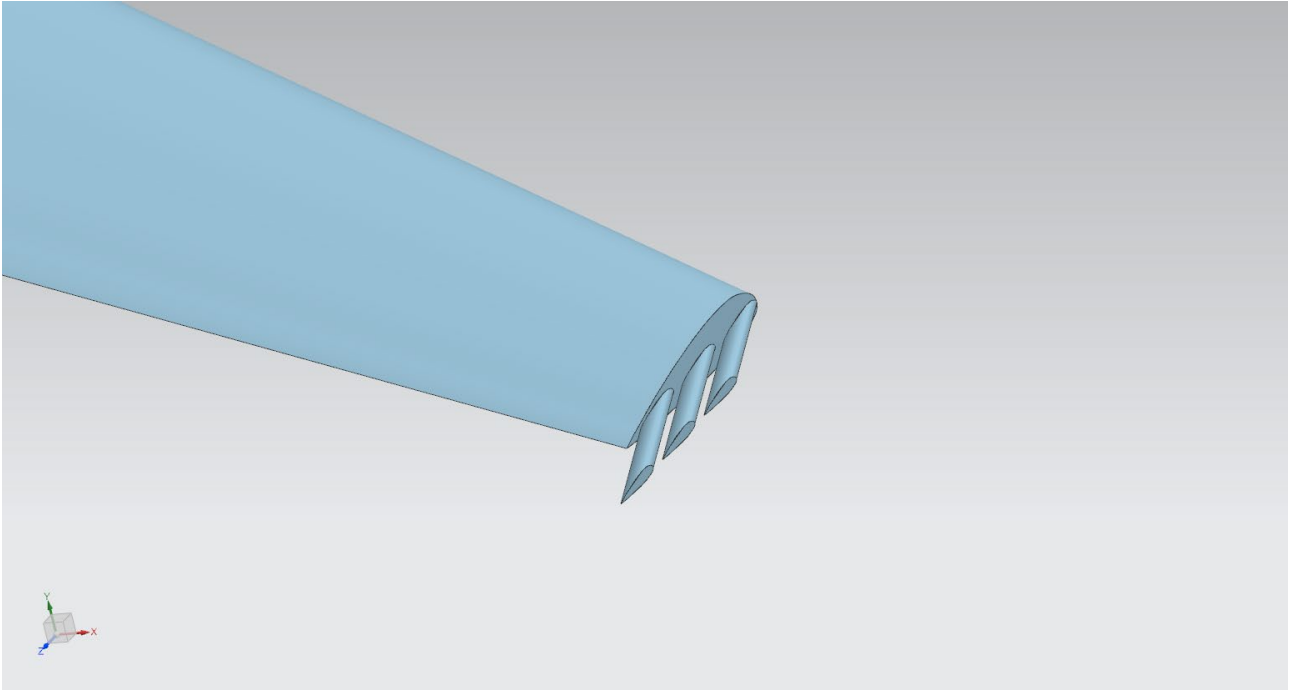


Figure 2.50 – Winglet 1

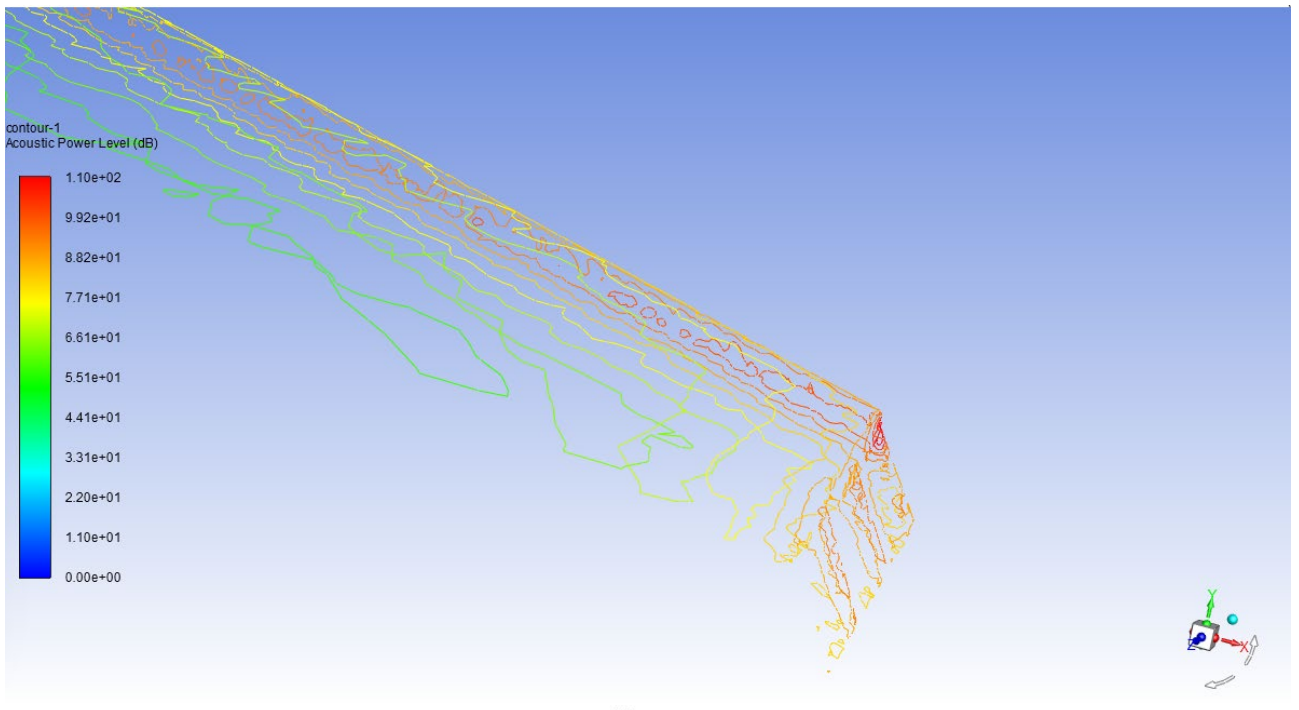


Figure 2.51 – Noise absorbed by winglet 1 - 110.194 dB

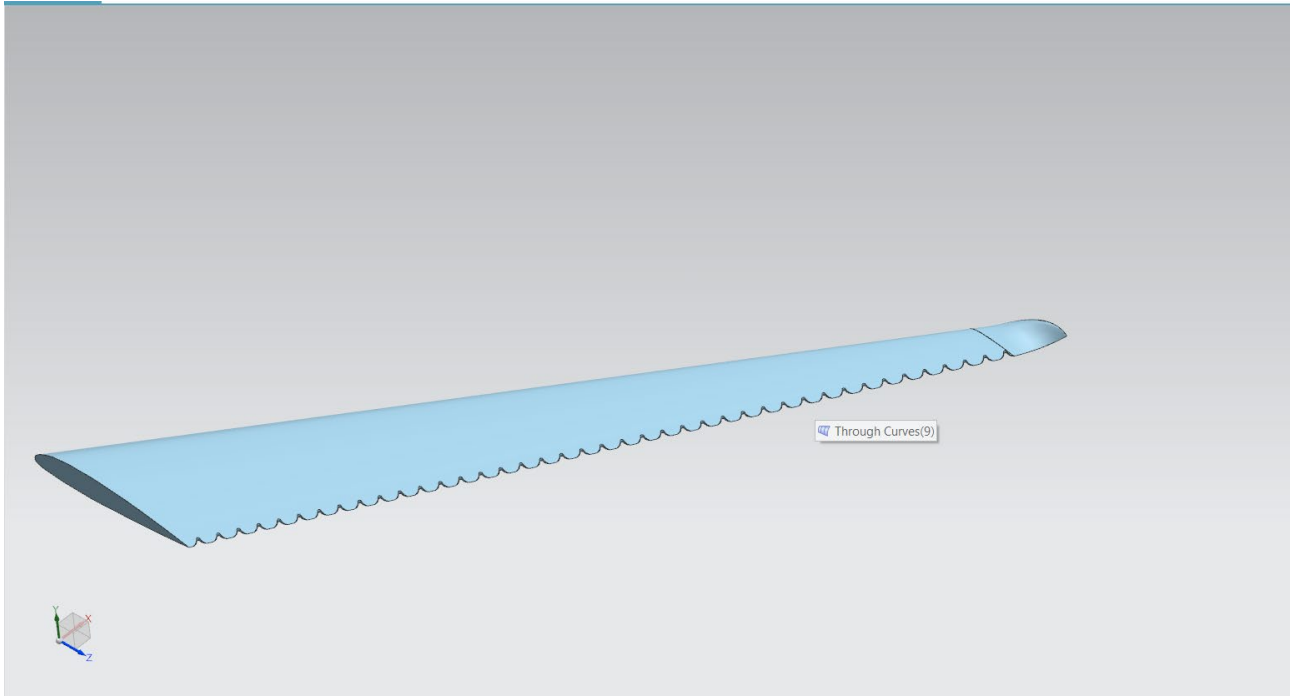


Figure 2.52 - Winglet 2

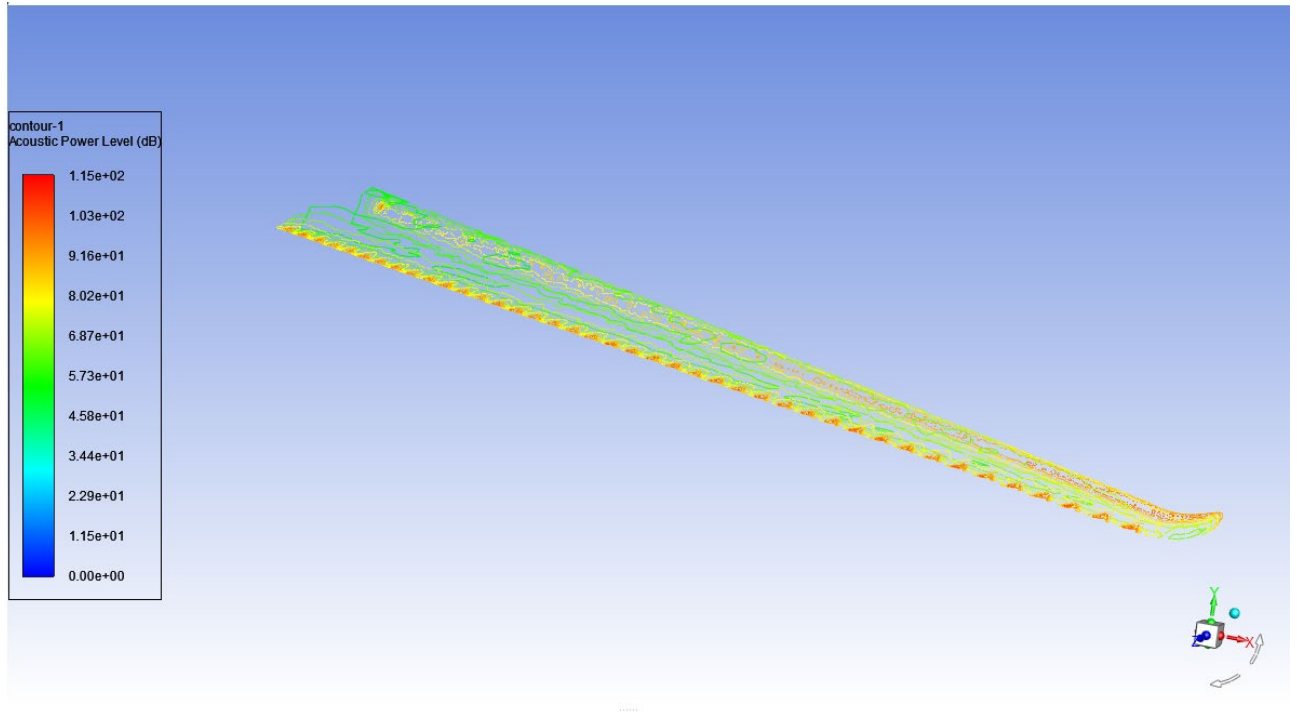


Figure 2.53 – Noise absorbed by winglet 2 – 114.5 dB

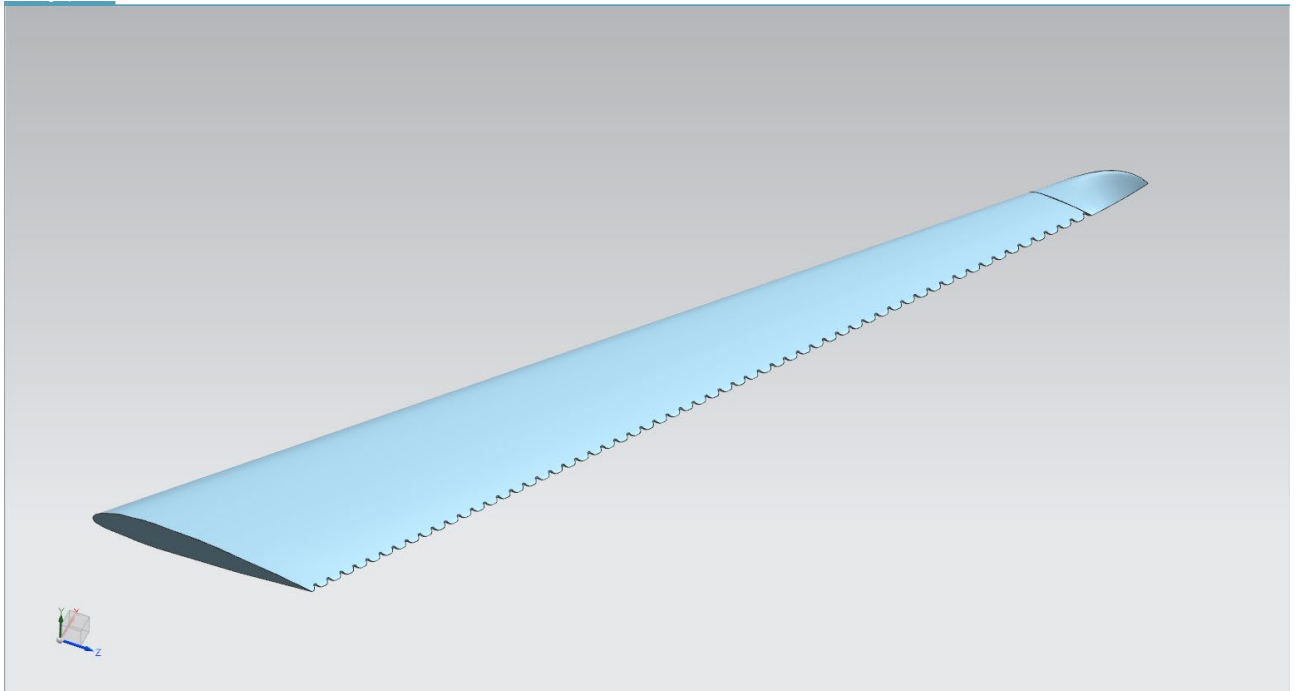


Figure 2.54 – Winglet 3

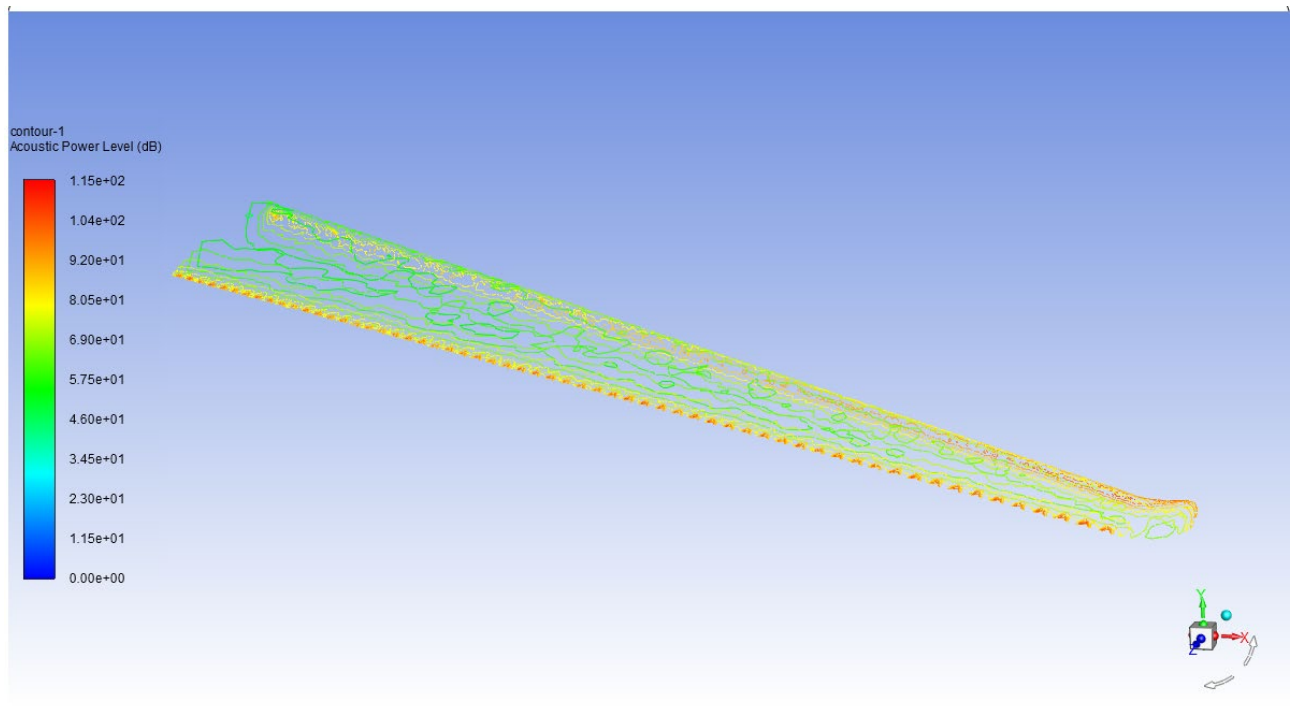


Figure 2.55 – Noise absorbed by winglet 3 – 115.04

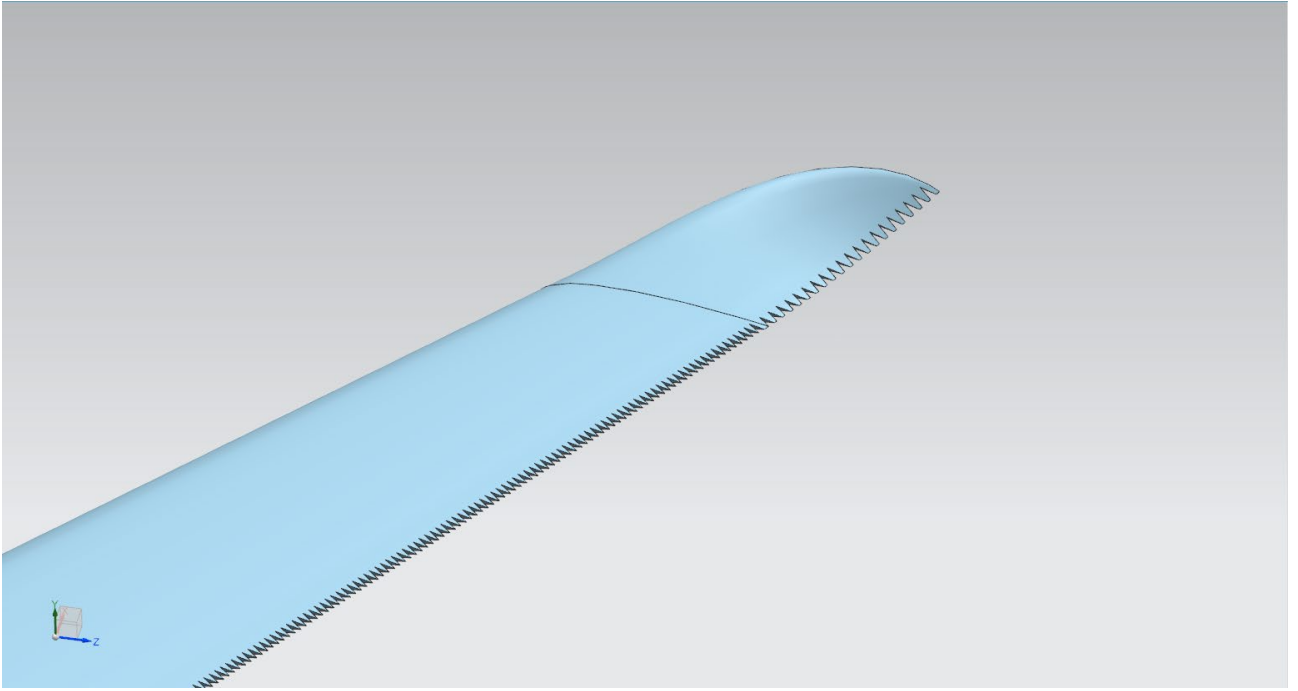


Figure 2.56 – Winglet 4

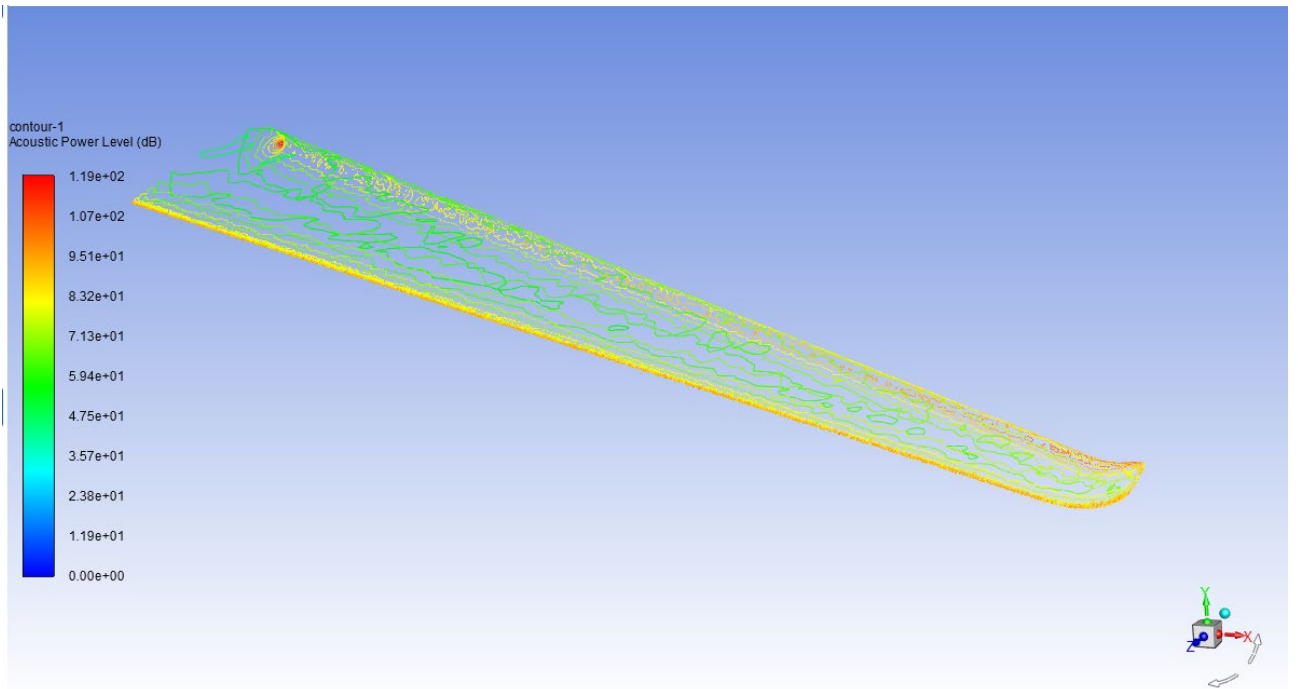


Figure 2.57 – Noise absorber by winglet 4 – 118.87 dB

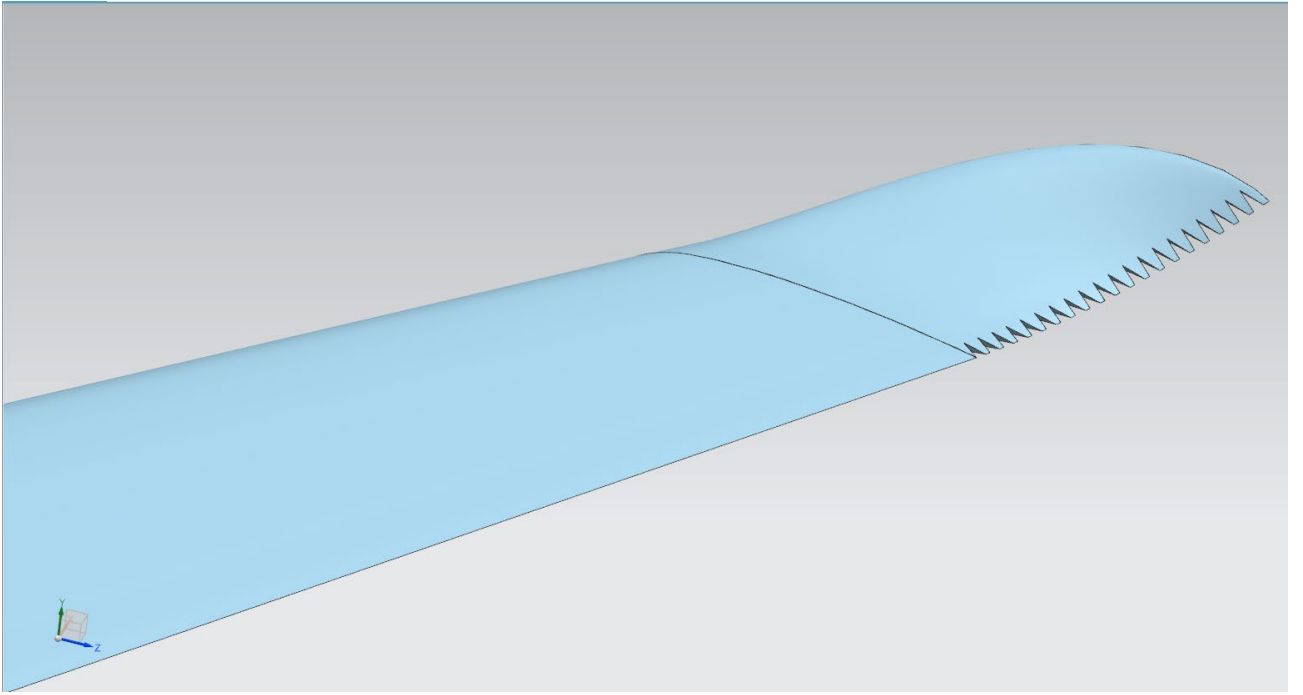


Figure 2.58 – Winglet 5

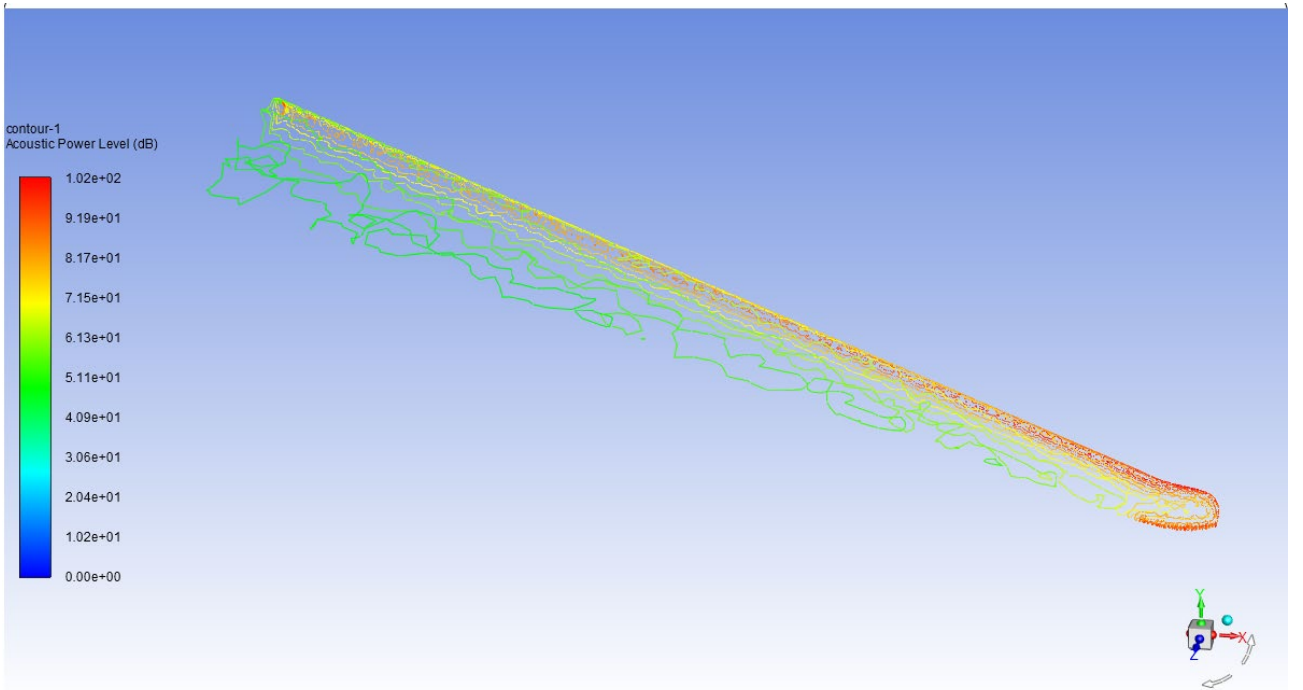


Figure 2.59 – Noise absorbed by winglet 5 – 102.15 dB

2.2.5 Results

Table 2.3 – Comparative analysis of the winglets

Winglet Designs	Velocity (m/s)	Acoustic Power (dB)
Existing Winglet	75	105.02
Winglet 1	75	110.194
Winglet 2	75	114.5
Winglet 3	75	115.04
Winglet 4	75	118.87
Winglet 5	75	102.15

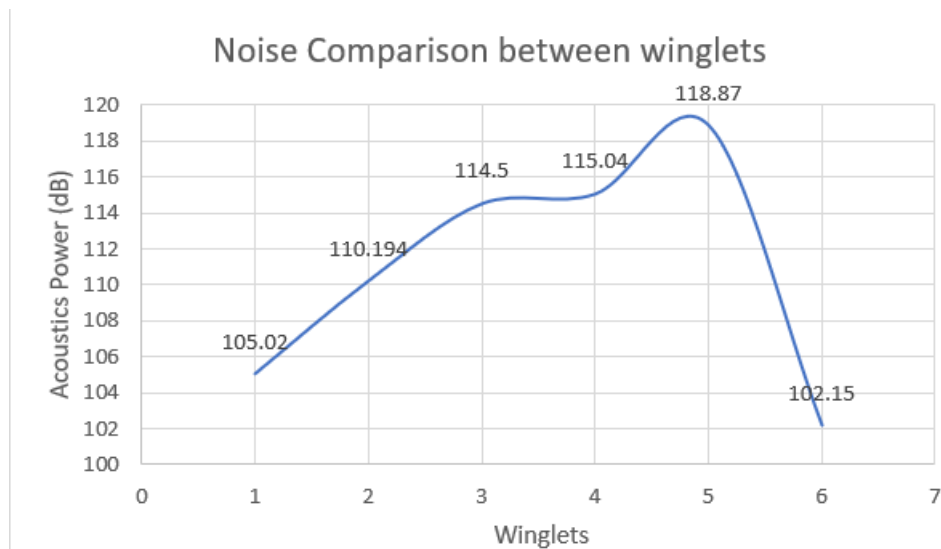


Figure 2.60 – Noise comparison between Winglets

2.2.6 Conclusion

Winglet is designed to be reduced for noise reduction. In this we have modified the design of the wing and winglet. Among this 5 types of design, we have analysed each wing with velocity of 75 m/s.

By comparing the results, Winglet 5 has suitable range of acoustic power with 102.15 dB. Which is less than Existing Winglet, it has 105.02 dB.

3 ECONOMIC SECTION

3.1 Competitive advantages of the designed aircraft and assessment of its possible volumes of its implementation in the sales markets

3.1.1 Characteristic of tactical and economic indexes of the designed long-range passenger aircraft as a commodity product

The main indicators affecting economic indicators are:

- take-off mass of the aircraft, $m = 117977$ kg
- payload, $m_{pl} = 18000$ kg;
- passenger capacity, $n_{pass} = 120$
- board flight-navigation equipment and automatic control of the aircraft provides: automatic and director control (functions "Autopilot" and "Flight Director") in the following flight control modes:

- 1) Automatic speed control (function "Automatic traction") in the modes;
- 2) Category IIIa automatic approach;
- 3) Speed protection functionality to withstand flight speed in the VLS – VMS range, calculated for the current configuration and flight conditions;
 - an indication and recording system allow on-board data to be recorded on a standard memory card of the PCMCIA type (removable memory card) and automated wireless transmission of aircraft data on the ground to calculate production and forecast the remaining aircraft resource;
 - required field length 1500 m;
 - maximum flight Mach number and cruising flight speed $M = 0.85$ and $V_{cruise} = 840$ km/h;
 - mass of aircraft structure $m_{st} = 19600$ kg

3.1.2 Consumer qualities of the aircraft, affecting the competitive advantages and economic costs when designing aircraft structures in the Design Bureau

Designing aircraft has a lower required mass of fuel for the flight with a maximum payload on the flight range $L = 6400$ km its $m_{fuel} = 14446$ kg, which is less than that of analogues.

The equipment allows take-off and landing at the aerodrome classes A, B, C, D according to the classification in the CIS countries and classes from 3C to 4E according to the international classification. Indication and recording system provide an opportunity to study the operating conditions of already flying aircraft, to conduct improvements to the design and equipment on the modifications of the aircraft for operation that is more efficient and greater profit.

Mass of structure $m_{st} = 19600$ kg less than that of analogue aircraft, which reduces the metal consumption and the cost of raw materials for the production of the designed aircraft.

Market analysis based on marketing research and determining the volume of possible sales of finished aircraft.

The Global Commercial Aviation Market is projected to register a CAGR of 7.65%

- Largest Market by Sub-Aircraft Type - Passenger Aircraft : The sub-aircraft type segment is dominated by passenger aircraft. Increasing air passenger traffic and the growing middle-class population in emerging countries are driving the market's growth.
- Largest Market by Body Type - Narrowbody Aircraft : A fleet of narrowbody aircraft adds flexibility in terms of fleet management and helps reduce the operating costs of the airlines, thereby resulting in its rapid adoption.
- Largest Market by Country - United States : The country is expected to register a major revenue share during 2022-2028 due to increasing levels of air transportation and a rising number of commercial aircraft orders from major airlines.
- Largest Market by Region - North America : Rising domestic and international air traffic levels in the region are driving the airlines to procure more aircraft, thereby boosting the growth of the regional commercial aircraft market.

According to the UNWTO, tourism contributes 10% of the world's GDP, making it one of the main sources of income in the modern world, with 57% of cross-border travellers using aircraft. In the last 15 years, the number of passengers in commercial aviation has doubled.

Over the next 20 years, Airbus estimates that more than 38,000 new airplanes will be delivered, some of which will replace the current fleet's more aged aircraft.

The COVID-19 pandemic affected air passenger traffic globally in 2020, reducing flight activity and impacting airline cash flows. As a result, most airlines decided to cancel or defer their aircraft orders. However, the commercial aviation industry recovered gradually in 2021, which led to a significant increase in aircraft deliveries compared to 2020. Airlines are looking for aircraft with better fuel efficiency and range, and the development of newer aircraft will help the OEMs attract more airline customers in the years to come.

Since the domestic passenger demand is anticipated to return to pre-COVID-19 levels earlier than the international passenger demand, the market for narrow-body aircraft is anticipated to rebound faster than the demand for wide-body aircraft. The 737 MAX's return to service in late 2020 may also support the expansion of the narrowbody market.

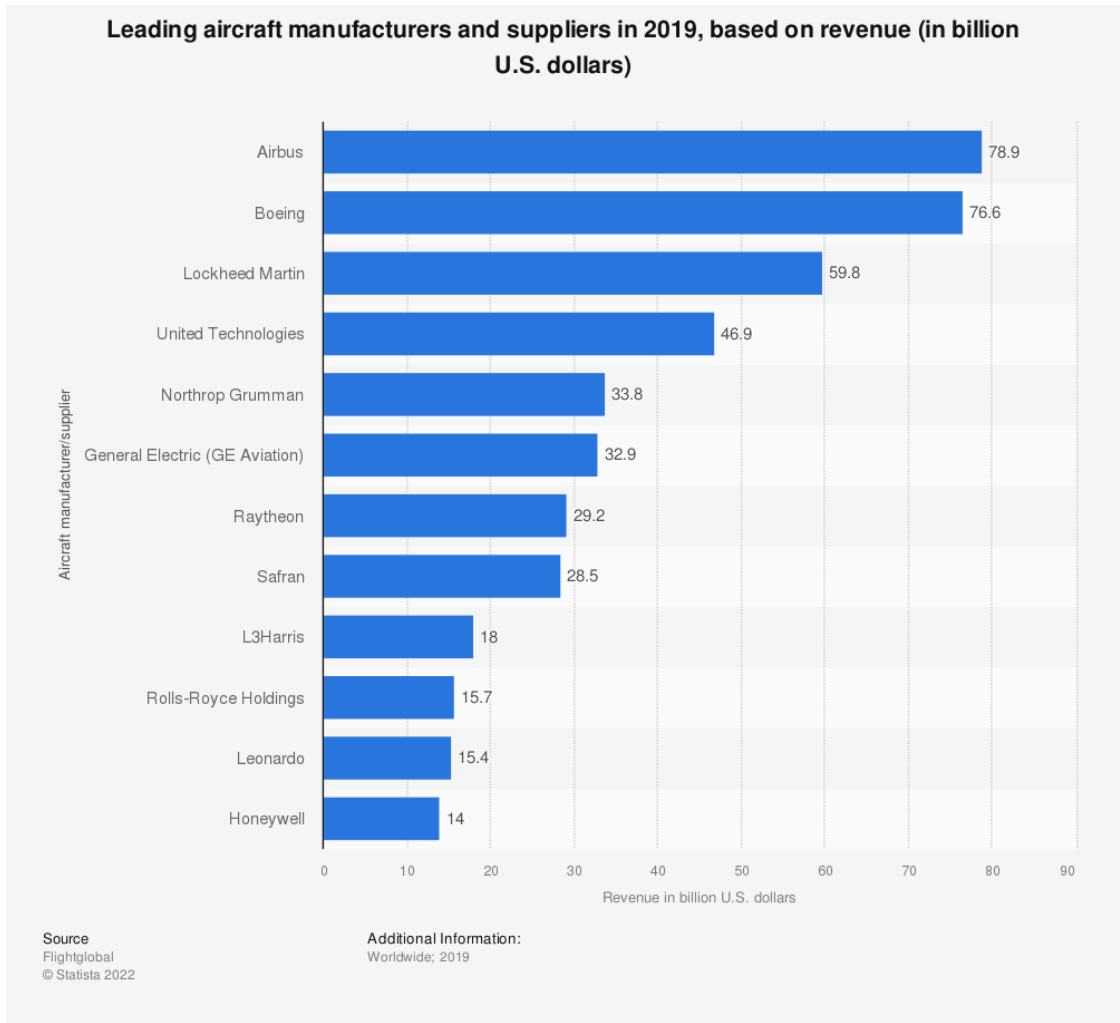


Figure 3.1

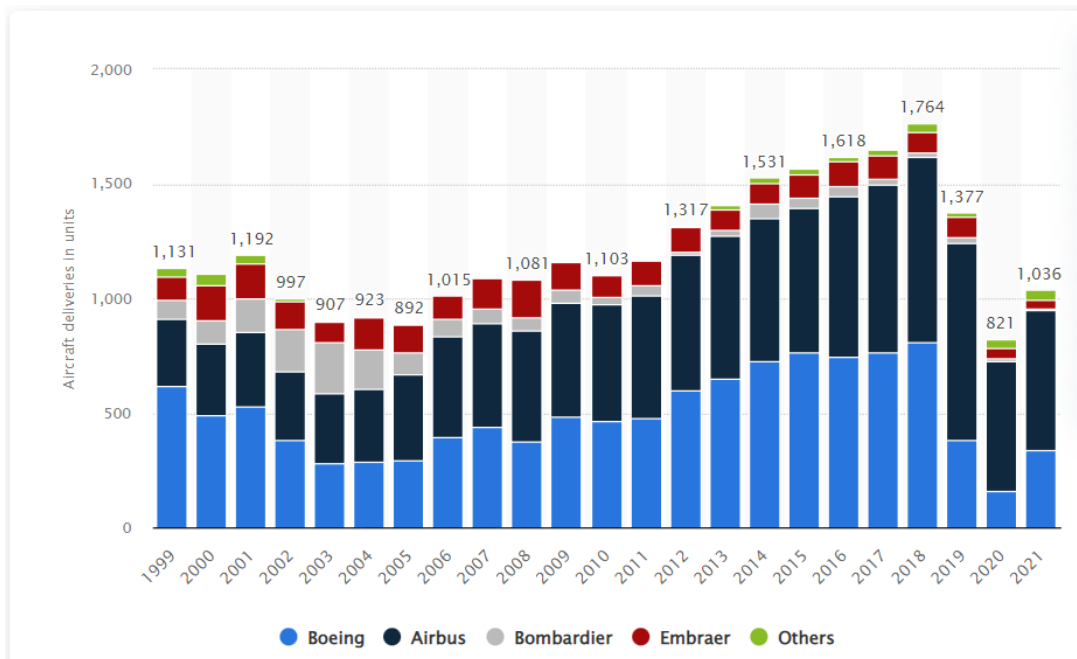


Figure 3.2

Figure 3.1 & Figure 3.2 – Distribution of commercial aircrafts

3.2 Initial data for the calculation of technical and economic performance indicators for the creation of an aircraft

3.2.1 Data for calculating costs in the experimental design bureau

To calculate the costs in the experimental design bureau, mass characteristics of the aircraft structure and equipment, speed characteristics, namely the maximum flight Mach number and maximum flight speed will be needed V_{max} , km/h.

Mass characteristics of the aircraft, taken from this note:

- $m_{airfr} = 19600$ kg – mass of airframe;
- $m_{eq} = 2700$ kg – mass of equipment.

Speed characteristics taken from this note:

- $M_{max} = 0.9$ – maximum Mach number of aircraft;
- $V_{max} = 870$ km/h.

3.2.2 Data for calculating the costs of mass production of aircraft

To calculate the cost of mass production, you will need the relative masses of the structure of the parts of the aircraft, the annual output of the aircraft, the mass of the crew, power plants, and airframe.

Mass characteristics of the aircraft, taken from this note:

- $m_w = 27370$ kg – wing structure mass;
- $m_{fus} = 24990$ kg – fuselage structure mass;
- $m_{TU} = 4970$ kg – tail unit structure mass;
- $m_{LG} = 12670$ kg – landing gear mass;
- $m_{crew} = 500$ kg – crew mass;
- $m_{pp} = 7000$ kg – power plant mass;
- $m_{airfr} = m_{st} = 19600$ kg – airframe mass;
- $m_{eq} = 2700$ kg – mass of aircraft equipment;
- $m_{empt} = 18000$ kg – empty mass.

Annual aircraft production $N = 53$ machines.

The number of engines installed on one aircraft is equal to two.

3.3 Calculation of the main technical and economic indicators of design and production of aircraft

3.3.1 Calculation of costs of the experimental design bureau

Preliminary enlarged determination of costs carried out at the design stage. Costs at the stage of transferring documentation to a serial plant can be neglected. Therefore, the calculation of costs carried out separately by stages:

- design;
- prototype manufacturing;
- testing and refinement.

Total design costs determined by the formula [8]:

$$MO\{S_{des}\} = 1.5 \cdot K_{c.tax} \cdot m_{airfr}^{0.1} \cdot \frac{\Gamma(M+1)}{a^{M+1}},$$

where S_{des} – design costs, dollar;

$K_{c.tax}$ – coefficient taking into account taxes, assessed contributions, deductions in the design costs, $K_{c.tax} = 1.61$;

m_{airfr} – the mass of the aircraft structure with equipment, including the mass of overhead and crew without the mass of power plants, $m_{airfr} = 19600$ kg;

Γ – gamma-function, $\Gamma = 0.096177$;

M – maximum number of flights, $M = 0.9$;

a – parameter characterizing the probable deviation of a random variable from number M , $a = 0.0186$;

$$MO\{S_{des}\} = 1.5 \cdot 1.61 \cdot (19600)^{0.1} \cdot \frac{0.096177 \cdot (0.9+1)}{(0.0186)^{(0.9+1)}} = 2300.875 \text{ th. dol.}$$

Costs for manufacturing each prototype [8]:

$$S_{Nman} = 1.5 \cdot K_{c.tax} \cdot m_{airfr}^{1.237} \cdot V_{max}^{0.699} \cdot N^{-0.2},$$

where V_{max} – maximum airplane speed, $V_{max} = 1000$ km/h;

N – serial number of the prototype.

$$S_{1man} = 1.5 \cdot 1.61 \cdot (19600)^{1.237} \cdot 1000^{0.699} \cdot 1^{-0.2} = 6157.97 \text{ th. dol};$$

$$S_{2man} = 1.5 \cdot 1.61 \cdot (19600)^{1.237} \cdot 1000^{0.699} \cdot 2^{-0.2} = 5360.82 \text{ th. dol};$$

The sum of the cost of manufacturing two prototypes:

$$S_{man} = S_{1man} + S_{2man} = 6157.97 + 5360.82 = 11518.79 \text{ th. dol.}$$

The costs of fine-tuning and testing of prototypes determined by the formula [20]:

$$S_{test} = 1.5 \cdot K_{c.tax} \cdot 10^4 \cdot n_{fl.sam}^{0.9} \cdot [1 + 0.01 \cdot (n_{fl.sam} - 1)] \cdot K,$$

where $K = 1500^{-0.03} = 0.803$;

$n_{fl.sam} = 1$ – number of flight samples.

$$S_{test} = 1.5 \cdot 1.61 \cdot 10^4 \cdot 1^{-0.9} \cdot [1 + 0.01 \cdot (1-1)] \cdot 0.803 = 19392.45 \text{ th. dol.}$$

The total costs of the design bureau determined by the formula [20]:

$$\begin{aligned} S_{des.b} &= MO\{S_{des}\} + S_{man} + S_{test} = 2300.875 + 11518.79 + 19392.45 \\ &= 33212.115 \text{ th. dol.} \end{aligned}$$

Project cost:

$$C_{des.b} = 1.25 \cdot S_{des.b} = 1.25 \cdot 33212.115 = 41515.114 \text{ th. dol.}$$

3.3.2 Calculation of mass production costs

Factory average cost of one plane of the annual volume in N pieces cost without engines defined by the formula [8]:

$$S_{fact} = M_0 + PI + STEQ + SE + SSE + W_0 + IE_w + IE_{fact} + AC + ACT_{TOT} + H_R,$$

where M_0 = cost of basic materials, raw materials and finished products for general industrial use and the cost of purchased semi – finished products;

PI = cost of purchased items;

$STEQ$ = manufacturing, repair and restoration costs special technological equipment debited on the program for the first two years of serial production of the aircraft.

$$M_0 = 1.95 \cdot 10^4 \cdot m_{st}^{0.93} \cdot 0.9^{3.32 \ln N},$$

where m_{st} – mass of aircraft structure = 19600 kg;

N – annual aircraft production = 53.

$$M_0 = 1.95 \cdot 10^4 \cdot (19600)^{0.93} \cdot 0.9^{3.32 \ln 53} = 53547.63 \text{ dol};$$

$$PI = 1.95 \cdot (2.37 \cdot V_{max} + 14.15 \cdot m_{epmt} - 1280) \cdot N^{-0.09},$$

where V_{max} – maximum aircraft speed = 870 km/h;

m_{epmt} - empty mass = 18 t.

$$PI = 1.95 \cdot (2.37 \cdot 870 + 14.15 \cdot 18 - 1280) \cdot 53^{-0.09} = 1413.79 \text{ th. dol.}$$

Labor costs for manufacturing, overhaul, restoration of special technological equipment is determined when $m_{epm} > 3$ t and $M \leq 2.5$:

$$T_k = (2.943 + 0.0775 \cdot m_{epmt} - 2.58 \cdot 10^{-4} \cdot m_{empt}^2) \cdot 1.05^n,$$

where n – number of engines = 2.

$$T_k = (2.943 + 0.0775 \cdot 18 - 2.58 \cdot 10^{-4} \cdot 18^2) \cdot 1.05^2 = 4.19 \text{ mill. norm – hours.}$$

Overall labor costs in the manufacturing repair, restoration of special tooling up:

$$T_{ov.all} = T_k \cdot K_1 \cdot K_2 \cdot K_3 \cdot K_4 \cdot K_5;$$

K_1 – takes into account the entire volume of output:

$$K_1 = 2.27 \cdot 10^{-3} \cdot N + 0.64;$$

$$K_1 = 2.27 \cdot 10^{-3} \cdot 53 + 0.64 = 0.760;$$

K_2 – takes into account the lever of application of normalized snap;

$$K_2 = 1.2 - 0.005 \cdot \chi$$

where χ - level of application of normalized snap in % = 25%.

$$K_2 = 1.2 - 0.005 \cdot 25 = 1.075.$$

K_3 – takes into account the level of continuity of the created structure;

$$K_3 = 10^{-2} \cdot [220 - \sqrt{(250.6)^2 + (X - 220)^2}],$$

where X – percentage of parts transferred from the previous construction made at this plant, $X = 0.1$.

$$K_3 = 10^{-2} \cdot [220 - \sqrt{(250.6)^2 + (0.1 - 220)^2}] = 0.998.$$

K_4 – takes into account the manufacture of backups of equipment, its repair and restoration, $K_4 = 1.51$;

K_5 - coefficient taking into account whereby thrust is created, $K_5 = 1.12$.

So;

$$T_{ov.all} = 4.19 \cdot 0.760 \cdot 1.075 \cdot 0.998 \cdot 1.51 \cdot 1.12 = 5.8 \text{ mill. norm - hours.}$$

The value of the cost of manufacturing special equipment

$$CO = T_{ov.all} \cdot \bar{c},$$

where c – production cost of one norm - hour of special technological equipment equal to 2.5 – 2.7 dol.

$$CO = 5.8 \cdot 2.5 = 14.5 \text{ mil. dol.}$$

So;

$$STEQ = \frac{CO}{N_1 + N_2},$$

where N_1, N_2 – number of aircraft planned for release in the first and second years of mass production, $N_1 = 53, N_2 = 53$.

$$STEQ = \frac{14.5}{53 + 53} = 0.137 \text{ th. dol.}$$

SE – production costs caused by the development in serial production of a new aircraft and the development of its manufacturing process.

SSE – special expenses (expenses for testing serial aircraft).

$$SE = 0.44 \cdot STEQ;$$

$$SE = 0.44 \cdot 0.137 = 0.060 \text{ th. dol.}$$

$$SSE = 0.33 \cdot STEQ;$$

$$SSE = 0.33 \cdot 0.137 = 0.045 \text{ th. dol.}$$

$$W_o = 1.5 \cdot 3.013 \cdot 10^4 \cdot m_{st}^{0.93} \cdot M^{0.42} \cdot N^{-0.32} \cdot K_{prod},$$

where K_{prod} – coefficient taking into account the increase in labor productivity of the worker during the time from the development of the preliminary design, when the preliminary calculation of the price of the aircraft is carried out, before the start of mass production, $K_{prod} = 0.5835$ [8].

$$W_o = 1.5 \cdot 3.013 \cdot 10^4 \cdot (19600)^{0.903} \cdot (0.9)^{0.42} \cdot 0.5835 = 5321.72 \text{ mil. dol.}$$

Indirect workshop and factory expenses are equal:

$$IE_w = 1.92 \cdot 3.04 \cdot W_o \cdot N^{-0.129};$$

$$IE_w = 1.92 \cdot 3.04 \cdot 5321.72 \cdot 53^{-0.129} = 18612.094 \text{ th. dol.}$$

$$IE_{fact} = 1.92 \cdot 3.701 \cdot W_o \cdot N^{-0.359}$$

$$IE_{fact} = 1.92 \cdot 3.701 \cdot 5321.72 \cdot 53^{-0.359} = 9091.955 \text{ th. dol.}$$

Estimated assessed contributions for the annual aircraft release program:

$$AC = \frac{(l_{AC} + l_p) \cdot S_{IPP} \cdot N}{100},$$

where l_{AC} – total rate of mandatory contributions from labor costs of all categories of employees, $l_{AC} = 37\%$; l_p – the rate of deductions from labor costs of workers of all categories of industrial production personnel in the amount of 1% of the salary of each employee; SIPP – costs of the basic and additional wages of workers of all categories of industrial and production personnel, included in the factory average cost of one aircraft [8].

$$S_{IPP} = K_{S_{IP}} \cdot (STEQ + SE + SSE + W_o + IE_w + IE_{fact}),$$

where $K_{SIP} = 0.235$ – the share of labor costs for workers of all categories of industrial and production personnel in total costs for special equipment, installation costs, testing costs, the basic and additional wages of production workers, indirect costs of primary production workshops and indirect factory costs.

$$S_{IPP} = 0.235 \cdot (0.137 + 0.060 + 0.045 + 5321.72 + 18612.094 + 9091.955)$$

$$S_{IPP} = 7761.1 \text{ th. dol.}$$

$$AC = \frac{(37+1) \cdot 7761.1 \cdot 53}{100} = 156308.55 \text{ th. dol.}$$

ACT_{TOT} – total amount of assessed contributions and value added tax:

$$ACT_{TOT} = l_{gen} \cdot S_{IPP} \cdot \frac{N}{100},$$

where l_{gen} – generalized rate of labor costs – 58%.

$$ACT_{TOT} = 58 \cdot 7761.1 \cdot \frac{53}{100} = 238576.214 \text{ th. dol.}$$

Rate, included in the cost of i-th annual release program, is determined:

$$H_R = l_R \cdot S_{IPP} \cdot \frac{N}{S_{nnn}},$$

where l_R – utility tax rate 2 dol/pers;

S_{nnn} – average monthly wage per worker (400 dol).

$$H_R = 0.002 \cdot 7761.1 \cdot \frac{53}{0.4} = 2056.7 \text{ th. dol.}$$

Cost of aircraft without deductions for road maintenance, VAT and excise tax:

$$S_{fact} = 53.54 + 1413.79 + 0.137 + 0.060 + 0.045 + 5321.72 + 18612.094 + 9091.955 + 156308.55 + 238576.214 + 2056.7 = 431434.791 \text{ th. dol.}$$

Deductions for the maintenance of roads and the aerodrome of the plant:

$$D_{road} = 0.0153 \cdot S_{fact};$$

$$D_{road} = 0.0153 \cdot 431434.791 = 6600.952 \text{ th. dol.}$$

The factory cost of the aircraft from the annual output of 80 pieces without the cost of engines is [20]:

$$C_{fact} = S_{fact} + D_{road} + ACT_{TOT};$$

$$C_{fact} = 431434.791 + 6600.952 + 238576.214 = 676611.957 \text{ th. dol.}$$

Summing up the costs for all items, and get the total cost of the aircraft from the annual output of 80 aircraft:

$$S_{TOT} = 1.01 \cdot C_{fact};$$

$$S_{TOT} = 1.01 \cdot 676611.957 = 683378.077 \text{ th. dol.}$$

Engine price $P_{eng} = 71800$ th.dol.

The cost of one aircraft with engines will be:

$$S_{TOT+eng} = S_{TOT} + n \cdot P_{eng};$$

$$S_{TOT+eng} = 683378.077 + 2 \cdot 71800 = 826978.077 \text{ th. dol.}$$

Determine the price of the aircraft (P_{plan}) with profitability of 25%:

$$P_{plan} = 1.25 \cdot S_{TOT};$$

$$P_{plan} = 1.25 \cdot 826978.077 = 1033722.596 \text{ th. dol.}$$

Determine the price of an airplane with engines:

$$P_{plan+eng} = P_{plan} + 2 \cdot P_{eng};$$

$$P_{plan+eng} = 1033722.596 + 2 \cdot 71800 = 1177322.596 \text{ th. dol.}$$

Define the profit from sales of the designed aircraft:

$$P_r = P_{plan} - S_{TOT} = 1033722.596 - 683378.077 = 350344.52 \text{ th. dol.}$$

Profit after taxes:

$$P_{rtax} = 0.7 \cdot P_r;$$

$$P_{rtax} = 0.7 \cdot 350344.52 = 245241.16$$

Profitability:

$$PROF = \frac{P_r}{S_{TOT}} \cdot 100;$$

$$PROF = \frac{350344.52}{683378.077} \cdot 100 = 51\%$$

3.4 Evaluation of aircraft production efficiency depending on their sales volumes on sales markets

3.4.1 Break – even point determination

To determine the breakeven point, constructing graphical dependencies of profit and total production costs on the aircraft production program.

The formula for calculating the break-even point in physical terms (in units) [20]:

$$N_{br-e} = \frac{C_{des.b}}{P_{plan} - S_{TOT}},$$

where $C_{des.b} = 41515.114$ th. dol. - total fixed costs (costs of the experimental design bureau for aircraft design);

$P_{plan} = 1033722.596$ th. dol. – average aircraft price;

$S_{TOT} = 683378.077$ th. dol. - average variable costs for the release of one aircraft.

So, obtain:

$$N_{br-e} = \frac{41515.114}{1033722.596 - 683378.077} \approx 10 \text{ units.}$$

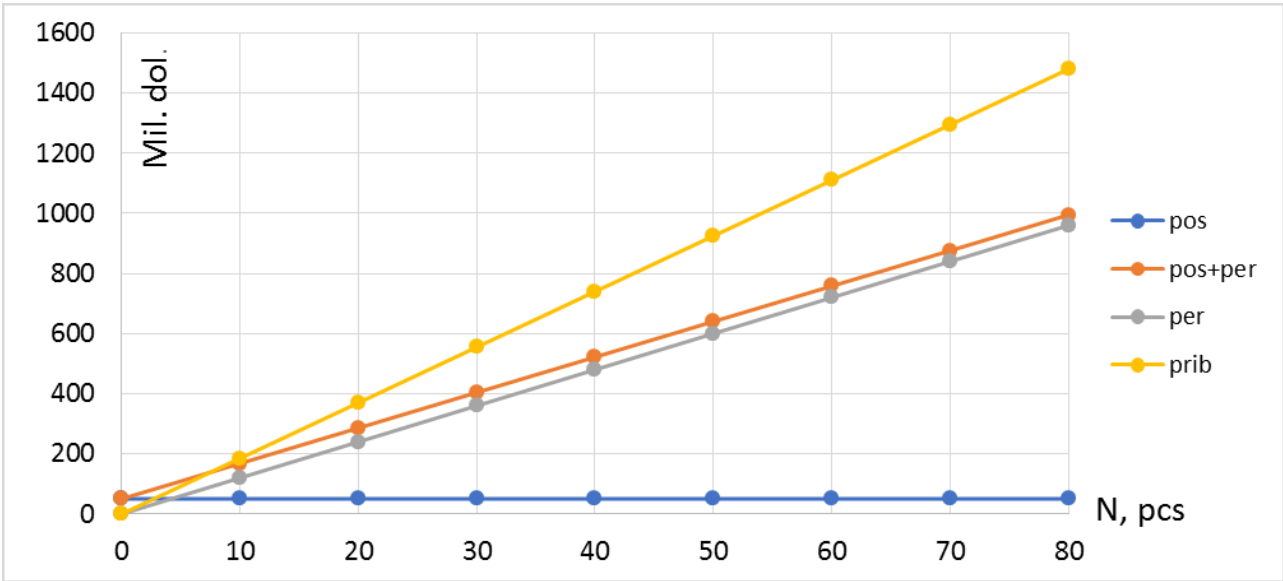


Figure 3.3 - Total Production Costs and Profits from the Aircraft Production Program

3.5 Economic Conclusion

The main technical and economic indicators of the design and production of the projected aircraft have been calculated.

The estimated cost of the projected aircraft for the design bureau is 41515.114 thousand dollars. The estimated cost of manufacturing the aircraft, is 676611.957 th. dol. The plan price of the aircraft with engines is 1177322.596 th. dol.

The company's income will exceed production costs with a program for the production of more than 10 aircraft.

CONCLUSION

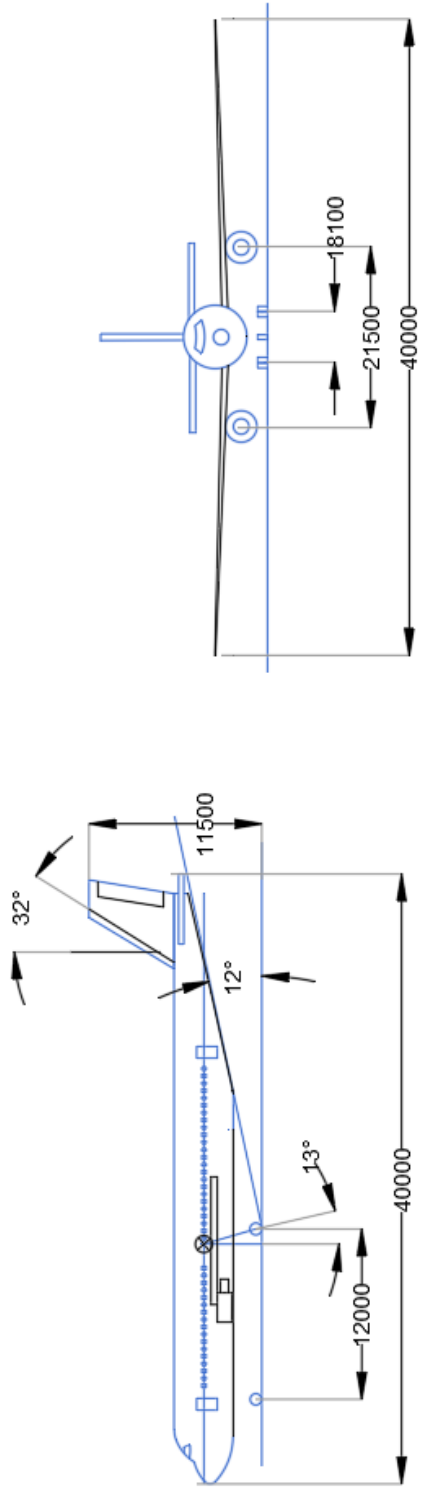
As a result of the implementation of the master's degree project by various research methods, the following results were obtained:

- 1 The main parameters and characteristics of analog aircraft are analyzed.
- 2 The take-off mass of the projected aircraft was determined in three approximations and amounted to 117977 kg. The masses of the main components of the aircraft, depending on the take-off mass of the aircraft, were calculated; wing mass – 27370 kg; fuselage mass – 24990 kg; tail mass – 4970 kg; power plant mass – 7000 kg; landing gear mass – 12670 kg; as well as fuel mass – 19776.8 kg.
- 3 The basic geometric parameters of the projected aircraft have been determined: $S = 130 \text{ m}^2$, $l = 40 \text{ m}$, $\eta = 4$, $\lambda = 10$, $b_A = 3.64 \text{ m}$, $L_f = 40 \text{ m}$.
- 4 The centering sheet of the projected aircraft has been calculated. The position of the center of mass is at 1.336 of b_A .
- 5 The values of the coefficients of the lifting force and the force of the frontal resistance are determined. Polars were built during cruise flight, takeoff and landing. It was determined that the maximum aerodynamic quality is 15.7 units.
- 6 Natural fibers composites are renewable and cheaper substitute than synthetic fibers such as glass and carbon fiber reinforcements in making structural components. Thus, from the analytical and experimental results, it is found that, kenaf has the highest sound absorption coefficient of 0.87 and to some extent jute also can be used in aircraft for sound absorption.
- 7 The estimated cost of the projected aircraft for the design bureau was calculated, which is \$41.5 million. The estimated cost of manufacturing the aircraft was \$6.76 billion. The company's income will exceed production costs with a program for the production of more than 10 aircraft.

REFERENCES

1. В. Н. Клименко, А. А. (1986). Приближенное определение основных параметров самолета [Текст]: учеб. пособие по курсу "Общее устройство самолетов и агрегатов", 40.
2. В. С. Кривцов, Я. С. (2003). Основы аэрокосмической техники [Текст]: учеб. для студентов вузов:, 620.
3. Техничко-экономическое обоснование конструкций самолетов и двигателей [Текст]: учеб. (2000). пособие по дипломному проектированию. – Х.: Нац. аэрокосмический ун-т «Харьк. авиац. ин-т», 51.
4. Житомирский, Г. (1991). Конструкция самолетов [Текст]. учебник для студентов авиационных ВУЗов, М, 400.
5. Авиационные правила. Часть 25. Нормы летной годности самолетов транспортной категории,. (1994). 1 - 22.
6. Joel E. Guerrero, D. M. (2011). Biomimetic spiroid winglets for lift and drag control. *Elsevier Publication*, 14.
7. Jorge P Arenas, F. A. (2017). Eco Materials with noise reduction properties. *ResearchGate*, 26.
8. Molin, N. (2019). Airframe noise modeling and prediction. *CEAS Aeronautical Journal*, 19.
9. *Mordor Intelligence*. (n.d.). Retrieved from <https://www.mordorintelligence.com/industry-reports/commercial-aircraft-market>
10. Whitcomb, R. T. (1976). A Design Approach and Selected Wind - Tunnel Results at High Subsonic Speeds for Wing - Tip Mounted Winglets. *NASA Technical Note*, 33.
11. А. К. Мялица, Л. А. (2010). Разработка аванпроекта самолета [Текст]: учеб. 233.
12. Harry H. Heyson, G. D. (1977). Theoretical Parametric Study of the Relative Advantages of Winglets and Wing - Tip Extensions . *NASA Technical Paper*, 80.
13. J.W. Wong, W. M. (2017). Sound absorption properties of kenaf bamboo particleboard at various mixing ratio and density. *AIP Conference Proceedings*, 6.

APPENDIX A



1	Ktflight	0.85
2	Lib	1500
3	L	6400
4	Mto	75250
5	m	70000
6	mc	18000
7	npass	120
8	Pto	8700
9	to	0.13
10	Number and type of engines	2 x PW1500G
11	Swing	130
12	S1c	33
13	S2c	24
14	rwing	4
15	xwing	30
16	Awing	10
17	fls	4
18	fls	32
19	fls	4
20	rws	2
21	xps	31
22	Aus	2
23	flusage	m 4
24	flusage	10
Handling Qualities		
Mass Data		
Power Plant Data		
Geometry		
Passenger Airplane		Scale
		200:1
		150FD, KtAI

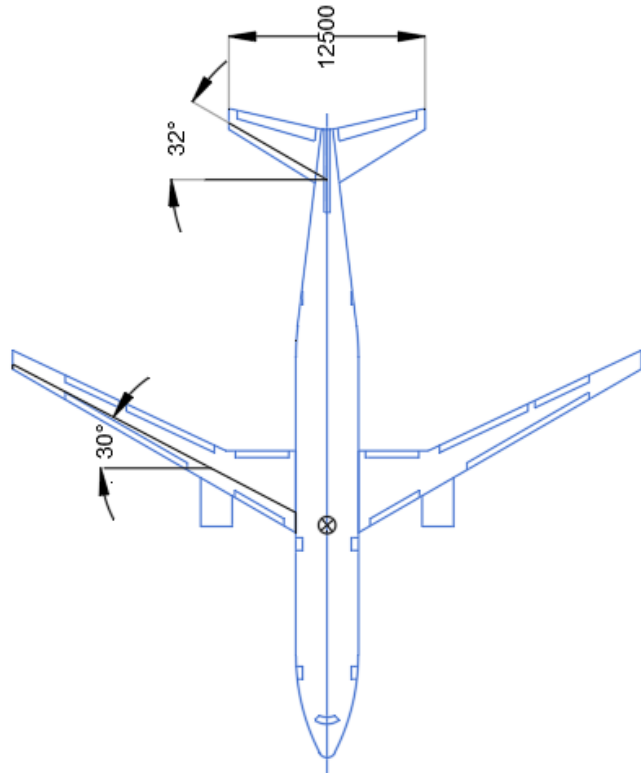


Figure A.1 – The general view drawing

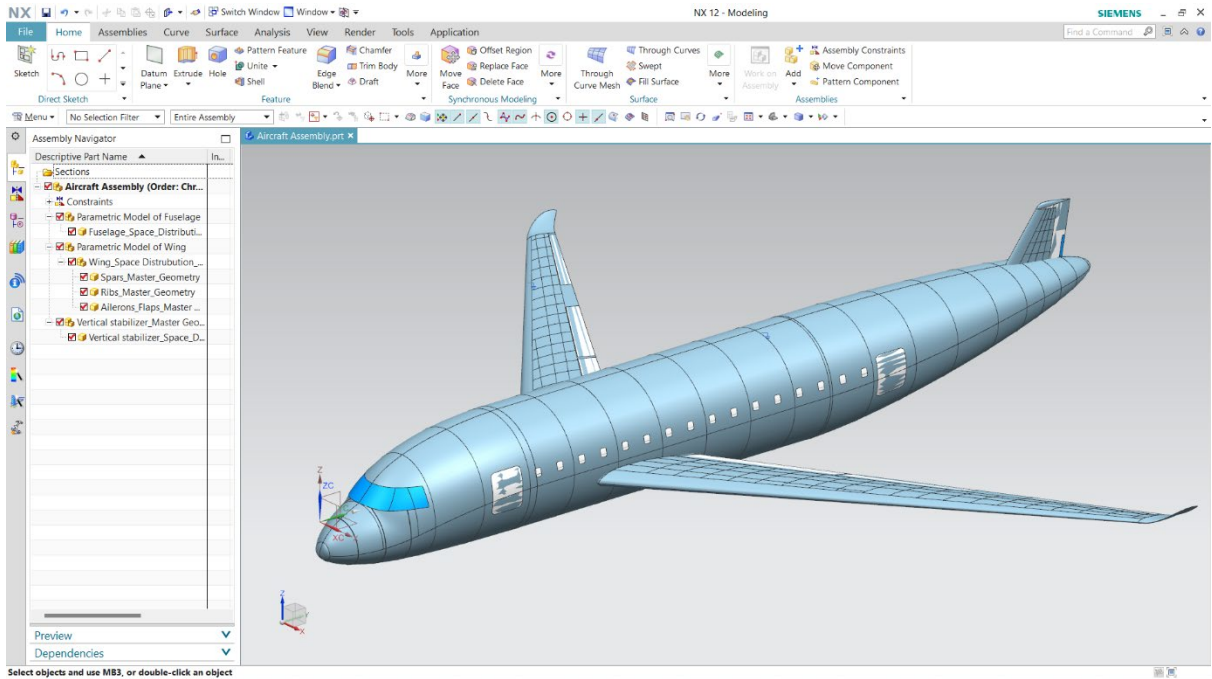


Figure A.2 – The master – geometry model

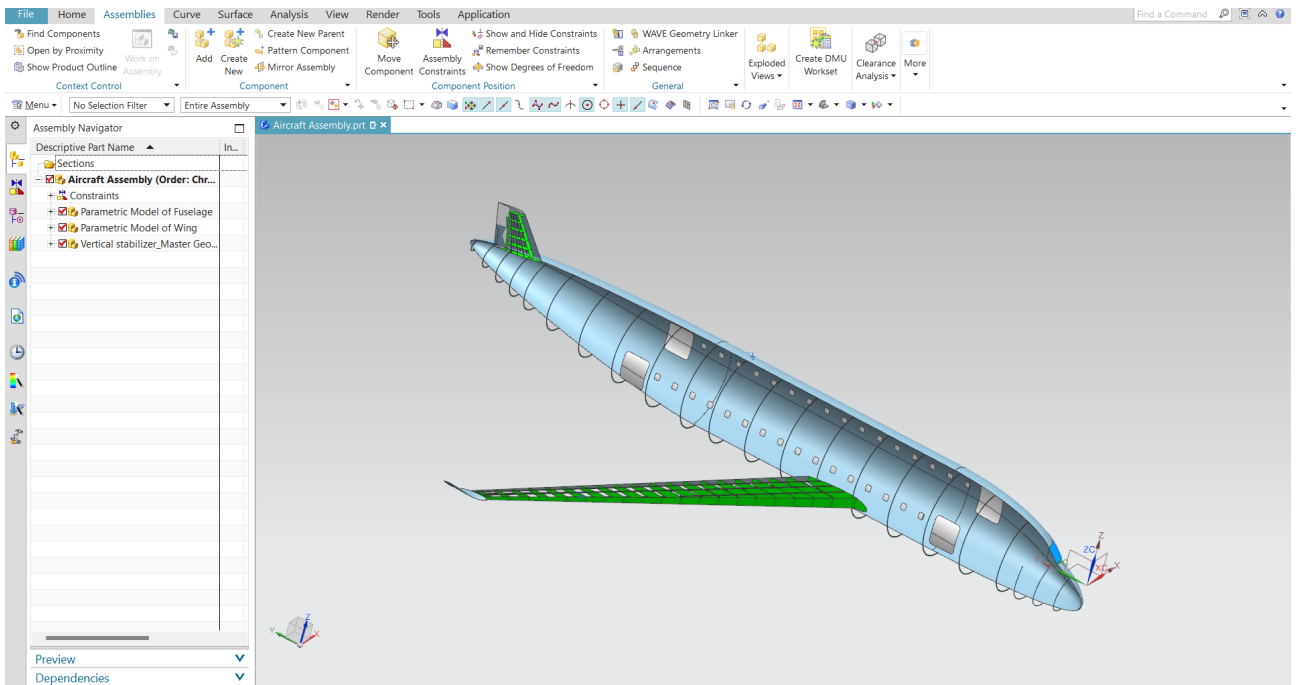


Figure A.3 – The space – distribution model of projected airplane